AN INVESTIGATION ON THE EFFECTS OF Ag ADDITION IN THE POWDER – IN – TUBE PROCESSING OF LONG MULTIFILAMENTARY (Bi,Pb) - 2223/Ag SUPERCONDUCTING TAPES

Thesis submitted to Cochin University of Science and Technology (CUSAT)

for the degree of

DOCTOR OF PHILOSOPHY

in

PHYSICS

BY

SOBHA. A.

REGIONAL RESEARCH LABORATORY
(COUNCIL OF SCIENTIFIC & INDUCTRIAL RESEARCH)
TRIVANDRUM-695 019

DECEMBER 2002

COUNCIL OF SCIENTIFIC AND INDUSTRIAL RESEARCH [CSIR]
REGIONAL RESEARCH LABORATORY
TRIVANDRUM - 695 019, INDIA

Dr. U. Syamaprasad
Scientist E II

Phone : 0091-0471-515233 (O), 741830 (R)
Fax : 0091- 0471- 491712, 490186; Grams : CONSEARCH
Email:syam@csrrltrd.ren.nic.in; usyamaprasad@hotmail.com

30 December 2002

CERTIFICATE

This is to certify that the thesis entitled " ***AN INVESTIGATION ON THE EFFECTS OF Ag ADDITION IN THE POWDER – IN – TUBE PROCESSING OF LONG MULTIFILAMENTARY (Bi,Pb) - 2223/Ag SUPERCONDUCTING TAPES***" is an authentic record on the research work carried out by Mrs. Sobha. A., under my supervision in *partial fulfilment of the requirement for the degree of* ***Doctor Of Philosophy*** *of the Cochin University of Science and Technology and further that no part of this thesis has been presented before for any other degree.*

U. Syamaprasad

DECLARATION

I, Sobha. A., hereby declare that, this thesis entitled " AN INVESTIGATION ON THE EFFECTS OF Ag ADDITION IN THE POWDER–IN–TUBE PROCESSING OF LONG MULTIFILAMENTARY (Bi,Pb)-2223/Ag SUPERCONDUCTING TAPES" is a bonafide record of the research work done by me and that no part of this thesis has been presented earlier for any degree, diploma of any other University.

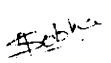

Sobha. A.

Trivandrum
30 December 2002

Dedicated to
my husband, parents and brothers.

ACKNOWLEDGEMENTS

With great pleasure, I express my deep sense of gratitude and respect to Dr. U. Syamaprasad, my supervising guide, Regional Research Laboratory, Trivandrum for his valuable guidance, constant encouragement and continuous support throughout the period of my Ph.D. work.

I am grateful to Dr. B.C. Pai, Acting Director, Regional Research Laboratory, Trivandrum and Dr. G. Vijay Nair, former Director of RRL, Trivandrum, for providing all the facilities to carry out this work and for their encouragement and valuable suggestions during this work.

I am greatly indebted to Mr. P. Guruswamy, Technical Officer, Regional Research Laboratory, Trivandrum for his constant encouragement, invaluable suggestions and sincere help during the entire course of this work.

My sincere thanks are due to Dr. K.G.K. Warrier, Dr. C. Pavithran, Dr. Peter Koshy and Mr. P. Prabhakar Rao, Scientists, Regional Research Laboratory, Trivandrum for their help during this work.

I owe my sincere gratitude to my senior colleague Dr. M. Sankara Sarma, Lecturer, Govt. Women's College, Trivandrum, and my colleagues Mr. R..P. Aloysius and Mr. R.. Rajeev Kumar, for their sincere help, constant encouragement and invaluable suggestions.

My heartfelt thanks are due to Mr. S.G.K. Pillai, , Mr. Krishna Pillai, , Mr. K. Sadasivan, Mr. M.R. Nair, Mr. P. Mukundan for extending different instrumental facilities.

I express my sincere gratitude to Dr. P. Vijayakumar, Head, Department of Physics, Cochin University of Science and Technology, Trivandrum for his kind cooperation and support at various stages of this work.

Finally I express my deep sense of gratitude to the Council of Scientific and Industrial Research, New Delhi for the award of Senior Research Fellowship.

Sobha. A.

CONTENTS

2. PREPARATION AND CHARECTERIZATION TECHNIQUES

3. PHASE EVOLUTION, MICROSTRUCTURE AND TRANSPORT PROPERTY OF (Bi, Pb)-2223/Ag TAPES PREPARED USING POWDERS OF VARYING PARTICLE SIZE DISTRIBUTION

4. PHASE EVOLUTION IN Ag, Ag_2O AND $AgNO_3$ ADDED (Bi,Pb)-2223 SUPERCONDUCTOR

6. PROPERTIES OF Ag SHEATHED (Bi,Pb)-2223-Ag NANOCOMPOSITE –PREPARED BY SOL-GEL METHOD

7. PREPARATION AND CHARECTERISATION OF LONG MULTIFILMENTARY Ag/(Bi, Pb)-2223-Ag COMPOSITE SUPERCONDUCTING TAPES

PREFACE

Silver sheathed (Bi,Pb)-2223 PIT tapes have been emerging as the most promising High Temperature Superconducting (HTS) current carriers for practical applications. However for the tapes to be commercially useful in systems like high field magnets, energy storage devices, motors/generators, fault current limiters and power transmission cables, they need to be processed into composite multifilamentary tapes of sufficient length with excellent mechanical properties. However, (Bi,Pb)-2223 is a complex system containing five cations and the processing parameters for obtaining good superconducting properties show wide variations over sintering temperature, duration and atmosphere. Also inherent to the system are the weak links and microcracks that may develop during processing/heat treatment. The presence of weak links and microcracks will deteriorate the critical current density (J_C) of the tapes. Intense research efforts are being carried out around the world to improve the superconducting properties of (Bi,Pb)-2223 system by careful optimization of the process parameters.

It is important that long superconducting tape must have desired strain tolerance (less reduction of J_C with applied strains) and stress tolerance (less reduction of J_C in applied stresses) for its use as coils and magnets. Ag addition to the BPSCCO system has many advantages with its physical and chemical inertness to the system, reduces the processing temperature, and promotes the grain growth, grain alignment and connectivity. All these not only enhance the critical current density of the tapes but also improve the mechanical properties. But the published results show very much scattering on the

type of Ag additive to be selected, method of addition and its optimum percentage. Also there are some negative reports in this regard. The present work has been undertaken to study the effect of silver addition in different forms (Ag powder, Ag_2O, $AgNO_3$) on the superconducting and mechanical properties of (Bi,Pb)-2223/Ag tapes and to find out a suitable form of Ag additive and its optimum percentage to have better superconducting and mechanical properties. Also it is the aim of the present work is to optimise the process parameters needed to prepare (Bi,Pb)-2223/Ag multifilamentary tapes of length ~ 12 m in solenoid and pancake coil forms with good critical current density and homogeneity of J_C along the length of the tapes.

First Chapter is an overview of the structure and property relations in HTS materials. Due importance is given to the properties of Bi based materials, their processing and application environments. Also different aspects of Ag addition collected from the literature are discussed. State of the art developments in the processing of long multifilamentary tapes are discussed along with their application vistas.

Preparation and characterisation methods of Ag/BPSCCO tapes are described in Chapter-2. Superconducting properties of the Bi-2223 tapes mainly depend on the complex fabrication process consisting of precursor synthesis, mechanical deformation and heat treatment. Among these the quality of the precursor powder is most important and is governed by the phase assemblage and particle size distribution. Chapter 3 describes the effect of particle size distribution of the precursor on phase evolution, microstructure, J_C and J_C -B characteristics of Bi-2223/Ag tapes. The results show that the tapes prepared using coarser powder, the reaction kinetics was slower and the microstructure contained smaller grains with many misalignments and voids. On the other hand, use of extremely fine precursors yielded

tapes with a larger fraction of secondary phases due to the degradation of crystallinity of the precursor and consequent change in the reaction sequence.

Chapter 4 describes the studies conducted initially in order to find out the relative effect of Ag powder, Ag_2O and $AgNO_3$ on the sequence of phase evolution, kinetics of (Bi,Pb)-2223 formation, density variation and finally the transport current in bulk BPSCCO system. Experiments were conducted by varying the silver content in the composition. Phase evolution of the samples at different stages of heat treatment, microstuctural examination and superconductivity characterisation suggested that Ag addition in BPSCCO accelerates the Bi-2223 phase formation and J_C to different extents depending on the form of Ag additive.

As a continuation of the work on bulk BPSCCO, the effects of Ag powder, Ag_2O and $AgNO_3$ on the phase evolution, microstructure and critical current density in (Bi,Pb)-2223/Ag tapes were also carried out and results different from those of bulk samples were obtained and these are described in fifth Chapter of the thesis. The results of the studies on mechanical strength of the Ag added mono and multifilamentary (Bi,Pb)-2223/Ag tapes also is described in this chapter. It was found that the strain tolerance and tensile strength of Ag added tapes improve remarkably as the Ag content in the matrix increases. The strain limit of monofilamentary tapes increases by about twofold by the addition of 7wt% Ag. The mechanical properties of multifilamentary tapes were found to be better than that of monofilamentary tape. It was concluded that multifilamentary tape with 7wt% silver addition have a strain tolerance more than three times and a tensile stress tolerance of 142% higher than that of pure monofilamentary tape.

Chapter 6 deals with the studies conducted to improve the transport property and microstructure of Ag added tapes by introducing well dispersed ultrafine silver particles in molecular level to the precursor. The method further improved the phase formation and J_C. Transport property of 1 wt% and 3 wt% Ag added samples was better than the pure sample of which 3 wt% Ag added sample shows the highest J_C. 3 wt% Ag added tape shows slight improvement in J_C-B characteristics.

All the experiments conducted on the preparation and characterization of long multifilamentary Ag added (Bi,Pb)-2223 superconducting tapes are given in Chapter 7. 3 wt% $AgNO_3$ added sol-gel derived powder has been used and long multifilamentary tapes were prepared after optimising the parameters such as wire diameter in the first and second stages, filament number, final tape thickness etc to maximise J_C as well as mechanical strength in short length. Studies on long length tapes include testing of homogeneity of J_C along the length of the tape at 77K, susceptibility measurements and whole length J_C measurements in solenoid and pancake coil forms. 12 m long tapes prepared under the optimum conditions have shown J_C in the range 12-16 $kAcm^{-2}$ at 77K and self-field. Pancake coils with ID: 5-8 cm and OD: 8-10 cm and turn number upto 50 have been made using tapes by W&R and R&W approaches.

The overall conclusions drawn from the investigations are summarised in Chapter 8.

LIST OF PUBLICATIONS OF SOBHA. A.

I. Research Papers Published in International Journals

1. Superconducting and Mechanical Properties of (Bi,Pb)-2223/Ag Tapes in the Wire-In-Tube Geometry, ***Physica C***, accepted for publication 2002
2. Development of HTS conductors for electrical power applications ***Metals Materials And Processes,*** 2001, Vol. 13, No. 2&3
3. Phase evolution, microstructure and transport property of (Bi, Pb)-2223/Ag tapes prepared using powders of varying particle size distribution ***Superconductor Science and Technology*** (UK) 14 (2001) 417-424
4. Bend Strain and tensile Stress Characteristics of (Bi, Pb)-2223/Ag-Cu alloy sheathed tapes ***Superconductor Science and Technology*** (UK) 14 (2001) 85-89
5. Strain tolerance and tensile strength of Ag added mono and multifilamentary (Bi, Pb)-2223/Ag tapes ***Superconductor Science and Technology*** (UK) 13 (2000) 1487-1491
6. Processing of Long Multifilamentary HTS Tapes and Coils ***Metals Materials And Processes,*** 2000, Vol. 12, No. 4, pp 301-310
7. Fabrication of (Bi, Pb)-2223/Ag-Cu alloy sheathed tapes: Optimization of Cu composition in the sheath with respect to the Cu stoichiometry in the system. ***Physica C*** 328 (1999) 221-229 (NH).

8. Effects of Ag, Ag_2O and $AgNO_3$ additions in (Bi, Pb)-2223/Ag powder-in-tube tapes. ***Physica C*** 316(1999) 63-68 (NH)
9. Optimisation of tape width and powder packing density in the powder-in-tube processing of (Bi, Pb)-2223/Ag tapes. ***Physica C*** (NH) 309(1998) 203-207
10. Phase evolution in Ag, Ag_2O and $AgNO_3$ added (Bi, Pb)-2223 superconductor ***Physica C*** (NH) 307 (1998) 277-283
11. Enhanced critical current density in multilayered Ag/(Bi,Pb)2223 tapes prepared using pretextured monolayered tapes ***Superconductor Science and Technology*** (UK) 10 (1997) 987-990
12. Preparation and characterization of (Bi,Pb)-2223-Ag/Ag nano composite tapes. Communicated to ***Superconductor Science and Technology(UK)***
13. Nano size MgO addition: Enhanced flux pinning in (Bi,Pb)-2223/Ag superconducting tapes. Communicated to ***Superconductor Science and Technology(UK)***

II. PAPERS PUBLISHED IN EMINARS/SYMPOSIA PROCEEDINGS

1. Ag addition in (Bi, Pb)-2223 superconductor: Effects of Ag, Ag_2O and $AgNO_3$ on the phase evolution. Presented at DAE ***Solid State Physics Symposium SSPS'97,*** Kochi, Dec. 27-31.p- 286 (1997)
2. Effects tape width and powder packing density in the PIT processing (Bi, Pb)-2223/Ag superconducting tapes. Presented at DAE ***Solid State Physics Symposium SSPS'97***, Kochi, Dec. 27-31.p-287 (1997)
3. Structural and superconducting properties of mono and multilayered Ag/(Bi,Pb)-2223 tapes. Presented at the ***XXI National Conference on Electron Microscopy Society of India***, Trivandrum, Dec. 17-19 (1997)
4. Development of long length multilayered Ag/(Bi,Pb)-2223 superconducting tapes and pancake coils. ***DAE-BRNS Workshop on Thin Film Multilayers.*** BARC, Mumbai, Oct. 6-8 (1999)

III. **Patents Filed**

1. Conduction cooling high temperature superconducting current lead
   Indian Patent NF-390/99 dated 11.01.2000

2. Liquid nitrogen level sensor-monitor device using high TC superconductors and method of manufacture thereof
   US Patent Application No. 4062-25 filed on 20.03.2002.

CHAPTER 1

PROPERTIES AND PROCESSING ASPECTS OF Bi-BASED SUPERCONDUCTORS

1.1. High T_C Superconductor Materials

In 1911, Kammerlingh-Onnes observed that the electrical resistivity of mercury vanished below a temperature of 4.2 K. [1] Since then this phenomenon of disappearance of electrical resistivity of materials as they are cooled to low temperatures has been called superconductivity and the materials which exhibit this property are called superconductors. Also the temperature at which transition from normal state to superconducting state occurs is called the superconducting transition temperature, or critical temperature, T_C. It is an important parameter of any superconductor. Over the last ninety years, many different classes of superconducting materials have been identified and Table 1.1 lists some of these classes along with specific examples. It can be seen from the table that most of these classes of superconductors possess low transition temperatures. In fact, until 1986, the maximum T_C reported for a conductor was that observed in Nb_3Ge thin films, 23.2 K. [2] In 1986, J.G. Bednorz and K. A. Muller reported the observation of T_C ~30 K in an oxide containing La, Ba, Ca and Cu. [3] This unexpected observation of record breaking T_C in a copper oxide (cuprate) compound attracted world wide attention and the work that followed during the last one and a half decade resulted in the

discovery of a whole new class of cuprate superconductors with distinctively higher transition temperatures than that existed ever before.

Table 1.1. Various families of superconductors and their transition temperature [4-12]

Sl.No.	Type	Example	T_C (K)
1	Amorphous superconductors	Amorphous Ga	8.4
2	Cheveral phases $M_xMo_6X_8$ (M = Pb, Sn, Cu, Ag, La; X = S, Se, Te)	$PbMo_6S_8$	12.5-14.7
3	Elements	Nb	9.4
4	Carbides	NbC	11
5	Nitrides	NbN	15
6	Transition metal alloys	MoTc	16
7	C15 type Laves Phases	V_2Zr	9
8	Nitrocarbides	$NbN_{0.7}C_{0.3}$	18
9	A15 type Laves Phases	Nb_3Ge	23
10	Intercalation compounds	$TaS_2(C_5H_5N)_{1/2}$	3.5
11	Organic superconductors	$(TMTSF)_2PF_6$	1 (at 12 kbar)
12	Semi-metal superconductors	La_3Se_4	10
13	Heavy Fermion superconductors	UPt_3	
14	Magnetic superconductors	$ErRh_4B_4$	8.6
15	Oxides	$BaPb_{0.75}Bi_{0.25}O_3$	13
16	Cuprates	$YBa_2Cu_3O_{7-\delta}$	92
17	Bismuthates	$(Ba_{0.6}K_{0.4})BiO_3$	30
18	Oxycarbonates	$Bi_2Sr_4Cu_2CO_3O_8$	
19	Borocarbides	YNi_2B_2C	15
20	Fullerides	Rb_2C_{60}	45
21	Borides	MgB_2	39

In Table 1.2, some of the cuprate superconductor families are listed along with their T_C values. It may be noted that a large range of transition temperatures are exhibited by the individual members. Also many of the new superconducting compounds have T_C exceeding 77 K, the boiling point of liquid nitrogen. Compounds belonging to families such as Y-Ba-Cu-O(YBCO), Bi-Sr-Ca-Cu-O (BSCCO), Tl-Ba-Ca-Cu-O

(TBCCO) and the more recently discovered Hg-Ba-Ca-Cu-O (HBCCO) belong to this category.

In order to appreciate the importance of high T_C, it is imperative to understand the variety of applications to which traditional low T_C superconductors are employed. Superconducting materials possess an unquestioned first place in three of the most active research areas of physical science viz. sensors, satellite communication and energy technology. While the ability to carry high currents without resistive energy loss offers applications such as power transmission, energy storage and powerful electromagnetic systems, the interaction of superconducting state with magnetic field and temperature has been enabling sensor and microwave applications. However, as has been stated earlier, the LTS materials exhibit these fascinating properties only on cooling to extremely low temperatures, thereby necessitating the use of expensive liquid helium and the associated cryogenic recycling facilities. Many of the new HTS copper oxide superconductors, on the other hand, can be operated at liquid nitrogen (LN_2) temperature (77 K) thereby reducing the investment on cryogenic facilities substantially. Moreover, many of these materials are able to retain superconducting state upto higher magnetic fields in comparison with LTS materials. Similarly, the payload considerations have been instrumental in attracting LN_2 operated devices for satellite communications. However, the promises borne by the HTS materials have been slow to be utilised in reality. This is mainly because of the key differences in both the properties and processing aspects of these new materials when compared to those of conventional LTS materials. Therefore a review of the properties and structure of cuprate superconductor is presented in the following sections

Table 1.2. Compounds of HTSC cuprate family of superconductors [13-14]

Compound	T_C(K)
$La_{1.85}(Ba/Sr)_{0.15}CuO_4$	35
$La_2CuO_{4+\delta}$	45
$La_{1.6}Sr_{0.4}CaCu_2O_{6+\delta}$	60
$YBa_2Cu_3O_7$	92
$YBa_2Cu_3O_8$	82
$TlBa_2Ca_{n-1}Cu_nO_{2n+3}$	120 (n = 3)
$TlBa_2Ca_{n-1}Cu_nO_{2n+4}$	127 (n = 3)
$Bi_2Sr_2Ca_{n-1}CunO_{2n+4}$	110 (n = 3)
$HgBa_2Ca_{n-1}CunO_{2n+2+\delta}$	134 (n = 3)
$CuBa_2Ca_{n-1}CunO_7$	120
$Sr_2Ca_{n-1}Cu_nO_4$	90
$Pb_2Sr_2(Ca,Y,Nd)Cu_3O_8$	70
$Pb_2(Sr,La)_2Cu_2O_6$	32
$PbBaSrYCu_3O_8$	50
$(Pb,Cu)(Ba,Sr)_2(Y\ Ca)Cu_2O_7$	53
$Pb_{0.5}Sr_{2.5}\ (Y,Ca)\ Cu_2O_7$	104
$(Pb,Cu)\ (Sr,La)_2\ CuO_5$	32
$(Nd,\ Ce)_2CuO_{4-\delta}$	24
$(Nd,Ce,Sr)CuO_{4-\delta}$	28
$(Pb,Cu((Eu,Ce)_2\ (Sr,Eu)_2\ Cu_2O_9$	25
$(Eu,Ce)_2\ (Ba,Eu)_2Cu_3O_{10}$	43
$Bi2Sr_2\ (Gd,Ce)2Cu_2O_{10}$	34
$Tl_{0.5}Pb_{0.5}Sr_4Cu_2(CO_3)O_7$	70
$(BaSr)_2CuO_2(CO_3)$	40
$Sr_{4-x}Ba_2Tl_Cu_2(O_3O_7)$	62
$Tl_{0.5}Pb_{0.5}Sr_2Gd_{2-x}Ce_xCu_2O_{9-\delta}$	45
$NbSr_2(GdC_3)_2Cu_2O_4$	27
$Bi_2Sr_{6-x}Cu_3O_{10}\ (CO_3)_2$	40
$(Cu_{0.5}C_{0.5})Ba_2Ca_{n-1}Cu_nO_{2n+3}$	117 (n = 4)
$YCaBa_4Cu_5(NO_3)_{0.3}(CO_3)_{0.7}O_{11}$	82
$CuSr_{2-x}La_xYCu_2O_7$	60
$GaSr_2Ln_{1-x}Ca_xCu_2O_7$	73
$(C_{0.35}Cu_{0.65})Sr_2(Y_{0.73}(C_{0.27})_2Cu_2O_x$	18
$Bi_4Sr_4CaCu_3O_{14+x}$	84
$(Sr_{x-2}Bi_x)(Ln_{2-y}Ce_n)Cu_2O_{8-\delta}$	30
$Sr_2Nd_{1.5}(e_{0.5}NbCu_2O_{10-\delta}$	28

1.2. Properties of HTS Materials

1.2.1. Basic Properties

The temperature at which a material becomes superconducting is known as the transition, or critical temperature (T_C) and it varies for different materials from close to absolute zero to as high as 135K. In addition to temperature, a material's ability to superconduct depends heavily on two other variables. The first is the strength of the magnetic field in which they are placed and second the current density they can carry in the superconducting state. Superconductivity is lost when any of these parameters exceed beyond a certain critical value. Thus superconductivity is limited by three phase regions viz. transition temperature (T_C), critical magnetic field (H_C) and the critical current density (J_C)

1.2.2. Type-II Nature and The Mixed State in Superconductors

The transition from superconducting state to the normal state is greatly influenced by the coherence length ξ, which is roughly the distance over which superconducting state can appear or disappear and which also distinguishes different types superconductors. When ξ is greater than $\sqrt{2}\lambda$, (where λ is the penetration depth) as in the case for most pure elemental superconductors with high normal state conductivities, the superconductor is classified as type I. The transition to the normal state occurs sharply at a fairly low critical field, H_C of less than 0.2 T. When ξ is less than $\sqrt{2}\lambda$, as is frequently found for alloys and compounds, the superconductor is classified as type II. In this case transition to the normal state occurs gradually over a wide range of

magnetic field from H_{C1} to H_{C2}. It invokes a " mixed state" in which superconducting and normal regions coexist on a fine scale with in the material.

The lower critical field of Type-II superconductors, $H_{C1} \sim [\varphi_0/4\pi\lambda^2]\ln\kappa$, (where φ_0 and κ are flux quantum and the GL parameter) is the minimum field required for flux to penetrate into the superconductor in the absence of demagnetization effects, and the upper critical field, $H_{C2} = \varphi_0/2\pi\xi^2$, is the field above which the system goes into the normal state. For fields that fall in the range $H_{C1}<H<H_{C2}$, the system goes into the mixed state, in which an array of flux vortices, or vortex lattice is present. Each flux vortex has a normal core with a radius of order ξ, and contains exactly one flux quantum φ_0 within a region of circulating current with a radius of order λ. Fig. 1.1shows plots of magnetization vs. field for a type-I and an ideal type-II superconductor. Cuprates are known to be extreme type-II superconductors.

Type-II superconductors are generally preferred over type-I for most bulk applications, such as magnets, coils etc because of the higher upper critical field H_{C2}. An "ideal" type-II superconductor with a reversible M-H plot, as shown in Fig.1.1 is quite useless for such applications because each flux vortex experiences a "Lorentz" force per unit length $F_L=J_S \times \varphi_0$, where the flux φ_0 is directed along the vortex. In the absence of pinning the vortices will thus move perpendicular to the current in a process known as flux flow and produce a voltage along the longitudinal direction. The combination of both voltage and current along the same direction implies that power is being dissipated, which is undesirable for most bulk applications.

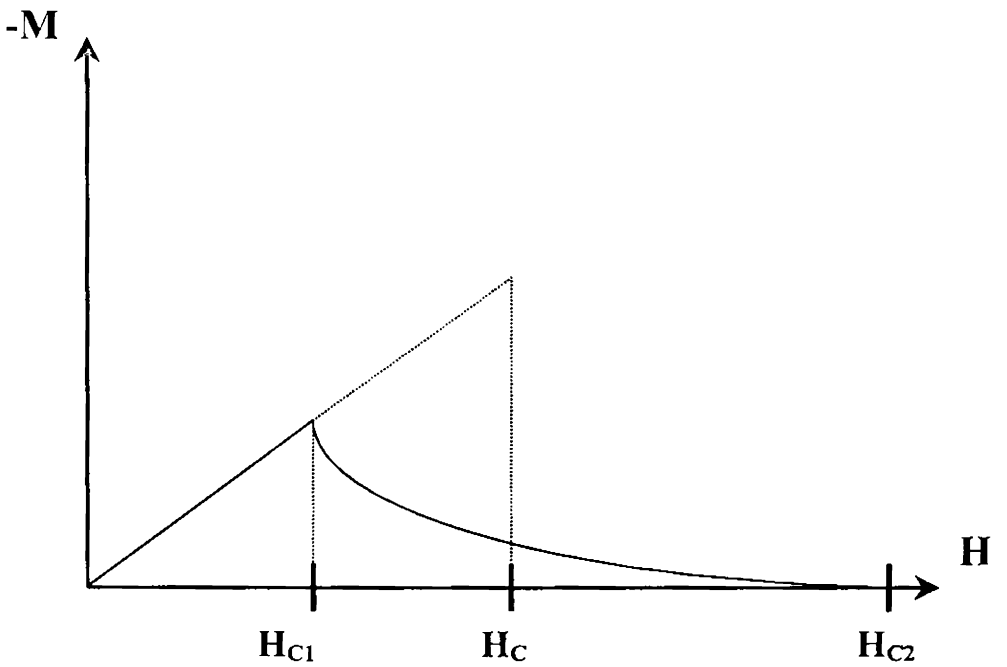

Fig. 1.1. M vs. H for a type-I (dotted line) and type II superconductor with no flux vortex pinning centres (solid line)

1.2.3. Flux Creep in Type-II Superconductors

All HTS superconductors are of type-II, whose mixed state is characterized by a vortex lattice in which the Abrikosov vortices are arranged to minimize the free energy. Most HTS materials contain fluctuations in the densities of point defects, impurities and other inhomogeneities. The vortex lattice thus becomes distorted and pinned and consequently, the magnetization vs. field (M-H) curves becomes irreversible. The simplest model capable of describing an irreversible loop, first proposed by Bean, [15] is known as the critical state model. One of the characteristic features of the magnetic behaviour of cuprate superconductors is their large and nonexponential or "giant flux creep".[16]. Experimental measurements [17] of magnetic relaxation due to

flux creep in oxides, organic, Chevrel phase, and heavy fermion superconductors demonstrate that their magnetic relaxation rates are large at temperature in the millikelvin range.

1.2.4. Irreversibility Line

The temperature dependence of the dc magnetization [18] showed that the field-cooled and zero-field-cooled curves merged into a common reversible behaviour above a certain temperature called the "irreversibility temperature" T_{irr} which is less than the critical temperature T_C, and depends on the magnetic field. The irreversibility field H_{irr} for a given temperature can be determined by plotting an M-H hysteresis loop and noting the field above which the curve merge and the magnetization becomes reversible nonhysteretic. This field is less than the upper critical field H_{C2}, and can be plotted on a phase diagram of field vs. temperature as shown in Fig.1.2 and the corresponding boundary in the H-T plane is now known as the irreversibility line.

The Meissner state in Fig. 1.2. is that for which the field is less than the lower critical field H_{C1} and the sample completely expel the magnetic flux. The irreversibility line corresponding to the temperature above which the flux lattice "melt" and becomes a vortex liquid [19] in high quality single crystal with few pinning centers. A particularly interesting prediction involves the existence of a re-entrant behaviour of the melting phase boundary at low fields in weakly pinned flux line lattices. At low field values, the melting temperature $T_m(H)$ is expected to increase with increasing field, reflecting the gradual stiffening of the lattice. This phase boundary should cross over to the more commonly studied high field regime, where $T_m(H)$ decreases with increasing H.

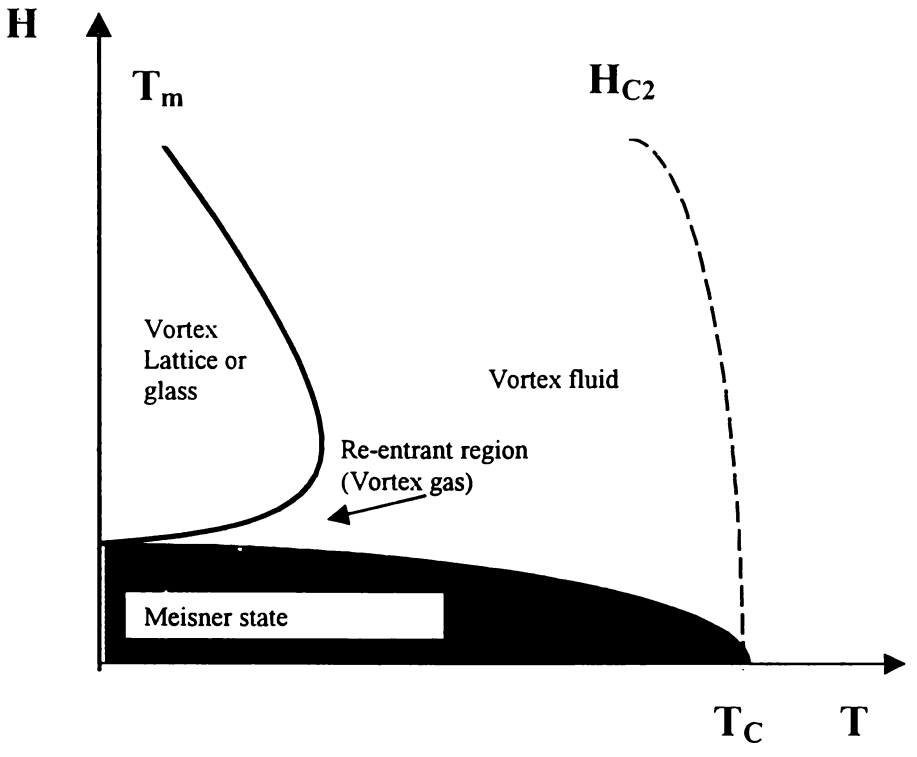

Fig. 1.2. Phase Diagram (H-T plane) of an extreme type –II superconductor , showing the various states as functions of temperature and field. The irreversibility line is shown as a solid line for nearly ideal samples (melting temperature)

1.2.5. Theoretical Efforts

Even though Kammerlingh-Onnes' discovery of superconductivity dates back to 1911, a successful microscopic explanation for the phenomenon arrived only by 1957 through the BCS theory. [20] According to this theory, the normal state electrons in a

metal behaves as a Fermi liquid. However, as temperature is lowered, at T_C, spontaneous formation of cooper pairs occurs which subsequently condenses in the Bose-Einstein sense, as once paired, the electrons behave as bosons. The basic pairing interaction was supposed to mediate through weak coupling between electrons and phonons. Quantitative verification of BCS formula like, $2\Delta(0)/kTc$ 3.5, $\Delta C_P = 1.43\gamma T_C$ etc. showed the validity of the theory for superconductivity in LTS materials.

However, as HTS materials were discovered, it was clear that BCS theory as applied for LTS could not be applied as such. For example, occurrence of T_C values higher than 20 to 40 K could not be explained by weak coupling BCS scheme [21] and experimentally determined energy gap was found to be twice as high as that of BCS derived formula.

A set of theories which have been forwarded for HTS relies in BCS type mechanism, e.g. strong phonon coupling, polaron mediated interactions, mediation through excitons, plasmons, spin fluctuations, resonating valence bond (RVB) theory, [22] anyon theory etc. More recently a new report from Berkely proposed that high T_C superconductivity involves fluctuations of the magnetic spins of atomic nuclei rather than phonon mediated mechanism of classical low T_C superconductors. In addition, they also studied [23] the single crystals of BPSCCO using low temperature (as low as 0.25 degree above zero) STM (Scanning Tunneling Microscope) by substituting Zn atom and observed that high T_C superconductivity originate from strongly interaction or paired electrons moving through copper oxide layers.

1.3. Applications of High Temperature Superconductors

The discovery of superconductivity generated interest in practical applications, mainly because of its potential to save energy. But there are certain practical limitations, which limit the widespread replacement of copper or other normal conductors by superconducting materials. The important ones are self-generated magnetic field, which tend to destroy the superconductivity when the current densities through the superconductors are increased to practical levels. A second problem was the cost and complexity of operating refrigeration equipment at lower temperatures, near to 4 K. In fact, removing one watt of heat generated at 4 K demands about 1000 W of refrigeration power at room temperature.

The discovery of HTS materials aroused tremendous excitement because many of them were superconducting above 77 K, and the applications earlier thought of with LTS, especially large-scale applications were just around the corner. In comparison to the operation at 4 K, removing one watt of heat generated at 77 K requires 10 W or less at room temperature. But these grandiose expectations soon led to disappointment as the current densities in HTS materials also lead to be naturally too low for technological applications, while there are persistent problems with poor mechanical properties. The practical problems pertinent to HTS are related to their ceramic, granular, anisotropic nature; they need to be formed at high temperatures in presence of oxygen; being brittle they are very difficult to shape and handle; while long flexible, superconducting ones are necessary for many large scale-applications. Other problems inherent with HTSs are grain boundary weak links and the low flux pinning strength arising due

to the very small coherence length. Despite these limitations, vast research efforts over the past 15 years had realized some practical applications of HTS both on the small-scale low current systems and the large-scale high current systems.

1.3.1. Small-Scale Applications

The successful small scale applications of HTS are based on the Josephson quantum tunneling effects, most notably HTS SQUIDS, are now commercially available, having the advantage of smaller size and low power consumption. Other devices that have reached commercial availability are HTS passive RF and microwave wave filters for wide band communications and radar. [24-26] They have the advantages of very low noise and much higher selectivity and efficiency than conventional filters. RSFQ (Rapid Single Flux Quantum) logic for integrated circuits and computers is still under development.[27-29] The logic elements are composed of superconductor rings with a Josephson junction shunted by a resistor. RSFQ logic circuits have speeds upto 100 times those of fast semi-conductor ICs combined with great accuracy.

1.3.2. Large-Scale Applications

LTS superconductors are already in quite common use for large-scale applications, but still have suitability problems due to the complex and expensive refrigeration required. Compared with the small-scale applications, a large-scale application generally means that much larger currents and lengths of superconductors are required. Applications

related to magnet technology are probably among the most significant that are under research at the present time. These include magnetic energy storage,[30] Maglev trains[31] (relying on repulsion between the magnet mounted on the train and guideway) and magnets for MRI and other medical imaging applications.[32-33] In all these cases, the superconductor must not only carry a large current with zero resistance under high magnetic field, but it must be possible to fabricate it into long lengths with high flexibility and high packing density. This is because for large electromagnets it is necessary to build high current ampere-turn windings. For the large-scale applications, the critical current density J_C must generally be greater than 10^4 A/cm^2 and the magnet must operate well in a magnetic field from about 0.2T for a transmission cable to about 4 T for a generator. Fig.1.4 shows how some HTS meet the requirements of the different applications. The performance of the common LTS superconductor NbTi is also shown for comparison.

Research on HTS large-scale applications has mainly focused on the BPSCCO family because it is difficult to grow other systems such as YBCO, Tl-1223, Hg-1223 etc in long length with the current densities required. A number of large-scale prototype devices using BPSCCO wires have shown to work satisfactorily and are listed in Table 1.5.

1.4. The Bi-Based Superconductors

There are three superconducting phases in the BPSCCO system such as (i) $Bi_2Sr_2CuO_6$ (Bi-2201) has a T_C ~ 7 to 20 K[34] (ii) $Bi_2Sr_2CaCu_2O_{8+y}$ (Bi-2212) has a T_C 85 K and (iii) $Bi_2Sr_2Ca_2Cu_3O_{10+y}$ (Bi-2223) has a T_C 110 K[35]. The three phases differ mainly by the

number of Cu-O layers that rest between the Bi-O layers, which cap the unit cell.

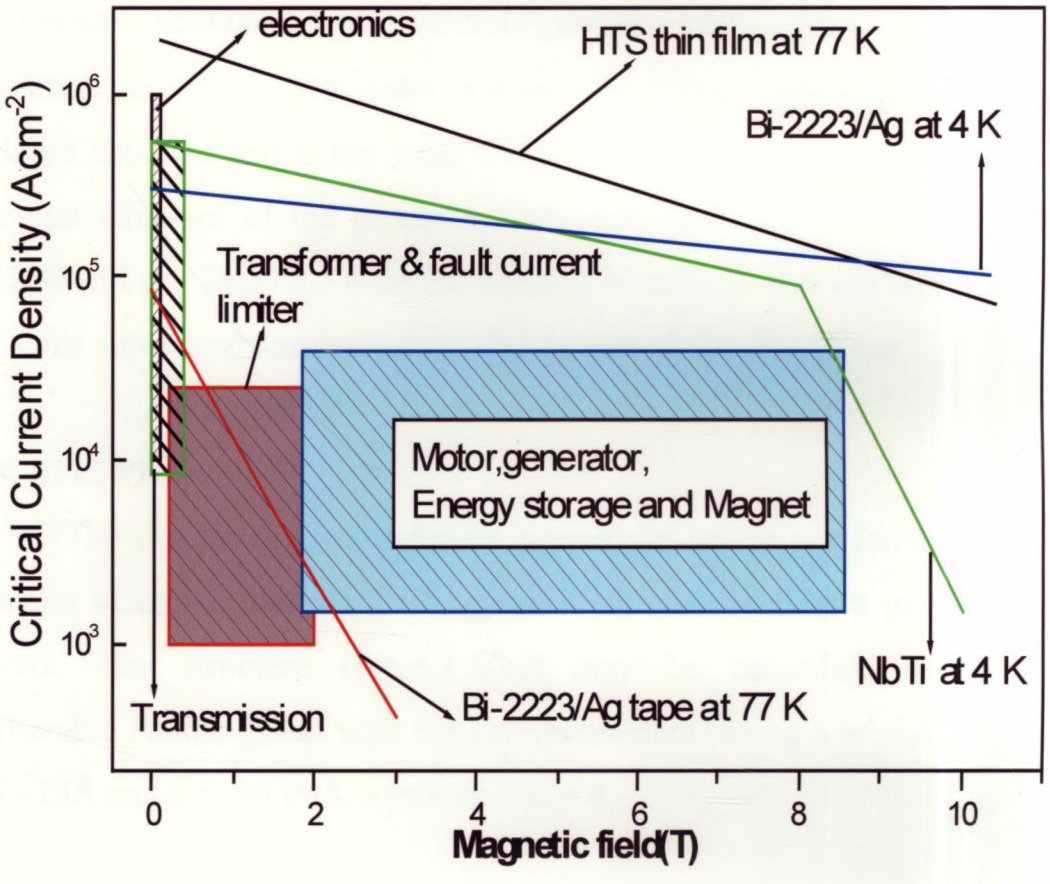

Fig. 1.4. Current and magnetic field demands for large scale applications compared with the performance of existing HTS superconductors. NbTi, a commonly used LTS material is also included for comparison.

1.4.1. Structural Features

(a). Bi-2201 Phase

This is a single layer compound, an apical oxygen atom sits above and below the copper atoms, as in a simple perovskite structure. This system contains two distinct phases with closely related composition in which the solid solution $Bi_{2-x}Sr_{2-y}Cu_1O_{6+\delta}$ shows a modulated structure and is the superconducting phase. Fig. 1.5(a) shows the crystal structure of the phase and the cell parameters a = 5.36Å, b=5.37 Å and c = 24.37Å. Also the number of formula unit per unit cell Z = 4. This superconducting phase is also known as Reveau phase.

(b). Bi-2212 Phase

The double oxygen deficient perovskite layers are formed by two layers of corner sharing CuO_5 pyramid interleaved with a plane of Ca ions. The structure (Fig. 1.5(b)) may be described in the orthorhombic Amma group with the cell parameters being a = 5.414Å, b = 5.428Å and c = 30.99Å, again with Z = 4.

(c). Bi-2223 Phase

In 2223 phase, the triple perovskite layer is formed by one layer of corner sharing CuO_4 square planar groups sandwiched by two layers of corner sharing CuO_5 pyramids. Two planes of Ca ions are interleaved between these layers. The space group assigned (Fig. 1.5(c)) to this phase is Amma with a = 5.39Å, b = 5.41Å, and c = 37.1Å with Z = 4 .

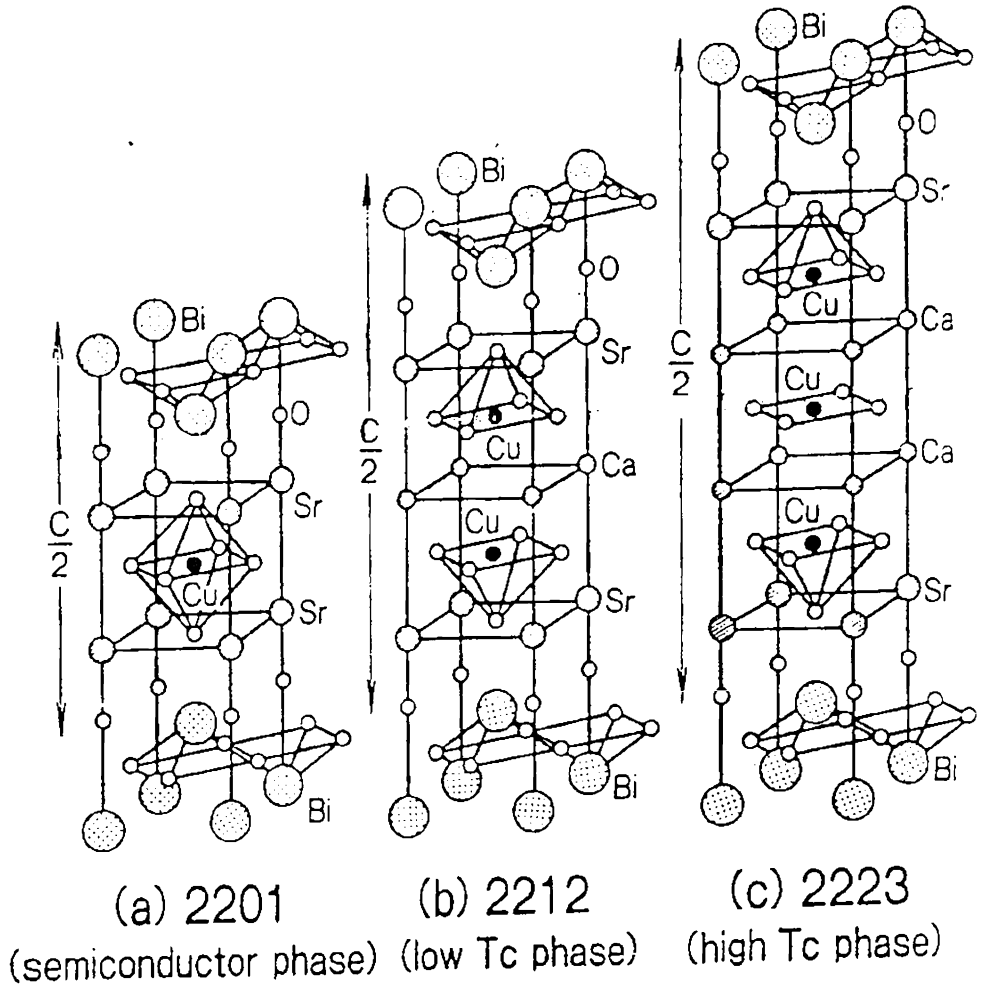

Fig. 1.5. Crystal structure diagram of (a). $Bi_2Sr_2CuO_6$, (b).$Bi_2Sr_2CaCu_2O_8$ and (c). $Bi_2Sr_2Ca_2Cu_3O_{10}$

All the three members of Bi series seem to show modulated structures. [36-37] As the modulated structures are difficult to study by conventional x-ray and neutron diffraction, electron microscopy has been employed and many possibilities like excess oxygen in the Bi_2O_2 layers, Sr atom deficiencies, atomic substitution (e.g. Bi for Cu) etc. have been forwarded as the source of structural modulation. Another

convincing argument has been the incommensurability between the Bi-O layer and the perovskite layer. This mismatch introduces co-operative atom displacements or extra oxygen in Bi-O layers.[38]

An important aspect of the structures has been the double layer of BiO characteristics to all three phases. The separation of 3.25 Å between the BiO layer is supposed to occur due to $6s^2$ lone pair of Bi^{3+} ions. [39] This weak bonding leads to unit cell splitting in to charge neutral sections and easy cleavage between the BiO layers.[40]

1.4.2. Importance of Lead and Liquid Phase Formation

It was discovered by Sunshine et al.[41] that the partial substitution of Bi by Pb enhances the formation and stability of Bi-2223 phase. Pb addition also lowers and broadens the partial melting temperature and facilitates the growth of 2223 phase.

Liquid phase is important for the formation of 2223 phase. However, it must be properly converted into 2223 in order to maximise the 2223 fraction and J_C. Uzumaki et al.[42] proposed that the formation of liquid phase is from the melting of Ca_2PbO_4 at ~ 822 ^{0}C in air and found that Ca_2PbO_4 and 2201 formed below 750 ^{0}C in air. They also suggested that 2223 is formed by a reaction between 2212 and Ca^{2+} in the liquid formed by melting of 2201 and Ca_2PbO_4. Liquid with lowest formation temperature (825 ^{0}C in air) was formed from a reaction between 2201 and Ca_2PbO_4 as proposed by Ikeda et al.[43] They stated that this liquid wetted both 2201 and 2212, but not 2223 plate-lets and this liquid converts 2212 to Pb-2212 and that Pb-2212 reacts with $(Ca,Sr)_2CuO_3$ and other liquid composition to from 2223. Several other researchers have also reported similar findings.[44-49]

1.4.3. Reaction Mechanism and Stability of 2223 Phase

(a). Mechanism of Formation of the 2223 Phase

The structural similarities of the three Bi-based compounds suggests the phase intergrowth of 2212 from 2201, and of 2223 from 2212 through an intercalation-diffusion of Ca and Cu atoms over a short distance. However there are conflicting reports in the literature regarding the mechanism of 2223 phase formation:

- A disproportionation reaction of the 2212 phase to form the 2223 and 2201 phases.[50-51]
- A 2223 precipitation from a partially molten phase.[52]
- A dissolution – precipitation process where the 2223 phase is formed from both the 2212 phase, from the decomposition of Ca_2PbO_4.[45]
- A formation of Bi/Pb – rich mobile liquid droplets which migrate over growing platelets.[47]
- A two- dimensional growth with decreasing nucleation rate. A liquid phase generated in the powder reacts with the 2212 matrix via Ca, Cu, and Pb ions diffusion, resulting in the nucleation of the 2223 phase, which spreads into the 2212 matrix but the outline of the original crystal shape remains.[53-57]
- An one-dimensional diffusion controlled nucleation and growth process with edge dislocations via the rapid intercalation of the CuO_2/ Ca Bi-layers into the CuO_2/ Ca/ CuO_2 blocks of 2212.[58-59]

The common point between these different models is the 2212 phase functioning as a precursor for the formation of the 2223 phase. Most of the works described above analyse the kinetics of the 2223 phase formation using the Avrami (1)[53-55] or the Johnson – Mehl-Avrami equation (2).[56-57]

$$C(t) = 1\text{-}\exp(-Kt^n) \quad (1)$$

$$C(t) = 1\text{-}\exp(-(Kt)^n). \quad (2)$$

Where C is the phase fraction after soak time t, n is the reaction order and $K = Ae^{-E/RT}$ is the Arrhenius rate constant.

(b). Stability of the 2223 Phase.

Among the Bi- based systems Bi-2223 is the stable phase with highest critical temperature. The preparation of a high fraction of 2223 phase is a very elaborate procedure and understanding the mechanism of formation has been the subject several studies. The annealing temperature was found to be very critical and a variation of $> \pm 1\text{-}3^0C$ from the optimum is undesirable. This is because 2223 formation is very slow and this phase is stable only within a very narrow temperature range.[60-61] Treating samples at temperatures outside this small optimum range resulted in increased concentrations of other low-T_C phases, as well as appearance of undesirable secondary phases.[62] The optimum temperature reported in the literature are quite different because they also depend on many other parameters, such as the nominal stoichiometry of the initial powder, particle characteristics , annealing atmosphere etc. Even though most of the reported work on 2223 has been done in air, there have been numerous studies that examined the effect of processing atmosphere on the formation of 2223.

1.5. Processing Methods of HTS

In order to put high-T_C superconductors into practical use high critical current density is the primary requirement. For fabricating high J_C conductors ordinary pressureless sintering may not be useful because of its inability to induce grain connectivity and grain alignment. Therefore, methods such as uniaxial as well as cold/hot isostatic pressing /rolling have been tried with better results. However, a significant improvement in this regard has come from the identification of melt texturing process. [63-64] In this process the material is taken above its peritectic temperature and cooled fast to the recrystallization temperature and then cooled slowly in a gradient furnace to assure the long columnar grains longitudinally.

Even though, melt texturing is a good method to produce monoliths, e.g. Current leads; parallel developments have been continued for finding out viable processes for making flexible wires/cables. The various methods towards this end have been, [65-69]

- Slurry extrusion of wires/tapes from polymer blends of HTSC powder
- Surface coating of HTSC on metal cores
- Melt-spinning of ribbons of HTSC
- Zone-melting of wires
- Oxide Powder-In- Tube Technique
- Metallic Powder-In- Tube Technique
- Ion beam deposition on tape surfaces
- Electrophortic deposition

There are mainly five HTS compounds identified as candidate for exploitation in conductors; they are YBCO, Tl-1223, Bi-2223, Bi-2212 and MgB_2. But the reaction and phase formation aspects of these superconductors are different and thus the choice of appropriate fabrication process are different for different materials. The criterion of choosing a particular process (and compound) then rest on the results obtained by experimenting with many (material, process) pairs. The oxide powder in tube approach has failed completely in the case of YBCO; no combination of mechanical working, wire drawing, rolling or pressing, has succeeded in producing texture in this material. Textured YBCO is produced by thin film deposition on a suitably textured substrate. Very limited texture has been achieved in Tl-1223 by powder in tube combined with rolling and partial melting. [70] Bi-2223 as well as MgB_2 conductors are being prepared by the powder in tube method; involving complicated schedules of wire drawing, roll flattening, pressing and annealing. Bi- 2212 can be textured with little difficulty, due to the magnitude of its anisotropy. The substrate, a silver or silver alloy tape, is coated either by dipping in a slurry or by electrophortic deposition from a suitable suspension and the tape conductors are fabricated by continuous partial melting of the coated substrate.[71] However its extreme anisotropy results in very weak flux pinning, related to the formation of "pancake vortices" [72], at liquid nitrogen temperature.

1.6. Powder-In-Tube Technique for Bi-Based Superconductor

After the discovery of Bi-based high temperature superconductor enormous efforts have been undertaken to improve their critical current

density (J_C). These efforts were hampered by the granular structure of the material. Even though the grains had a large J_C, the bulk material suitable for common use had disappointingly low J_C. The reason for this low J_C is due to poor current carrying capability of the links between the grains. A major step forward in obtaining better links was achieved with the introduction of silver- sheathed Bi-based superconductors.[73-76] These materials can be drawn and rolled into long flexible wires/ tapes which make them convenient for the use in practical applications. The advantage is that the ductility of the sheath metal makes mechanical working possible and thereby enabling grain alignment, while heat treatments in the final stage sinters ceramic grains into a wholesome core. Such a metal clad geometry is desirable for HTS wires/ tapes because the sheath not only protects the core form environmental corrosion and mechanical abrasion but also enhance the cryostability during operation.

1.7. Considerations in the PIT Technique for Tape Fabrication

1.7.1. Choice of Precursor Powder

Phase assemblage of the precursor powder is a critical factor, which determines the final tape performance. In order to achieve high transport J_C it is essential to maximise the crystallographic orientation of (Bi,Pb)-2223 plate-lets with their ab plane $\|$ to the rolling direction . This necessitates the use of the partially reacted precursor powder, which consists of mostly 2212 and secondary phases, and leads to a higher values of J_C than the fully reacted 2223 powder[77] . The liquid phases formed at heat treatment temperatures lead to better connection

of the 2223 grains and heal the cracks formed during the mechanical deformation process and thus increase the J_C values.[78] The amount of liquid phase depends on the phase content of the precursor powder.

1.7.2. Choice of Sheath Metal

For the fabrication of BPSCCO superconducting tapes silver is found to be the most appropriate sheath metal due to its high electrical and thermal conductivity. Other properties, which isolate silver as the option, include its non-poisonous nature and compatibility at the processing temperature. Silver sheath may even play a role in aligning the grains of Bi-2223 during formation process. In addition Ag sheath is permeable to oxygen during processing at elevated temperatures and it also helps 2223-phase formation by reducing the evaporation of lead from the powder. Luo et al [79] have shown that Ag cladding effectively prevent the evaporation loss of Pb under typical heat treatment conditions.

1.7.3. Powder Packing Density

The starting packing density of the powder into the silver tube is an important parameter in determining the critical current density and core density of the final tape. It also plays an important role in determining the final Ag:SC ratio of the composite tape. Several authors have reported that maximum BPSCCO powder density that can be achieved through wire drawing and/or rolling is about 75%. [80-81] The need to densify beyond this low green packing density is one of the reasons why tapes must be deformed between the heat treatments.

1.7.4. Thermomechanical Processing

A process of mechanical deformation (rolling or pressing) combined with subsequent heat treatment cycle is required to obtain tapes with high J_C. It is believed that deformation steps are necessary to develop the alignment of the plate-like 2223 grains. The grain alignment is considered to be one of the major contributing factors to increase the transport current density. Deformation steps also increase the density of the core, thus increasing its connectivity. Both effects correlate to an increased critical current density. An additional benefit of the deformation steps is that they break up the sintered grains and bring the reactants into more intimate contact, facilitating greater conversion of the precursor powder to 2223. [82] For these reasons deformation is a beneficial step in the fabrication of high performance 2223 tapes. However, if the deformation is not optimised it may result in oxide core cracking which cannot be healed during the subsequent sintering. [82-84] The active cross section of the core is then reduced, resulting in a decrease in the conductor J_C. The final heat treatment has a dual purpose: first to convert the remaining precursor phase into 2223, and second to use the residual eutectic liquid to heal deformation damage, as discussed by Parrell et al.[85]

1.8. Critical Current Density of Bi- 2223/Ag Tape

Although J_C is the single most important parameter to be maximised for applications, one of the main problem on the way to better conductors is the insufficient understanding of mechanism

limiting J_C. The critical current density can be defined as $J_C = I_C/A$ where I is the transport critical current density and A is the whole cross sectional area of superconductor. The fundamental limit of critical current density is determined by the depairing current density, $J_d = H_C/\lambda$, (the maximum supercurrent density circulating near the vortex cores) where H_C is the critical field and λ the penetration depth.[86] Unfortunately BSCCO-2223 is strongly anisotropic, leading to a strong suppression of the value of depairing current density (1-3 x 10^7 at 77 K) for practical use. Thus overall critical transport current density in a superconductor for practical application is determined by whichever is the lesser of the intragrain or the intergrain current densities. Flux pinning controls the intragrain current density and the intergrain current density is controlled by the grain-to-grain connectivity. The latter also depends on the porosity, cracks and other inhomogeneity in the microstructure.

1.8.1. Flux Pinning in Bi-2223

Flux pinning is determined by spatial perturbations of the free energy of the vortex lines due to local interactions of their normal cores and screening currents with microstructural imperfections.[87] The main obstacle for HTS conductor is that their current carrying capacity deteriorates rapidly with increasing temperature and magnetic field. The J_C vanishes at the irreversibility field H^* (T), which is far below H_{C2} (T) at 77 K and this suppression of H^* (T) at higher temperature is due to the layered structure of HTSs, which greatly facilitates depinning of stacks of weakly coupled pancake vortices by thermal fluctuations. [88-89] For $H < H^*$ (T), vortex fluctuation cause thermally activated creep of

magnetic flux [90] producing measurable dissipation well below J_C defined at $1\mu Vcm^{-1}$. Anisotropy strongly enhances the effect of thermal vortex fluctuations, [91] thus suppressing H^* and enhancing flux creep in Bi-2223 much more than in YBCO. Both H^* and J_C can be significantly improved by irradiation, which creates effective columnar pinning tracks.[107] For e.g. neutron irradiation of U-doped Bi-2223 tapes fissions the U and produces heavy –ion tracks that raise H^* (77 K) to over 1 T, while also reducing the anisotropy of J_C. [92]

1.8.2. Grain Boundaries

Grain boundaries are strong barriers to current flow in HTS conductors and the critical current density J_b across the grain boundary drop exponentially, $J_b=J_0 \exp(-\theta / \theta_c)$ as a function of the misorientation angle θ between the neighbouring crystallites, [93-96] where θ_c depends on intergrain J_C. The *micaceous* nature of grains of Bi-2223 phase cause delamination and misorientation among the adjacent grains under mechanical working. Grain boundaries can be differentiated as *basal* and *nonbasal* and the former consist of both a-axis tilt boundary and c-axis twist boundary. That is, when the grain boundaries become basal plane faced, there appears a quasi-ohmic dissipation at low voltages that we interpret as being the signature of c-axis current flow, which is both more dissipative and qualitatively different (e.g. it does not have a definable H^*) from a plane flow seen in [001] and [100] tilt grain boundaries. Thus the basal plane boundaries are important for J_C studies. This extreme sensitivity to misorientation, coupled with the intrinsic anisotropy of the HTS compounds, dictates the need to texture conductors into the tape forms so as to shift the grain boundary

misorientation distribution to as small a value of θ as possible. For Bi-2223, rolling deformation used to make the tape produces a marked uniaxial, c-axis texture.

1.8.3. Current Percolation in Bi-2223

All HTS conductors are brittle, making cracks and are prone to porosity. The net result is that current percolates through a polycrystalline network containing many obstructions, some of which partially block the current while others result in a total block. [97] Thus the local fraction of current carrying cross-section is less than unity and the magnitude of J_C defined by I_C /A can be much less than the flux pinning limit. Magneto-optical imaging is an effective method of visualising non-uniformities of current flow in polycrystalline conductor forms.[98-99]

In Bi-2223 tape, these non- uniformities caused mainly by quasiperiodic fluctuations of the superconductor thickness and residual rolling damage. [97] In addition, there is a tendency for the highest- J_C regions to be located at the Ag-superconductor interface. Such a local variability is because BPSCCO is a six component system and it is hard to control the phase conversion reaction of Bi-2212 and other constituents to Bi-2223. Even though earlier reports [98,75-76] suggested that high J_C regions were confined mainly to the Ag/interface regions, better processing can produce much more uniform J_C distribution across Bi-2223/Ag tapes.

1.8.4. The Need for Texture

The difficulty with the high temperature superconductors is that factors other than flux pinning have a strong, even controlling, influence on their ability to sustain a transport current. Structurally the mixed oxide superconductors are tetragonal, or near tetragonal, with a, b lattice parameters lying in the range 0.535-0.545 nm, and c-axis parameter 3-12 times greater. This structural anisotropy leads to anisotropy in the physical properties of the compounds. In single crystals the critical current densities in the ab plane is many times greater than that in the c direction, normal to the ab plane. In addition, the superconducting coherence length, ξ, is very small in these compounds, of similar magnitude to that of the lattice parameter, and hence to that of the region of crystallographic disturbance in the boundary between two grains. The material needs to be textured so that the c-axis of the grains is close to being normal to the direction of current flow, and that the ab planes of the grains are in near parallelism to one another. Thus thermomechanical processing should be designed in such a way as to improve the c- axis alignment.

1.9. Bi-2223 Coated Conductor

PIT tape should have high level of J_C and J_E (engineering current desity) for the successful utilization as practical conductor. The critical issues for the enhancement of conductor performance include c-axis alignment of the Bi-2223 grains, the existence of an impurity channel in the centre of the filaments, filament uniformity, fill factor of the HTS, high cost of the silver sheath. A coated conductor approach was initiated

at ORNL to investigate these issues and as a potential alternative technique to fabricate better, cheaper and stronger superconducting conductors.

In this method a thin layer of Bi-2223 is deposited onto a low cost high strength flexible metallic substrate, with the inclusion of a silver (Ag) cap-layer to prevent lead loss. In this coated conductor approach, a variety of substrate materials, from polycrystalline Ag foil to biaxially textured RABiTS^{TM} (Rolling Assisted Biaxialy textured substrate) substrates, may be employed. Bi-2223 precursor can be deposited by various techniques such as spray pyrolysis and dip coating, whereas Ag cap layer can be deposited by thermal evaporation and sputtering etc. Multilayered Bi-2223 coated conductors can also fabricated using these methods. But the extension of this coated conductor into long length with proper thermo mechanical treatment schedule has to be developed.

1.10. Importance of Mechanical Strength of the Tape

The Bi-2223/Ag composite tapes consist of brittle BPSCCO fibres and a soft, ductile metal matrix. They may be subjected to strains resulting from different thermal contractions of the tape's elements, from tension and bending during the winding and finally from electromagnetic forces acting in the coils. Therefore several authors have tried to study the influence of the mechanical strain (mainly bending and tension) on the transport properties of Bi -2223/Ag. [100-106] Existing studies show that during bending or tensile tests, the critical current decrease is rather small, upto so-called irreversible strain. A further increase of the load beyond this level leads to a rapid decrease of the critical current, due to the damage of the superconducting core and

current flow path. The level of the irreversible strain vary with the filament number, [103,107] Ag content in the oxide core, [108] and the sheath metal[109-111]

1.11. Role of Silver in Bi-2223 Superconductor

Silver has been used for making BPSCCO superconductor wires, tapes and multifilaments and it has been found to be the only candidate among the noble metals that is non-poisoning to ceramic superconductors. This non-poisoning behaviour is of significant technical importance in the fabrication of Ag-superconductor composites.

There has been many studies on the effect of silver on J_C, T_C, microstructure, I-V characteristics, mechanical properties and flux pinning. However conflicting reports on various aspects have been reported in the literature.[112-116] For e.g. Dou et al [117] found that the detrimental effect of silver in the BPSCCO system can be prevented only by treating the composite specimen in low oxygen partial pressure (0.03-0.07 atm).Their observation was in sharp contrast to that of Jin et al [118], who found silver to be innocuous even when specimen containing 20 wt% silver were sintered and cooled in pure oxygen. Lowering of the bulk zero resistivity temperature and the transport critical current density have also been reported by Tsudo et al [119], when they sintered BPSCCO-Ag powder in air. On the other hand, the attainment of very low resistance contacts was reported by Selim et al [120] when they melted silver on lead stabilized bismuth cuprate samples before the final oxygen treatment which showed that

Ag/Superconductor surface interactions are not detrimental to the properties.

1.11.1. Sintering Temperature.

Addition of Ag results in a lowered partial melting point of the precursor powder and an accelerated 2223 phase formation and these were the common conclusions in most of the work. The effect of Ag on sintering temperature depends on various factors such as form and type of silver addition, heat treatment atmosphere etc and some of them are listed in the table 1.4. It is clear from the table that again the partial melting temperature depends on the form of Ag and the sintering atmosphere.

Table. 1.4. Effect of Ag addition on partial melting temperature of Bi-2223 precursor collected from the literature.

Form of Ag	Amount of Ag	Sintering Atmosphere	Reduction in $T_m^{partial}$ with silver addition	Reference
$AgNO_3$	5-40 wt%	Air	10^0C	121
Ag	5 wt%	7.5%O_2/Ar	15^0C	122
Ag_2O	Upto 3.5 at%	Air	10-15^0C	123
$AgNO_3$	20-80 wt%	Air	15-20^0C	124
Ag	-	Air	10^0C	125
Ag	10 wt%	7.0 %O_2	20^0C	126

Hence the sintering temperature should also depend on them.The actual mechanism for the reduction of melting temperature in Ag added precursor was reported differently by many of them. For e.g. Dou et all [114,127] proposed that addition of Ag causes the formation of Ag-PbO-CuO low melting eutectic liquid, which lowers the melting point of the Ag/2223 system. Also, Parrella at al [128] have shown that mixing a small amount of Ag (~ 1wt%) in the powder helps to distribute the liquid phase uniformly and leads to more homogeneous microstructure. The silver addition was found to accelerate the formation of process of high T_C (2223) phase by lowering the partial melting temperature of the samples.

1.11.2. Grain Alignment and Texture

Ag addition has beneficial effects on grain alignment and texture. An increased alignment of BSCCO grains near the interface between Ag sheath and BSCCO core, compared to the centre of the tape was observed by many of the authors [129-132]. They suggest that the highly aligned grains near the Ag/BPSCCO interface carry more supercurrent than the grains in the centre of the BPSCCO tapes. A smooth interface results in better-textured 2223 in the interface than in the centre and also Ag provides a geometrical constraint on the 2223-grain growth, and this also leads to some texturing.[133-134] Addition of Ag to the BPSCCO core will increase the Ag/BPSCCO interface area. R.Zhou et al [135] found that by adding Ag particles of average particle size 38μm these were stretched into long thin ribbons during rolling and these ribbons not only eliminate the cracking, necking and sausaging of the superconductor core during mechanical deformation, but also provide additional

Ag/superconductor interfaces to help superconductor phase formation and grain alignment.

1.11.3. Mechanical Strength

The addition of Ag to the BPSCCO core substantially increases the strain tolerance of the BSCCO tapes also. J.P Singh et al [136] developed a BPSCCO –Ag composite tapes, in which 90% of the initial J_C was retained for a 1.2 % applied strain, compared to only 40% in the pure BPSCCO tape. Miller et al[137] and Li et al[138] used Ag additions to BSCCO-2212 powder or silver coated microfilament 2212 additions; subsequent processing produced Ag- sheathed superconductor tapes with improved strain tolerance. Similarly Ekin et al [139] studied the same for 20 wt% Ag added 2223 tapes and found that the strain tolerance has improved over that of 2212 wire. In the same study, similar improvements were also observed for multifilamentary 2223 tapes.

The optimum silver percentage in the core for getting higher phase formation, J_C and strain tolerance is different in most of the cases discussed above. In addition, for a given content of Ag particles, the interface area will be strongly depending on the nature of particle morphology. Compared to plate-like high T_C (2223) grains silver particles are thicker and irregularly shaped. The undesirable size and shape of silver particles results in high angle grain boundaries between superconductor grains and hence causes a degradation of the tapes J_C values. It is believed that fine and homogeneous powders are required to obtain dense and uniformly sintered bodies because dense, sintered polycrystalline materials with a minimum weak links have good superconducting and mechanical properties. Therefore, an improved

understanding of the effect of Ag addition (content and particle morphology) and thermo mechanical treatment on microstructural development and resulting J_C is needed for the optimised processing of Ag sheathed BPSCCO tapes.

1.12. Importance of Multifilamentary Geometry

Conductors for power applications are multifilamentary wires/ tapes in which many superconducting filaments are embedded in a matrix of a normal metal such as Ag or Ag alloys, which provide protection against magnetic flux jumps and thermal quenching. [140] Such wires must have sufficient strength to withstand the fabrication process, device winding cool-down and electromagnetic stresses and be capable of being made or cabled to sufficient size to carry operating currents from hundred to thousand of amperes. In addition to the above property in multifilamentary (Bi,Pb) –2223 tapes the silver/superconductor interface area is much higher resulting in higher texture and thus J_C.

1.13. Application Prototypes- Current Status

1.13.1. International Scenario

Highly promising results have been obtained in long length Bi-2223/Ag powder-in-tube wires manufactured by ASC (American Superconductor Corperation) and IGC (Intermagnetic General Corperation). A 1180 meter length of BPSCCO /Ag wire with J_C of 12,500 Acm^{-2} along the entire wire length was fabricated by ASC and a J_C of 12,000 Acm^{-2} was produced by IGC in 1260 meter BPSCCO wire.

Besides, a different laboratories and companies are also working together on Bi-based superconducting tapes and the Fig. 1.6 shows the J_C performance versus length for Bi-2223 tapes made by various manufactures around the world. These wires are successfully incorporated into the near term applications such as high capacity cables, compact and powerful magnets and environmentally benign transformers with fault current limiting functionality (Table 1.5).

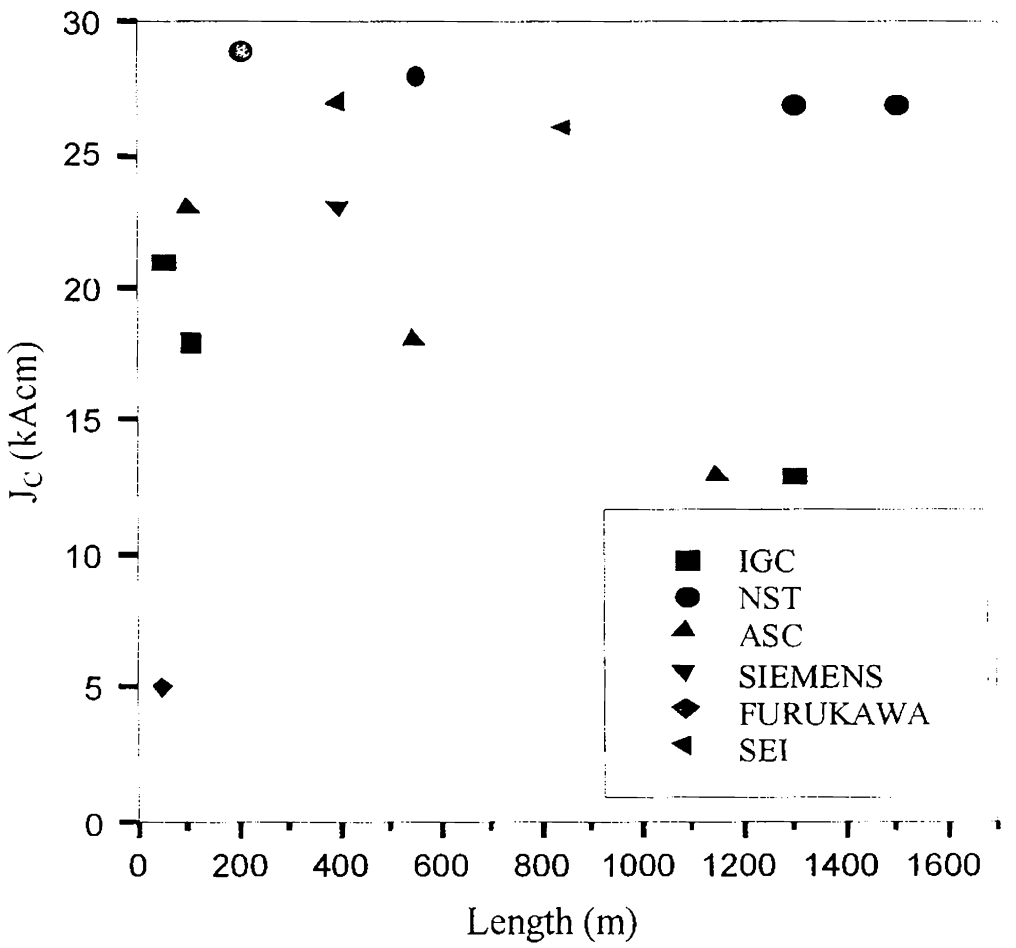

Fig. 1.6 . J_C values verses length for Bi-2223 tapes made by various manufactures.[141]

Coils made with Bi-2223 wires are being realised which generate a field above 0.5 T at 77K and nearly 3.3 T at 4.2 K. A demonstrator levitation system has been constructed which consist of nine double pancake coil. This coil provide 4770 ampere turn, 0,42 T gap induction and a lifting force of 354 N[142] with a current of 5A. Fig. 1.7 describes the recent program in US coil developement

Table 1.5. Shows the overview of present status for a various application prototypes[143-144]

Items	Present Status	Features
Transformer	800kVA	Non-flammable
SMES	100j coil at 77K & 1kj at 35K	2Hz operation
Magnets	3T with 40mm RT bore 4T with 50mm RT bore 7T with 50mm RT bore	Fast cycle operation 4T in 10 seconds 7T in 1minute
Cables	7m & 1kA 3 phase cables 50m & 3kA conductor 50m model 30m, 66kV& 1kA cable	Magnetic shielding structure Machine stranding 66kV voltage evacuation L N_2 cooling system

1.13.2. National Scenario

Research and development on HTS research is still at infancy stage in the country compared to the international scenario eventhough some significant development was made on LTS technology. Melt

textured YBCO with high J_C have been developed by DMRL. A host of new varieties of rare eath based substrate materials for HTS were developed and patented by RRL, TVM[145-150]. Short length of (Bi,Pb)-2223/Ag tapes of J_C (0T, 77 K) ~ 10^4 Acm^{-2} was developed jointly by RRL and BHEL in 1996. Thereafter the intense research efforts by RRL , TVM the J_C has been raised to 30$kAcm^{-2}$ for monofilamentary short length tape and an I_C of above 60 A for multifilamentary tape. The work presented in this thesis is part of HTS wire development program, especially long length multifilamentary (Bi,Pb)-2223/Ag tapes and other technology development being pursued at RRL Trivandrum.

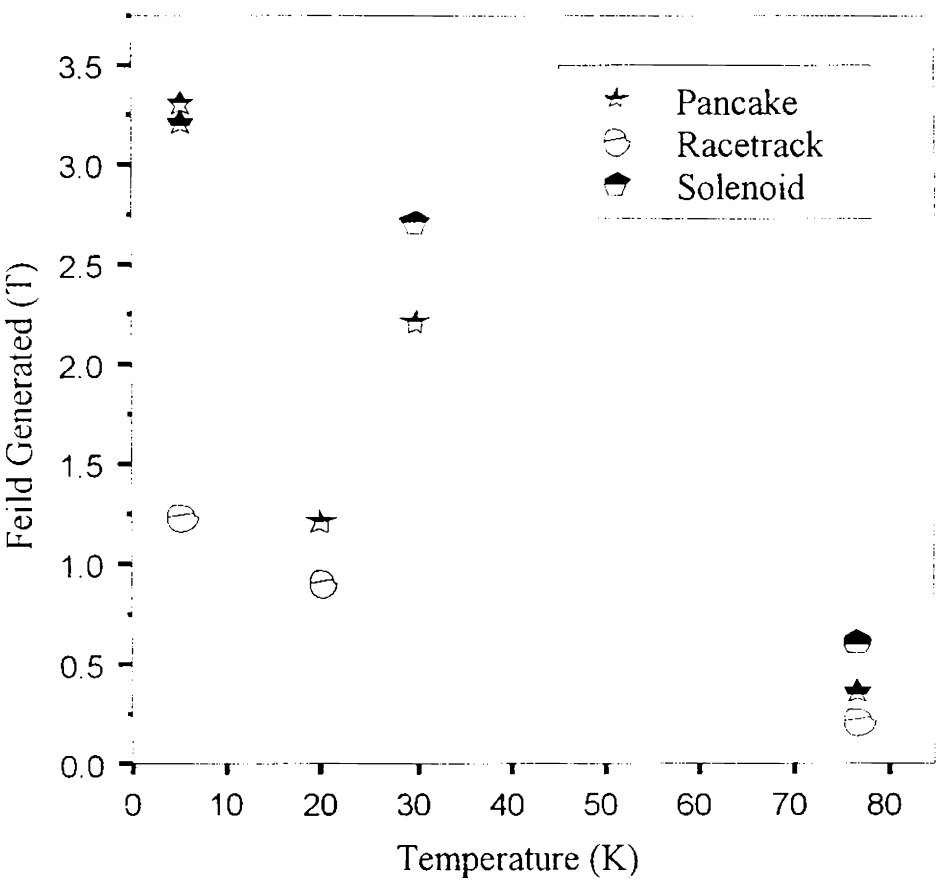

Fig. 1.7. Performance of the HTS coils that have been produced recently by three US companies.[141]

1.14. Scope of the Present Work

The brief overview presented above highlighted the importance of HTSC materials particularly BPSCCO and the need to improve the critical current density and the mechanical properties of the (Bi,Pb)-2223 tapes for the successful utilization of these for application prototypes. Fabrication of long multifilamentary conductors in the form of wires/tapes is an important step towards the exploitation of the application potentials of the Bi-based superconductor. Powder-in-tube technique followed by wire-in-tube technique is found to be suitable for fabrication of long multifilamentary tapes. The present thesis describes fabrication of long multifilamentary tapes with improved mechanical and superconducting properties. The investigations conducted mainly focused on following aspects.

- Finding an optimum particle size distribution for the precursor powder, which can have the best reactivity favouring the Bi-2223 formation.
- Selection/optimization of the suitable form, type and percentage of silver for improving the superconducting as well as mechanical properties of the tape.
- Optimization of geometrical parameters of the multifilamentary tape.
- Processing and characterization of long multifilamentary tape and pancake coils.

Fine and homogeneous precursor powder is an important requirement for the fabrication of Ag/BPSCCO tapes. But too fine a precursor will lead to early melting and formation of undesirable phases, which cannot be recovered on further heat treatment steps. In the present

work we systematically varied the particle size of a sol-gel derived precursor and investigated its effect on the tape characteristics. The results showed that the particle size has a great influence on reaction kinetics, ultimate phase fraction, microstructure and transport property. Relative effect of Ag powder, Ag_2O and $AgNO_3$ was studied by adding them in the precursor powder both in bulk pellets and in tapes. It was found that among these additives $AgNO_3$ was most effective in promoting the Bi-2223 phase formation and J_C. Effect of varying percentage of $AgNO_3$ on strain tolerance as well as tensile strength of mono and multifilamentary tapes showed that these properties improve remarkably as the Ag content in the matrix increases. Another important work done is the introduction of silver in molecular level into the system. The method yielded the best result in terms of phase formation as well as J_C among all forms of Ag addition. 3 wt% Ag addition in molecular level improved the J_C as well as J_C-B characteristics of the tapes. The geometrical parameters of the multifilamentary tapes such as filament number, initial and final wire diameter, final tape thickness etc were optimised with respect to critical current and mechanical strength. Based on the results obtained from the above studies, an optimized process for fabricating long multifilamentary tapes has been worked out and successfully developed multifilamentary Ag/BPSCCO-Ag composite tapes upto a length of 12 m with J_C (0T; 77K) more than 16 $kAcm^{-2}$. The quality of the tapes were further tested and evaluated by making pancake coils following R&W and W&R approaches. W&R is found to be better than R&W for obtaining higher critical current in the coils. The properties of the tapes are found to be at par with or better than those achieved by the leading international groups.

References

[1]. H. Kammarlingh Onnes, *Leiden Commn.* **120b, 122b, 124c** (1911).

[2]. J. R. Gavaler, *App. Phys. Lett.* **23**, 480 (1973)

[3]. J. G. Bednorz and K. A. Muller, *Z. Phys. B* **64**, 189(1986)

[4]. Various Chapters of the book *"Practical Superconducting Materials", Superconductor Materials Science: Metallurgy, Fabrication and Application,* Ed. S. Toner and B.B. Schwwartz (New York, Plenum Press 1981).

[5]. A.W. Sleight, J.K. Gillson and P.E. Bierstedt, *Solid State Commun.* **17**, 27 (1975).

[6]. M.K. Wu, J.R. Ashburn, C.J. Torng, P.H. Hor, R.L. Meng, L. Gao, Z.J. Huang, Y.Q. Wang and C.W. Chu, *Phys. rev. Lett.* **58,** 908 (1987).

[7]. L.F. Mattheiss, E.M. Gyorgy and D.W. Johnson Jr., *Phy. Rev. B* **37**, 3745 (1988).

[8]. R.J. Cava, B. Batlogy, J.J. Krajewski, R. Farrow, L.W. Rupp Jr., A.E. White, K. Short, W.F. Peck and T. Kometani, *Nature* **332**, 814 (1988).

[9]. D. Pelloquin, M. Caldes, A. Maignam, C. Michel, M. Hervien and B. Ravean, *Physica C* **208**, 121 (1993).

[10]. R. Cywinski, Z.P. Han, R. Berwoly, R. Cubitt, M.T. Whlie, E.M. Forgan, S.L. Lee, M. Warden, S.H. Kilarnjne, *Physica C* **233,** 273 (1994).

[11]. Z. Iqbal, R.H. Banyhman , B.L. Ramakrishna, S. Khare, N.S. Murthy, H.J. Bornemann and D.E.Morris, *Science* **254**, 826 (1991)

[12]. The Review of MgB2 in SUST.

[13]. C. Park and R.L. Snyder, *J. Am. Ceram. Soc.* **78**(12), 3171. (1995)

[14]. M.G. Aranda, *Adv. Mater.* **6,** 905(1994) and References therein.

[15]. C. P. Bean, *Phys. Rev. Lett.* **8**, 250 (1962)

[16]. Y. Yeshurun and A. P. Malozemoff, Phys. Rev. Lett. **60**, 2202 (1998)

[17]. A. V. Mitin, *Sov. Phys. JETP* **66**, 335 (1987); A. C. Mota, A. Pollini, P. Visani, K. A. Muller, and J.G. Bednorz, *Phys. Scr.* **37**, 823 (1988); A. Pollini A. C. Mota, , P. Visani, G. Juri, and J. J. M. France, *Physica B* **165&166,** 365 (1990); A. C. Mota, G. Juri, P. Visani, A. Pollini, T. Teruzzi, K. Aupke, and B. Hilti, *Physica C* **185-189**, 343 (1991); S. Uji, H. Aoki, S. Takebayashi, M. Tanaka, and H. Hashimoto, *Physica C* **207**, 112 (1993)

[18]. K. A. Muller, M. Takashige, and J.G. Bednorz, *Phys, Rev. Lett.* **58**, 1143 (1987)

[19]. D. R. Nelson, Phys. Rev. Lett. **60**, 1973 (1988); E. Brezin et al., Phys. Rev. B. **31**, 7124 (1985); E. H. Brandt, *Phys. Rev. Lett.* **63**, 1106 (1989)

[20]. D. R. Nelson, *Phys. Rev. Lett.* **60**, 1973 (1988)

[21]. D. R. Nelson and V. M. Vinokur *Phys. Rev. Lett.* **68**, 2398 (1992)

[22]. P. M. Anderson, *Science* **235 ,** 1196 (1987)

[23]. S.H. Pan, E.W. Hudson, K.M. Lang, H. Eisaki, S. Uehida and J.C. Davis, *Nature* **403,** 746(2000)

[24]. C. Hilbert and J. Clarke, *J. Low Temp. Phys.* **61**, 263 (1985)

[25]. M. A. Tarasov, G. V. Prokopenko, V. P. Koshelets, I. L. Lapytskaya, and L. V. Filippenko, *IEEE Trans. Appl.*

Supercond. **5**, 3226 (1995)

[26]. M. Muck, M-O. Andre, and J. Clarke, *Appl. Phys. Lett.* **72**, 2885 (1998)

[27]. A. V. Rylyakov, D. F. Schneider, and A. Yu. Polyakov, *IEEE Trans. Appl. Supercond.* **9**, 3623 (1999)

[28]. A. V. Rylyakov, *IEEE Trans. Appl. Supercond.* **7**, 2709(1997)

[29]. A. V. Rylyakov and S. V. Pololonsky, *IEEE Trans. Appl. Supercond.* **8**, 14(1998)

[30]. P. Komarek, Supercond. Sci. Technol.**13**, 456 (2000)

[31]. S. I. Yoo, T. Higuchi, N. Sakai, H. Fujimoto, and M. Murakami, *Mater. Sci. Eng.* B **53**, 203 (1998)

[32]. T. Kato et al, Proc. 15th Int. Conf. On Magnet Technology ed L. Lin, G. Shen and L. Yan (Science Press) 793 (1998)

[33]. F. Steinmeyer et al, *Adv. Cryogen. Eng.* 1999

[34]. C. Michel, M. Hervieu, M. M. Borel, A. Grandin, F. Deslandes, J. Provost and B. Raveau, Z.Phys. B.: *Condens. Matter* **68,** 421 (1987)

[35]. H. Maeda, Y. Tanaka, M. Fukutomi and T. Asano, *Jpn. J. Appl. Phys.* **27**, L209 (1988)

[36]. M. Onoda, A. Yamamoto, E. T. Muromacha and S. Takekawa, *Jpn. J. Appl. Phys.* **27**, L833 (1988)

[37]. T. M. Shaw, S. A. Shivashankara, S. J. Laplaca, J. J. Guonn, T. R. McGuire, R. A. Roy, K. H. Kelleber and D. S. Yee, *Phys. Rev. B* **37**, 9856 (1988)

[38]. H. W. Zandergen, W. A. Groen, A. Smit and G. van Tendeloo, *Physica C* **168**, 426 (1990)

[39]. O. Eibl, *Physica C* **168**, 215 (1990)

[40]. S. A. Sunshine, T. Siegrist, L. F. Schneemeyer, D. W. Murphy,

R. J. Cava, B. Batlogg, R. B. van Dover, R. M. Fleming, S. H. Glarum, S. Nakahara, R. Farrow, J. J. Krajewski, S. M. Zahurak, J. V. Waszczak, J. H. Marshall, P. Marsh, L. W. Rupp, Jr. and W. F. Peck, *Phys. Rev.B.* **38**, 893 (1988)

[41]. T. Uzumaki, Y. Yamanaka, N. Kamehara and K. Niwa, *Jpn. J. Appl. Phys.* **28**, L75 (1989)

[42]. Y. Ikeda, H. Ito, S. Shimomura, Z. Hiroi, M. Takano, Y. Bando, J. Takada, K. Oda, H. Kilaguchi, Y. Miura, Y. Takada, and T. Takada, *Physica C* **190**, 18 (1991)

[43]. S. S. Oh and K. Osamura, *Supercond. Sci. Technol.* **4**, 239 (1991)

[44]. W. Wong-Ng, C. K. Chiang, S. W. Freiman, L. P. Cook, and M. D. Hill, *Am. Ceram. Soc. Bull.* **71**, 1261 (1992)

[45]. Y. L. Chen, and R. Stevens, *J. Am. Ceram. Soc.* **75**, 1150 (1992)

[46]. Y. Yamada, B. Obst, and R. Flukiger, *Supercond. Sci. Technol.* **4**, 165 (1991)

[47]. P. E. D. Morgan, J. D. Piche, and R. M. Housley, *Physica C* **191**, 179 (1992)

[48]. H. K. Lee, K. Park, and D. H. Ha, *J. Appl. Phys.* **70**, 2764 (1991)

[49]. G. M. Zorn, R. Homung, H. E. Gobel, B. Seebacher, H. W. Neumuller, and G. Tomandl, *Supercond. Sci. Technol.* **8**, 234 (1995)

[50]. H. Nobumasa, K. Shimizu, Y. Kitano, andT. Kawai, *Jpn. J. Appl. Phys.* **27**, L846 (1988)

[51]. N. Kijima, H. Endo, J. Tsuchiya, A. Sumiyama, M. Mizuno, and Y. Oguri, *Jpn. J. Appl. Phys.* **27**, L1852 (1988)

[52]. T. Hatano, K. Aota, S. Ikeda, K. Nakamura, and K. Ogawa, *Jpn. J. Appl. Phys.* **27**, L2055 (1988)

[53]. J. S. Luo, W. Merchant, V. A. Maroni, D. M. Gruen, B. S. Tani, W. L. Carter, and G. N. Riley Jr. *Appl. Supercond.* **1-1/2** , 101 (1993)

[54]. Y. C. Guo, H.K. Liu and S. X. Dou, *Physica C* **235-240** , 1231 (1994)

[55]. Y. S. Sung, E. E. Hellstrom, , *J. Am. Ceram. Soc.* **78**, 2003 (1995)

[56]. W. Zhu and P. S. Nicholson, *J. Mater.Res.* **7-1**, 38 (1992)

[57]. I. Matsubara, R. Funahashi, T. Ogura, H. Yamashita, Y. Ozawa, K. Tanizoe and T. Kawai, *Physica C* **218**, 181 (1994)

[58]. W. Bian, Z. Yimei, Y. L. Wang, and M. Suenaga, *Physica C* **248**, 229 (1995)

[59]. Z. X. Cai, Y. Zhu, D. O. Welch, *Phys. Rev. B.* **52/17** 13035(1995)

[60]. A. Oota, J. Iwaya, P. Songsak, T. Saigou and M. Funakura, *Physica C* **214**, 9 (1992)

[61]. Y. Yamada, B. Oberst and R. Flukiger *Supercond. Sci. Technol.* **4**, 165 (1991)

[62]. K. Kanal, T. Kamo, and S. Matsuda *Supercond. Sci. Technol.* **4**, 207 (1991)

[63]. S. Jin, T. H. Tiefel, R. C. Sherwood, R. B. van Dover, M. E. Davis,G. W. Kammlott, and R. A. Fastnacht, *Phys. Rev. B* **37,** 7850 (1988)

[64]. K. Salama, V. Selvamanickam, L.Gao and K. Sun, *Appl. Phys. Lett.***54**, 2352 (1989)

[65]. T. Hikata, T. Nichikawa, H. Mukai, K. Sato and M. Hitotsuyanagi, *Jap. J. Appl. Phys.* **28**, 288 (1989)

[66]. M. Yang, M. J. Goringe, C. R. M. Grovenor, R. Jenkins, and H.

Jones, *Supercond. Sci. Technol.* **7**, 378 (1994)

[67]. K.C. Goretta, M. T. Lanagan, J. P. Singh, J. T. Dusek, U. Balachandran, S. E. Dorris and R. B. Poeppel, *Materials & Manufacturing Processes* **4(2),** 163 (1989)

[68]. A. Oota, C. Craven, D. Daly, E. R. Podtburg, J. Schreiber and L. J. Masur, *JOM* **45** (9), 48 (1993)

[69]. Sun- li Huang, David Dew- Hughes, M. Yang, C. Morgan, C. R. M. Grovenor, M. J. Goreinge, R. Jenkins, R. Storey, H. Jones, D. N. Zheng, A. M. Campbell, and D. M. Atill, *Supercond. Sci. Technol.* **8**, 32 (1995)

[70]. J. C. Moore, D. Hyland, C. J. Salter, S. Fox, David Dew-Hughes, C. R. M. Grovenor, (1996) (eds.) by U. Balachandran, P. J. Mc Ginn and J. S. Abell, *High Temperature superconductors: Synthesis, Processing and Large Scale Applications. The Minerals, Metals and Materials Society. Warrendale* pp 311-320

[71]. J. W. Burgoyne, C. G. Morgan, C. J. Eastell, R. J. Storey, David Dew- Hughes, H. Jones, C. R. M. Grovenor, and M. J. Goreinge, (1996) (eds.) by U. Balachandran, P. J. Mc Ginn and J. S. Abell, *High Temperature superconductors: Synthesis, Processing and Large Scale Applications.* The Minerals, Metals and Materials Society, Warrendale pp 167-175.

[72]. J. R. Clem *Phys. Rev.B* **43**, 7837 (1991)

[73]. S. X. Dou, H. K. Liu, J. Wang, M. H. Apperley, C. C. Sorell, S. J. Guo, B. Loberg, and K. E. Easterling, *Physica C* **172**, 63 (1990)

[74]. K. Sato, T. Hikata, and Y. Iwass, *Appl. Phys. Lett.* **57,** 1928 (1990)

[75]. Y. Yamada, B. Oberst, and K. Flukiger,*Supercond. Sci. Technol* **4**, 165 (1991)

[76]. K.Heine, J. Tenbrink, and M. Thioner, *Appl. Phys. Lett.* **55**, 2441 (1989).

[77]. U. Syamaprasad, M. S. Sarma, P. Guruswamy, V. Prakash Kumar, R. Ragini, K. G. K. Warrier, A. D. Damodaran, *Physica C* **297**, 85 (1998)

[78]. Y. L. Chen, R. Stevens, *J. Amer. Ceram. Soc.* **75**, 1150 (1992)

[79]. J. S. Luo, N. Merchant, V. A. Maroni, S. E. Dorris, M. T. Lanagan, and B. S. Tani, *J. Am. Ceram. Soc.* **78**, 2785 (1995)

[80]. M. Karuna, J. A. Parrell, and D. C. Larbalestier, *IEEE Trans. Appl. Supercond.* **5**, 1279 (1995)

[81]. B. Wolf, P. Paufler, M. Schubert, C. Rodig, and K. Fischer, *Supercond. Sci. Technol.* **9**, 589 (1996)

[82]. J. A. Parrell, S. E. Dorris, D. C.Larbalestier, *Advan. Cryogenic Engin.* **40**, 193 (1994)

[83]. P. Kovac, I. Husek, W. Pachla, T. Melisek, V.Kliment, *Supercond. Sci. Technol.* **8**, 341 (1995)

[84]. J. A. Parrell, A. A. Polyanskii, A. E. Pashittski, D. C.Larbalestier *Supercond. Sci. Technol.* **9**, 393 (1996)

[85]. J. A. Parrell, S. E. Dorris, D. C.Larbalestier, *Physica C* **231**, 137 (1994)

[86]. Qiang Li, M. Suenaga, T. Hikata, K. Sato, *Phys. Rev. B*, **46**, 5957 (1992)

[87]. A. M. Campbell, and J. E. Evetts, *Adv. Phys.*, **21**, 194 (1972)

[88]. F. H. Brandt, *Rep. Prog. Phys.* **58**, 1465 (1995)

[89]. G. Blatter, M. V. Feigelman, V. B. Geshkenbein, A. I. Larkin, V. M. Vinokur, *Rev.Mod. Phys.* **66**, 1125 (1991)

[90]. Y.Yeshurun, A. P. Malozemoff, A. Shaulov, *Rev.Mod. Phys.* **68**, 911 (1996)

[91]. L. Civale, *Supercond. Sci. Technol.* **10**, A11 (1997)

[92]. S. Tonies et al. , *Appl. Phys. Lett.* **78**, 3851 (2001)

[93]. H. Hilgenkamp and J. Mannhart, Rev.Mod. Phys. (in press)

[94]. D. Dimos, P. Chaudhari, J. Mannhart, *Phys. Rev. B* **41**, 4038 (1990)

[95]. N. F. Heinig, R. D. Redwing, J. E. Nordman, D. C. Larbalestier, *Phys. Rev. B* **60**, 1409 (1999)

[96]. D. Verebelyi et al. *Appl. Phys. Lett.* **76**, 1755 (2000)

[97]. A. A. Polyanskii, *IEEE Trans. Appl. Supercond.* **11**, 3269 (2001)

[98]. A. E. Pashitski, A. Polyanskii, A. Gurevich, J. A. Parrell, D. C. Larbelestier, *Physica C* **246,** 133 (1995)

[99]. U. Welp, et al., *Appl. Phys. Lett.* **66**, 1270 (1995)

[100]. P. Kovac, L. Kopera, I. Husek and L. Cesnak, *Supercond. Sci. Technol.* **9**, 792 (1996)

[101]. S. Salib, M. Mironova, C. Vipulanandan, and K. Salama, *Supercond. Sci. Technol.* **9**, 1071 (1996)

[102]. B. ten Haken, A. Beuink, H. H. J. ten Kate, *IEEE Trans. Appl. Supercond.* **7**, 2034(1997)

[103]. B. Ullmann, A. Gabler, M. Quilitzand W. Goldacker, *IEEE Trans. Appl. Supercond.* **7**, 2042 (1997)

[104]. B. Ullmann, A. Gabler, M. Quilitzand W. Goldacker, *Applied Superconductivity* (Inst. Phys. Conf. Ser. 158) pp 1259 (1997)

[105]. P. Kovac, I. Husek, and L. Kopera , *Supercond. Sci. Technol.* **10**, 982 (1997)

[106]. P. E. Richens, H. Jones, M. Van Cleemput, and D. P.

Hampshire, *IEEE Trans. Appl. Supercond.* **7**, 1315 (1997)

[107]. S. Salib, A. N. Iyer, C. Vipulanandan, K. Salama, and U. Balachandran, *Appl. Supercond.***6**, 1 (1998)

[108]. A. Sobha, R. P Aloysius, P. Guruswamy, and U. Syamaprasad, *Supercond. Sci. Technol.* **13**, 1 (2000)

[109]. R. P Aloysius, A. Sobha, P. Guruswamy, and U. Syamaprasad, *Supercond. Sci. Technol.* **14**, 1 (2001)

[110]. K. Fisher, T. Fahr, A. Hutten, U. Schlafer, M. Schubert, C. Rodig, and H. P. Trinks, *Supercond. Sci. Technol.* **11**, 995 (1998)

[111]. W. Goldacker, J. Kebler, B. Ullmann, E. Mosang, and M. Rikel, *IEEE Trans. Appl. Supercond.* **5**, 1834 (1995)

[112]. S. X. Dou et al., *Appl. Phys. Lett.* **56**, 493 (1990)

[113]. Y. Ishida, J. Matsuzaki, T. Kizuka, and H. Ichinose, *Physica C*, **190,** 67 (1991)

[114]. A. Oota, T. Horio, K. Ohba, and K. Iwasaki, J. Appl. Phys., **71** , 5997 (1992)

[115]. A. K. Sarker, I. Maartense, and T. L. Peterson, *J. Mater. Res.* **7,** 1672 (1992)

[116]. I. Kusevic, E. Babic, M. Prester, S. X. Dou, H. K. Liu, *Solid State Commun.* **88**, 241 (1993)

[117]. S. X. Dou, K. H. Song, H. K. Liu, C. C. Sorrel, M. H. Apperley, A. J. Gouch, N. Savvides, and D. W. Hensley, *Physica C*, **160,** 533 (1989)

[118]. S. Jin, R. C. Sherwood, T. H. Tiefel, G. W. Kammlott, R. A. Fastnacht, M. E. Davis, and S. M. Zahurak, *Appl. Phys. Lett.* **52**, 1628 (1988)

[119]. H. Tsudo, Y. Miura, K. Tsuchida, and A. Katto, *Ceram. Int.* **17**,

5 (1991)

[120]. R. Selim, R. Caton, A. M. Buoncristiani, C. E. Byvik, R. A. Edahl, Jr. , and S. Wise, *J. Appl. Phys.* **67** , 376 (1990)

[121]. G. V. Rama Rao, K. Swaminathan, O. M. Sreedharan, S. Venkadesan and S. I. Mannan, *J. Mater. Sci.* **33**, 1511 (1998)

[122]. Y. S. Sung, and E. E. Hallstrom, *Physica C* **255,** 266 (1995)

[123]. S. X. Dou, Y. C. Guo, R. K. Wang, M. Lonescu, H. K. Liu, *IEEE Trans. Appl. Supercond.* **5,** 1830 (1995)

[124]. T. Matsushita, A. Suzuki, T. Kishida, M. Okuda, and H. Naito, *Supercond. Sci. Technol.* **7**, 222 (1994)

[125]. Y. C. Guo, H. K. Liu, and S. X. Dou, *J. Mater. Research* **8,** 2181(1993)

[126] M.T. Malachevsky and D. A. Esparza, *Thermochimica Acta* 2424 (1995)

[127] S. X. Dou, H. K. Liu, Y. C. Guo, R. Bhasale, Q. Y. Hu, E. Babic, and I. Kusevic, *Appl. Supercond.* **2**, 191 (1994)

[128]. R. D. Parrella, Y. S. Sung, and E. E. Hallstrom IEEE Trans. Appl. Supercond. **7**, 2042 (1997)

[129] M. Lelental, T. N. Blanton, C. L. Barnes, and H. J. Romanofsky, *Physica C* **193**, 395 (1992)

[130]. J.S. Luo, N. Merchant, V. A. Maroni, G. N. Riley,Jr. and W. L. Carter, *Appl. Phys. Lett.* **63**, 690 (1993)

[131]. Y. Feng, Y. E. High, D. C. Larbalestier, Y. S. Sung, and E. E. Hallstrom, *Appl. Phys. Lett.* **62**, 1553 (1993)

[132]. A. F. Pashitski, A. Polyanskii, A. Gurevich, J. A. Parrell and D. C. Larbalestier, *Physica C* 246, 133 (1995)

[133]. N. Merchant, J.S. Luo, V. A. Maroni, G. N. Riley,Jr. and W. L. Carter, *Appl. Phys. Lett.* **65**, 1039 (1994)

[134]. J. W. Anderson, J. A. Parrell, P. V. P. S. S. Sastry, and D. C. Larbalestier, *IEEE Trans. Appl. Supercond.* 7, 2062 (1997)

[135]. R. Zhou, W. L. Hults, R. J. Sebring, J. F. Bingert, J. Y. Coulter, J. O. Willis, J. L. Smith, *Physica C* **255**, 275 (1995)

[136]. J. P. Singh, J. Joo, N. Vasanthamohan, and R. B. Poeppel, *J. Mater. Res.* **8 (10)**, 2458 (1993)

[137]. T. A. Miller, J. E. Ostenson, Q. Li, L. A. Schwartzkopf, D. K. Finnemore, J. Righi, R. A. Gleixner, and D. Zeigler, *Appl. Phys. Lett.*, **58(19)**, 2159 (1991)

[138]. Q. Li, J. E. Ostenson, and D. K. Finnemore, *J. Appl. Phys.* **70(8)**, 4392 (1991)

[139]. J. W. Ekin, D. K. Finnemore, Q. Li, J. Tenbrink, a nd W. Carter, *Appl. Phys. Lett.* **61(7)**, 17 (1992)

[140]. M. Wilson. *Superconducting Magnets* (Clarendon , Oxford,1983)

[141]. Informations published in the website of various companies and laboratories such as

(i) American Superconductor Corporation (www.amsuper.com);

(ii) Loss Alamos National Laboratory (www.lanl.gov),

(iii) University of Wisconsin Madison (www.asc.wisc.edu)

(iv) Argone National Laboratory (www.anl.gov)

(v) Intermagnetics General Corporation (www.igc.com.)

(vi) Oxford Instruments, UK, (www.oxfordinst.com)

(vii) BICC Cables, UK (www.bicc.com)

(viii) Electric Power Research Institute, USA (www.epri.com)

(ix) Superconductor Week (www.superconductorweek.com)

[142]. P. Goodall, C. MacLeod, A. El Abbar, H. Jones and A. M. Campbell. *Advances in Superconductivity* IX 1393 (1997)

[143]. Y. Aiyama, T. Ageta, *Cryogenics* **41,** 179(2001)

[144]. T. Matsushita, *Supercond. Sci. Technol* **13,** 51(2000)

[145]. J. Koshy, J. Kurian, P.K. Sajith, K.S. Kumar, R. Jose, A.M. John and A.D. Damodaran, ***U.S. Patent*** No. 5741747 dated 21.4.1998.

[146]. J. Koshy, J.K. Thomas, J. Kurian, Y.P. Yadava and A.D. Damodaran ***U.S. Patent*** No. 5856276 dated 5.1.1999.

[147]. J. Koshy, J.K. Thomas, J. Kurian, Y.P. Yadava and A.D. Damodaran ***U.S. Patent*** No. 6040275 dated 21.3.2000.

[148]. J. Koshy, J.K. Thomas, J. Kurian, Y.P. Yadava and A.D. Damodaran ***U.S. Patent*** No. 6121206 dated 19.9.2000.

[149]. J. Koshy, J.K. Thomas, J. Kurian, Y.P. Yadava and A.D. Damodaran ***European Patent*** No. EP 0 679 615 B1 dated 21.7.1999.

[150] J. Koshy, J. Kurian, P.K. Sajith, K.S. Kumar, R. Jose, M.J. Asha and A.D. Damodaran ***European Patent*** Appl. 96308464.5-2208 dated 22.11.1996.

CHAPTER 2

PREPARATION AND CHARECTERIZATION TECHNIQUES

2.1. Introduction

Processing of superconductor, especially high temperature superconductor, the stringent demands on phase purity, high degree of grain alignment, and the brittle nature of the core make it necessary to monitor the process carefully right from the selection of reactants to the final characterization by employing appropriate techniques. In this chapter, a brief description of the various techniques utilised during the tape fabrication and characterization are given.

2.2. Methods of Preparation

2.2.1. Powder Preparation

Ceramic powder can be prepared mainly by two methods (i) conventional ceramic route and (ii) wet chemical route. In the present study, both the methods are followed for the preparation of BPSCCO powder. (i). 'Solid state route' in which Bi_2O_3, PbO, $SrCO_3$, $CaCO_3$ and CuO were mixed in planetary ball mill using agate balls in acetone and (ii) 'acrylate polymer precursor route' in which an aqueous solution of metal nitrates were mixed with acrylic acid and heated. The mixtures obtained through both these techniques were then subjected to

calcinations at 750^0C and then at 800^0C with intermediate grinding in a programmable furnace. Also the furnace employed was having the facility for varying the oxygen partial pressure by controlling the O_2 flow. A dynamic vacuum also was attainable in the reaction chamber by operating a rotary oil pump and the pressure could be adjusted in the range of 760 to 2 mm of Hg by operating the inlet and outlet valves independently. In other words, the processing conditions such as temperature, duration, rate of heating, and oxygen partial pressure could be varied and controlled independently using the specially designed furnace.

2.2.2. Bulk Pellets

Bulk pellets were used for the initial studies on the effect of silver on phase formation, sintering characteristics and superconducting properties of the powders prepared. For this, 0.5 to 0.6 g of silver added calcined powder was pressed in rectangular dies by applying uniaxial pressure of 30 Mpa. The rectangular bar shaped specimens were typically of dimensions 20mm x 4mm x 2 mm.

2.2.3. Monofilament Tapes

Ag sheathed BPSCCO tapes were fabricated using the standard Powder-In-Tube (PIT) technique. For this, the ceramic powders of appropriate phase assemblage and particle size was filled to appropriate packing densities in seamless high purity (99.99%) silver tubes (Pyromet Inc, Pa, USA). Typical tube dimensions were outer diameter (OD)=10 mm, inner diameter (ID) = 8 or 7.5 mm. These powder filled

tubes were closed with silver plugs and sealed mechanically. After a vacuum-annealing (500^0C) step to remove any entrapped moisture the tubes were rolled through a series of grooves using a groove rolling machine to obtain monocore wires of diameter in the range 1.6 to 1.4 mm. The wires thus prepared were then flat rolled into tapes. In the wire stage rolling a diameter reduction up to 10 % per pass was used and in tape rolling stage a thickness reduction upto 5% per pass was used. Also intermediate annealing was performed at 400°C for 15 to 30 min after every six or seven passes to relieve the stress of the work hardened silver sheath. The rolled tapes were cut into convenient lengths after cleaning the surface and subjected to heating on alumina substrates.

2.2.4. Multifilament Tapes

The powder-in-tube (PIT) method followed by wire-in-tube (WIT) method has been widely accepted as the most viable process for making multifilamentary tapes in long length. Flow sheet showing the various stages of processing of multifilamentary Ag/Bi-2223 tapes is shown in Fig. 2.1. Monocore Ag sheathed wires were initially prepared by PIT process as described earlier. The wires thus prepared were cut into pieces and packed into different Ag tubes of OD/ID: 10 mm/8.5 mm. The wire filled tubes were then subjected to a second stage of groove rolling to yield multicore wires of diameters from 2.2 mm to 4.5 mm. These wires were flat rolled using a specially designed flat rolling machine. After cleaning the surface of rolled tapes, short length tapes were subjected to heating on high alumina substrates and long length tapes were heat treated by winding them helically on mullite mandrels.

2.3. Analytical Methods

In the present study, different analytical methods have been adopted for characterizing the samples after various stages of processing. Particle size analysis, differential thermal analysis etc were employed for the characterization of the precursor powder. X-ray diffraction technique was employed for phase analysis as well as kinetics of the reaction. Scanning electron microscopy and optical microscopy were carried out for microstructural analysis of the samples.

2.3.1. Particle Size Analysis

In the present work particle size analysis has been conducted for obtaining information on the effect of particle size distribution of the precursor powder on the reaction kinetics and the superconducting properties of the sample. A Micromeritics sedigraph 5100 particle size analyser was employed to determine the particle size distribution.

2.3.2. X-Ray Diffraction Techniques

In the present study, X-ray Diffraction technique (XRD) [1] was very frequently utilised for identifying the various crystalline phases formed in the reaction mixture, after various stages of heat treatment. Monitoring the phase assemblage is an important step in optimising the reaction conditions such as temperature, duration etc. The x-ray diffraction technique was employed to study phase conversion aspects during the powder processing stages and also the *in situ* conversion of filled powder to the desired high T_C phase in the PIT tape processing.

Apart from phase analysis, the XRD measurements have also been used to assess the kinetics of the reaction.

In a typical experiment, the powder samples were filled in aluminium sample holders. Care was taken to minimise the preferred stacking of crystallites, which is important owing to the basal plane growth exhibited by the grains of (Bi, Pb)-2212 or 2223 phases. The powder filled sample holders were kept at the centre of the vertical goniometer cell of a PW1710 model Philips Automated Power Diffractometer with a coupled θ - 2θ mode of Bragg Bentano geometry. Step or continuous scan could be made from 3^0C onwards in 2θ usually at 0.01 degree/step. For routine scans aimed at detecting phases the scan time took 19 minutes while specific runs to obtain information on structural features took up to one-hour duration. Most of the runs have been done applying 40 kV tube p.d. and 20mA tube current. CuKα radiation (wave length = 1.5418 Å) β- filtered by Ni has been used for all measurements.

In the case of tapes, the powder was taken out by cutting the tape specimens. As the amount of the powder thus obtained was often less it was required to use an appropriate sample holder and the entry slit width was to be reduced for restricting the beam on to the sample area. This caused a decreased overall intensity count, which was compensated by performing slower scans. The phase analysis was done by comparing the patterns with those given in JCPDS (Joint Committee for Powder Diffraction Standards) files as well as recent literature for many new phases.

The phase fraction calculations were based on the relation

$$F_X = I_X / \sum I$$

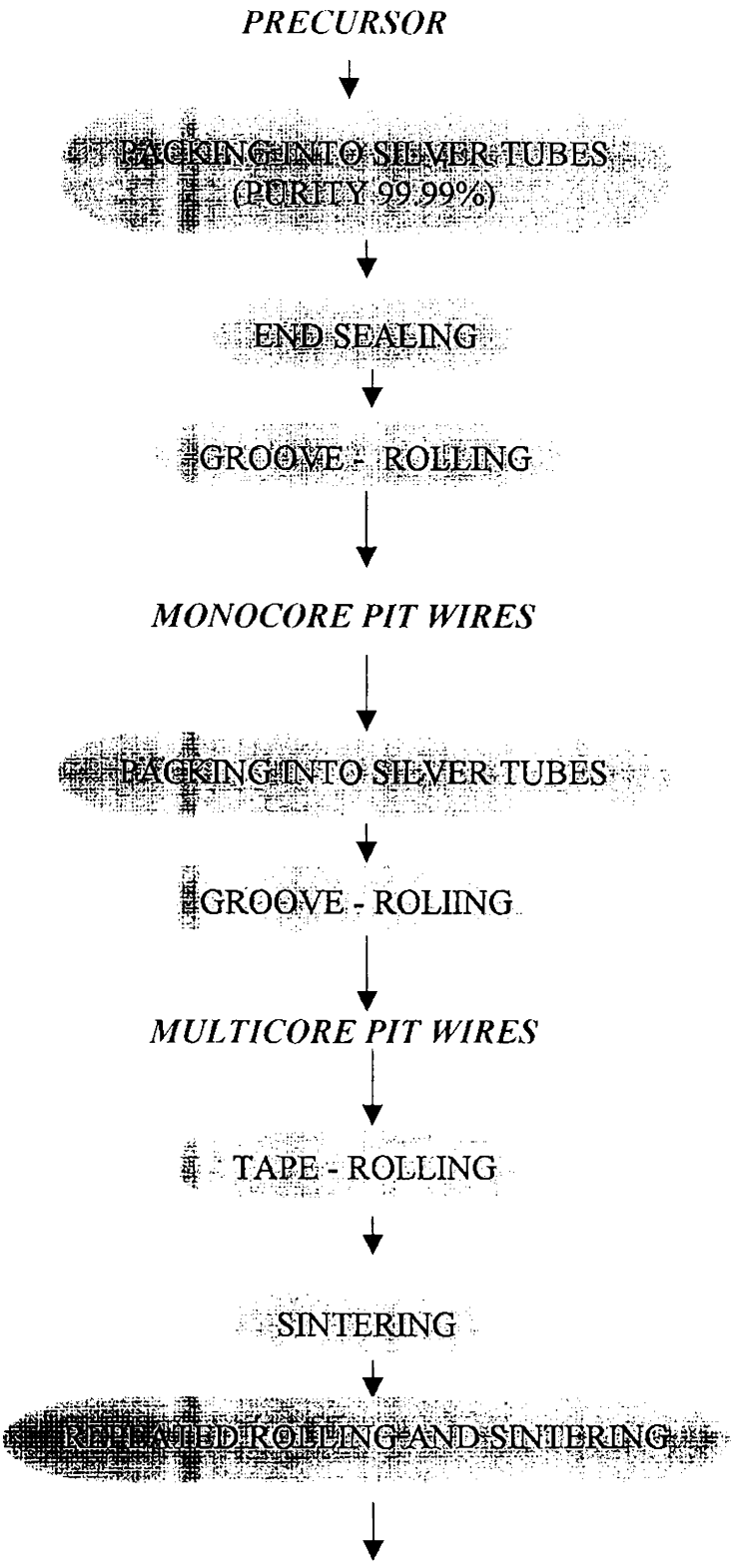

Fig.2.1. Flow sheet for preparation of multifilamentary HTSC tapes by PIT process

Where F_X is the phase fraction of the phase x, I_X is the integrated peak intensity of x and $\sum I$ is the sum of the integrated peak intensities of all the phases present. The integrated peak intensity of a particular phase was measured by selecting a representative peak of the phase from the XRD pattern using appropriate software.

2.3.3. Microstructural Analysis

While XRD is a powerful method to assess the average phase assemblage within the reaction mixture, specific properties like transport J_C are more dependent on the inter- and intra-granular structural details. Grain morphology, orientation, size and size distribution are all-important parameters in gaining an understanding on the process dependence of properties of materials in general. When second phase materials are either desirable in small amounts or are difficult to eliminate completely, often XRD methods fail in detecting them especially when such phases are not constituted by electron dense atoms. On the other hand the distinct morphology, size and reflectivity characteristics of different phases get manifested under microscopic examination thereby aiding not only the identification but also quantification of impurity phases.

2.3.3.1. Scanning Electron Microscopy

In the present study, the Scanning Electron Microscopy (SEM), in the back-scattered mode, has been performed mainly on superconducting core of bulk as well as Ag/ BPSCCO tapes. A JEOL

JSM 5600LV Scanning Electron Microscope was used for this purpose. The operating voltage generally used was 15 kV and the magnification range 500 to 4000. The features sought during SEM examination were (a) difference in grain morphology, suggesting the nature and growth of second phase grains, (b) the size and alignment of grains and (c) the distribution of silver particles and their effect in superconducting core of the tapes as well as bulk samples. Occasionally, SEM has also been used to compare the particle size distribution of the powder obtained through different mechanical deformation. Samples were prepared by fixing fresh fractured core material using silver paste, a thin gold coat was given on the surface using vacuum coating unit.

2.3.3.2. Optical Microscopy

Optical microscope is used for the microstructural examination of the polished section of the heat-treated sample. It is also used to study the morphology of the different sections of the multilayered tapes and to estimate the thickness and area of the superconductor core. Samples were prepared by moulding the sections of the tape using polymers; the surface of the mould along with tape was lapped by using fine emery papers, and subsequently polished using fine alumina suspension and polishing cloths. .

2.3.4. Thermal Analysis

Differential Thermal Analysis (DTA) was adopted for studying the reaction-taking place in the reaction mixture. [2] Supported by XRD phase analysis, these techniques help both in establishing the reaction

path way and in optimising the heat treatment temperature for the formation of a desired phase.

In the present study DTA was employed in determining the effect of particle size distribution and silver on the processing temperature. Shimadzu DTA 50 instrument was used and the DTA plots were taken at a heating rate of 10 ^{0}C min^{-1} in static air atmosphere.

2.4. Superconductivity Measurements

Superconducting state of the samples was characterized by using a number of characterization techniques such as measurement of critical current density with and without the application of external magnetic field and its dependence on bending strain and tensile stress, voltage – current characteristics, ac susceptibility measurements etc.

2.4.1. J_C Measurement

Traditionally two different types of J_C have been defined and studied in superconductivity measurements. The *magnetic* J_C is to be calculated from DC magnetisation of hysterisis measurement at a fixed temperature and slow field sweep. The formula connecting the hysterisis loop opening <M and J_C involves assumption on $J_C(H)$ dependencies collectively known as '*critical state models*'. Also geometry of sample comes into the formula. A more meaningful measurement from application side is the measurement of transport J_C. The measurement technique is the 4-probe method. After getting a V-I plot at the required temperature, a criterion is used for defining the J_C. In the electric field criterion, J_C is defined as the current density, which develops a fixed

value of electric field (usually 1 μV/cm) on the surface of the superconductor.

In the present study, both the sintered bar specimens as well as Ag sheathed tapes were characterized through J_C measurements. A schematic diagram of the set up described is given in Fig.2.2. In the case of bulk pellets, surfaces were freshly prepared by scratching with a razor blade. Four collinear and tiny spots were made along the length of the pellets by applying conductive silver paste. After curing the paste at 400^0C for 30 min, copper wires were connected by soldering. Current leads at the extreme ends were connected to an Aplab (India) constant DC current source (100A, 20V) with GPIB interface. The voltage across the inner leads was measured using a nanovoltmeter (Keithley model 181). In the case of tapes, current leads in the form of silver metal tapes were soldered using Pb:Sn solder and the specimens were fixed on thick substrate with GE paste.

2.4.2. J_C (B) Measurement

Dependence of critical current density on applied magnetic field is a very important characteristic. At low field strengths, the measurements may yield information on weak links. At intermediate field strengths information on intergranular flux pinning and in strong fields information on flux lattice melting can be obtained. In the present study we used a field upto 600 mT and the measurement set-up is shown in Fig. 2.3. The field was produced in a homemade electromagnet and the samples were kept at the centre of the two poles of the electromagnet (Fig. 2.4.). Samples could be easily rotated within the liquid nitrogen so

that the flat plane of the tape is parallel / perpendicular to the axial field of the electromagnets.

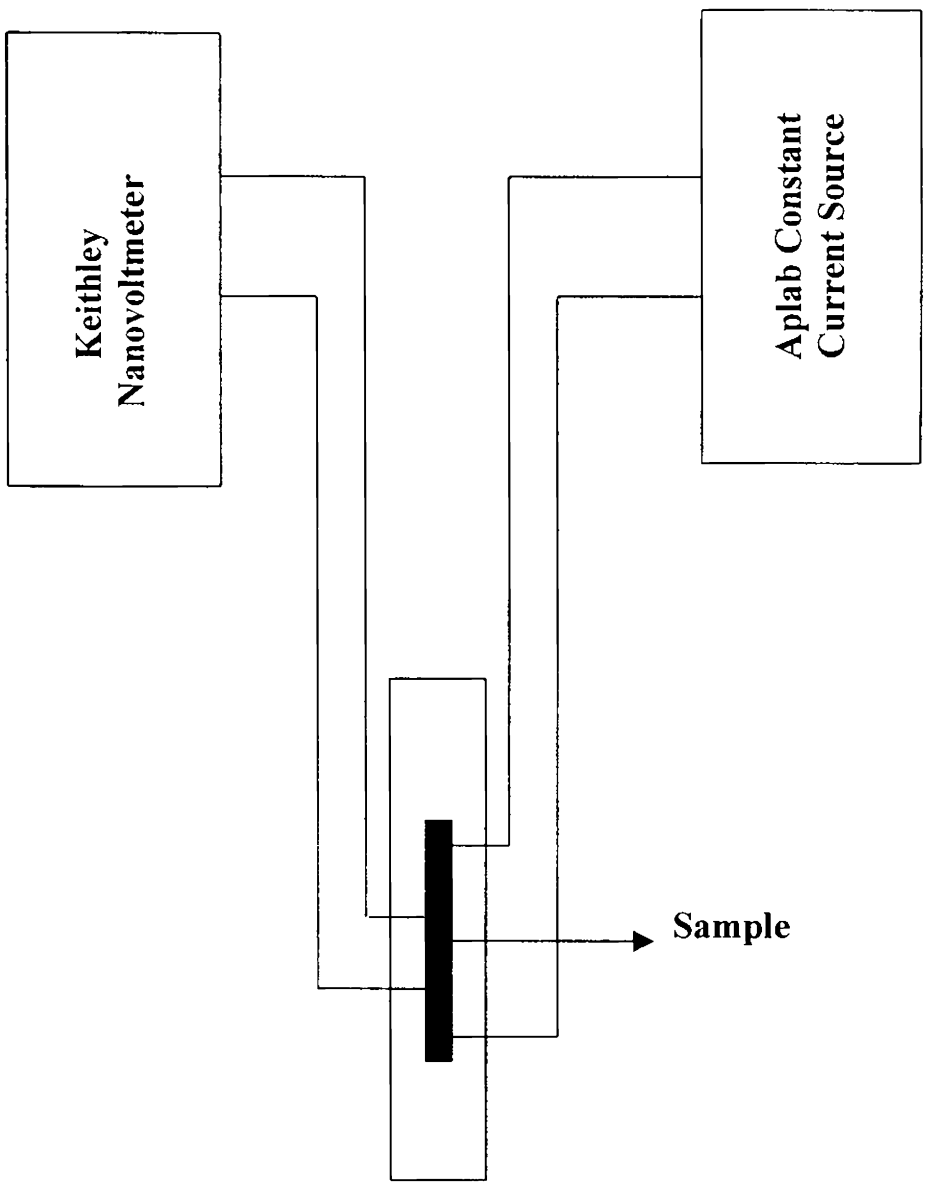

Fig. 2.2. Schematic Diagram showing the four probe connection used for J_C measurements. The samples were immersed in liquid nitrogen and the measurements were taken using appropriate software and are fully automated.

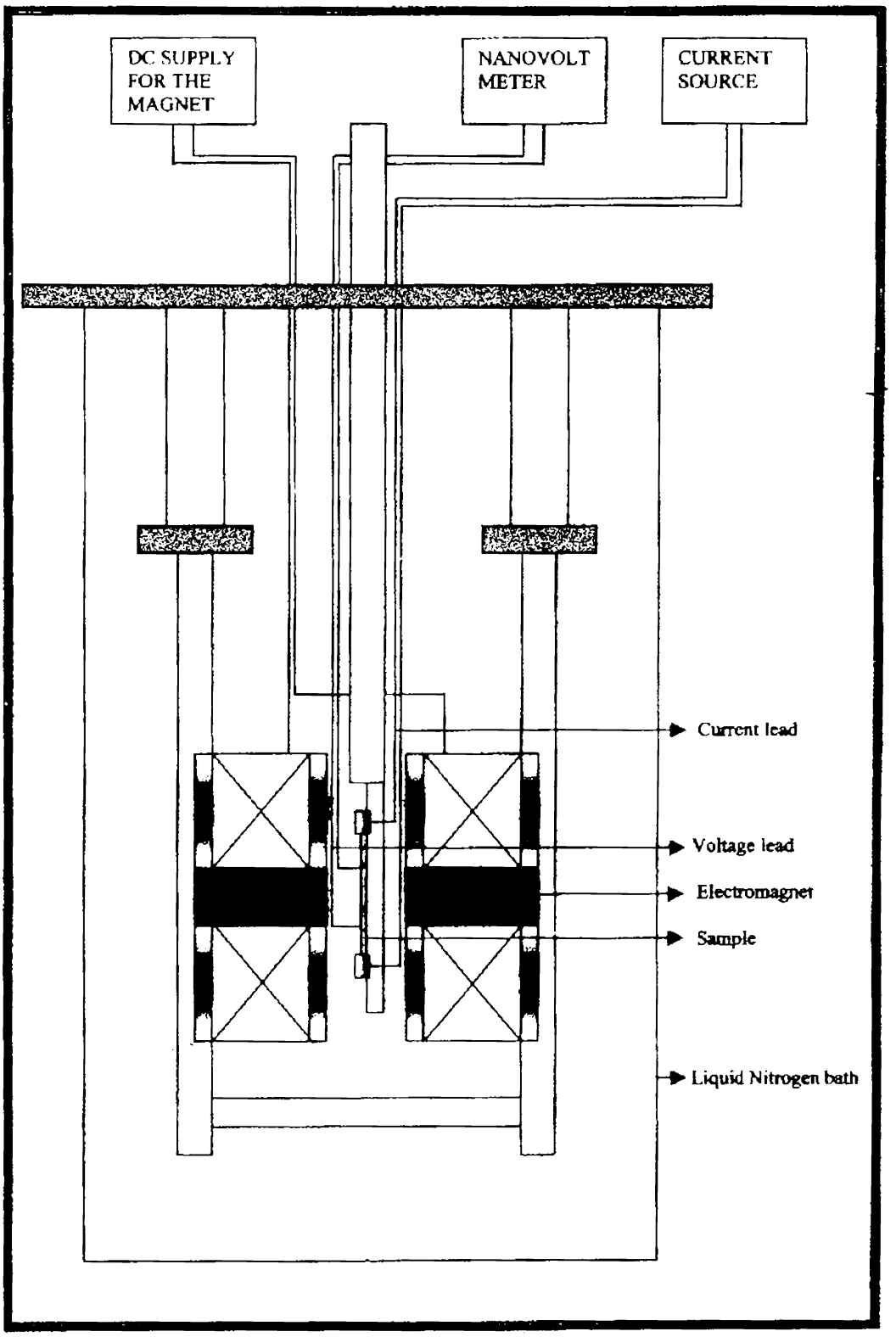

Fig.2.3. Experimental set-up for magnetic field measurements

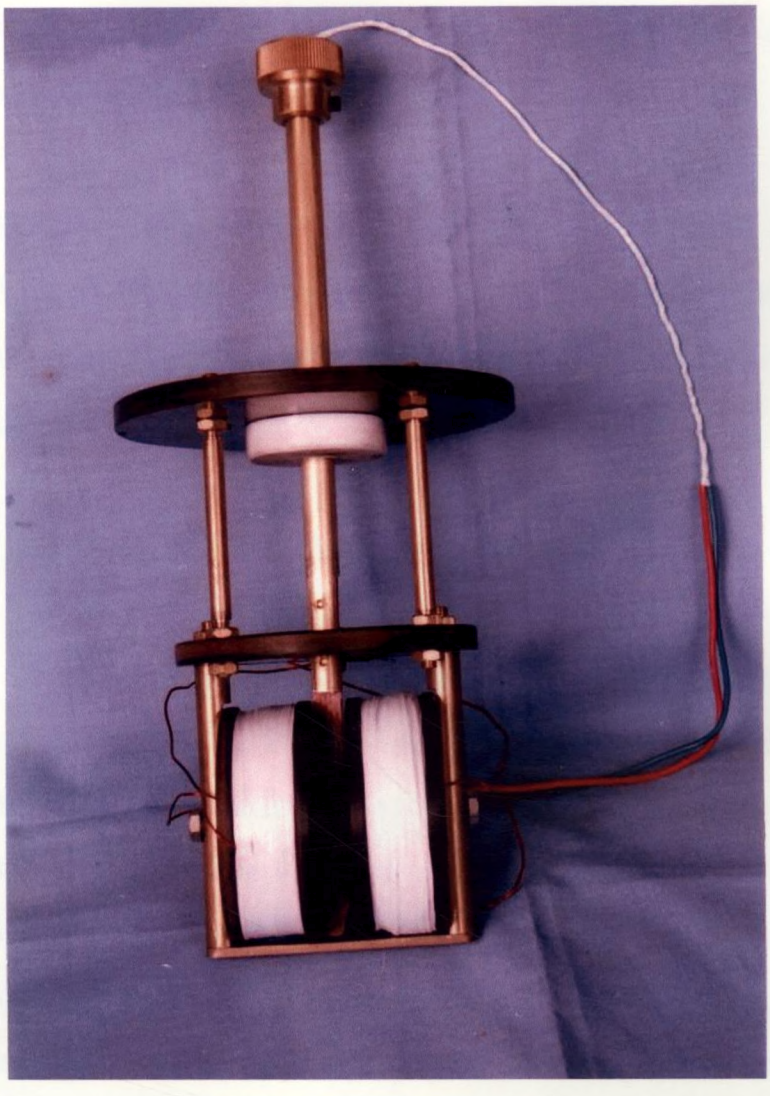

Fig. 2.4. Photograph showing the electromagnet used for magnetic field measurements

2.4.3. Bending Mode Measurements

Strain tolerance of the tape was evaluated by measuring the retained I_C after subjecting the tapes to a predetermined value of bend strain. In the present study, bending mode measurements were performed by bending the tapes on to cylindrical mandrels of predetermined radii at room temperature and measuring the I_C at 77 K by the four probe method using a $1\mu Vcm^{-1}$ criterion. The cycle was

repeated by varying the radius of curvature of the bend. The bend strain was calculated using the relation[3]

$$\varepsilon = t/(2R+t)$$

where **t** is the thickness of the tape and **R** is the radius of curvature. After plotting the variation of J_C/I_C with the percentage of applied strain, we determine the irreversible strain ε_{irr}, the strain level above which J_C/I_C degrades irreversibly.

2.4.4. Tensile Mode Measurements

Similar to the strain tolerance measurement, the tensile stress measurement also is very important. The I_C dependence on the tensile stress (tensile loading) was studied using an in-house-designed set-up with the provision for holding the sample in a vertical mode (Fig.2.5). Suitable guide bushes were provided in the vertical shaft (stainless-steel-rod), from which the stress is transferred to the sample in order to avoid lateral stresses. The samples were soldered to the sample holder (copper blocks) and the current terminals were insulated using teflon blocks. The flexibility of the design is that the I_C measurements can be performed in the on-load condition with the sample in the liquid nitrogen bath.

2.4.5. V-I or E-J Characteristics

The voltage versus current (V-I) or electric field versus current density (E-J) characteristics is an important measurement for superconductor characterization. Many groups have studied the non-linear relationship between V and I in high T_C superconductors in detail using power law dependence,

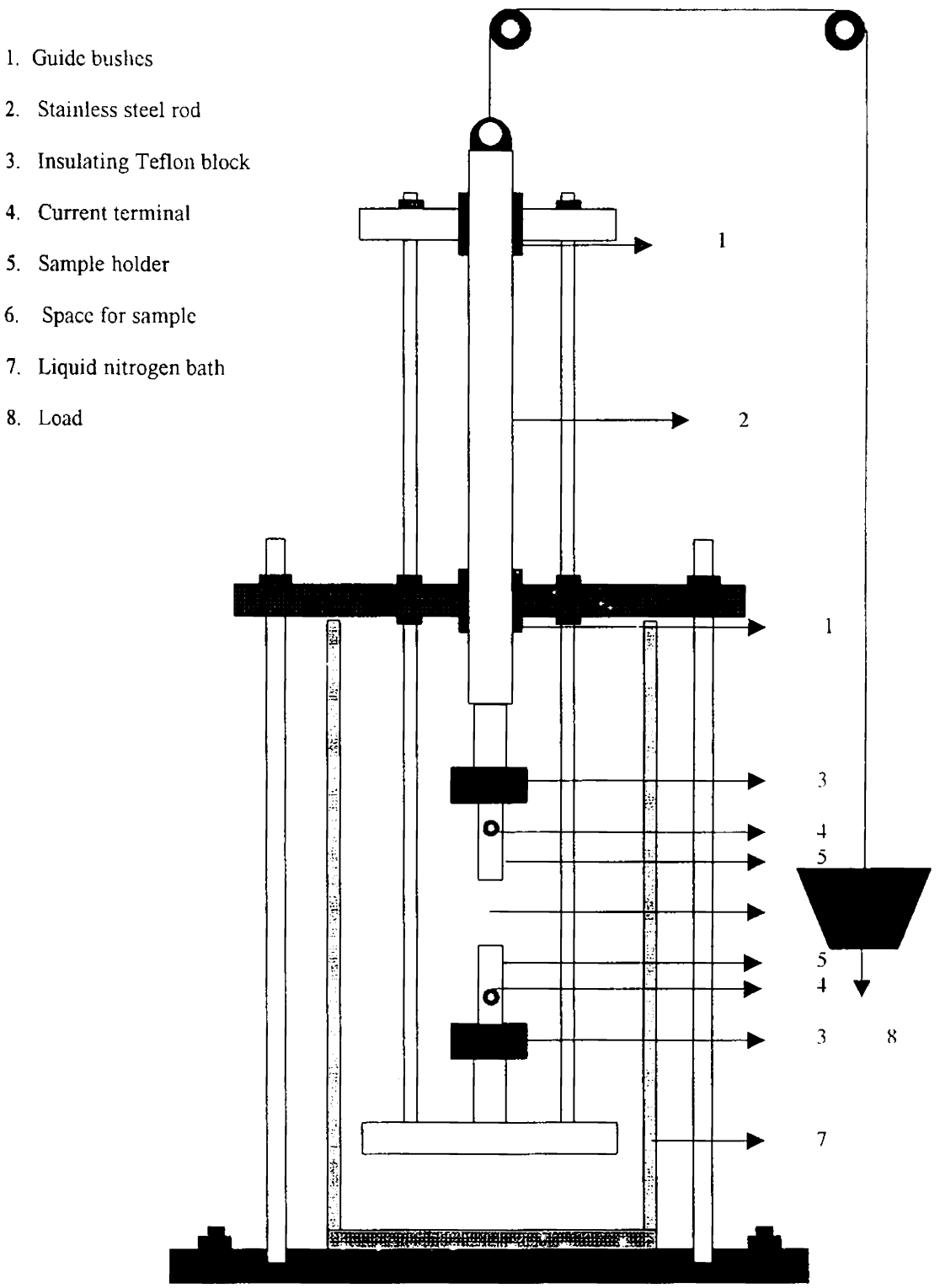

Fig. 2.5. Schematic diagram of the tensile mode measurement

$$V = k I^{\alpha}$$

where **k** is a constant and α is a function of applied magnetic field and temperature.The occurrence of power law behaviour has been ascribed to the collective motion of strongly correlated fluxoids under a large thermal disorder and pinning potential.[4] The strongly pinned conventional superconductors such as NbTi and Nb_3Sn show a nearly power law I-V behaviour with α varying from 15 to 70. [5] For HTSC, α ranges from 30 at 77 K upto 70 at 4.2 K in low magnetic fields.[4,6-8] The higher the value of α, the sharper the take off in the V-I characteristics at the critical current.

2.4.6. AC Susceptibility Measurement

AC susceptibility measurement also is an important magnetic characterization technique used for superconductors. [9] Direct information obtained from this experiment is the diamagnetic transition temperature- the magnetic analogue of resistive transition. The experimental arrangement consists of a primary coil at the centre of which there is a balanced secondary coil pair. The specimen is kept within one of the secondary winding. On the event of superconducting transition the balance is lost and non-zero signal generated.

The secondary coil voltage may be represented as $v = C\chi VfH_{rms}$, where **C** is calibration factor related to the difference of geometry of the coil assembly, **V** the volume of the sample, **f** the frequency of primary current and **H** the field produced by the primary coil. The non-linear interaction of superconductor causes appearance of harmonics of excitation frequency in the secondary. In a 'complex ' susceptibility description, $\chi = \chi' - \chi''$, where χ' is called the real part and χ'' the

imaginary part of susceptibility. With the help of a Lock-In-Amplifier, the two components appearing at the fundamental frequency with a quadrature phase difference may be detected and studied with respect to variation in temperature.

In the present study the set up utilised for susceptibility measurement is as shown in Fig. 2.6. The primary field used was 0.33 Oe and the excitation frequency 28 Hz. The rather low values of field has been employed because other wise information on weak link structure may get lost and the low frequency aided in minimising the eddy current contribution from conducting parts like silver. All the instruments for the above measurements were interfaced through a PC and the data collection was performed using appropriate softwares.

2.5. Conclusions

The major experimental facilities and techniques used for the preparation of various bulk as well as tape samples have been reviewed in the present chapter. Like any other modern ceramic system targeted for controlled properties, a rigid analysis of phase, morphology and reaction kinetics is demanded by the system under investigation. The present study utilised techniques such as particle size analysis, X-ray diffraction, electron microscopy and thermal analysis for studying these fundamental aspects. On the other hand the final product, viz., the superconducting tapes have been characterized by employing J_C, J_C (B), J_C (bend strain), J_C (tensile stress) V-I and ac susceptibility measurements.

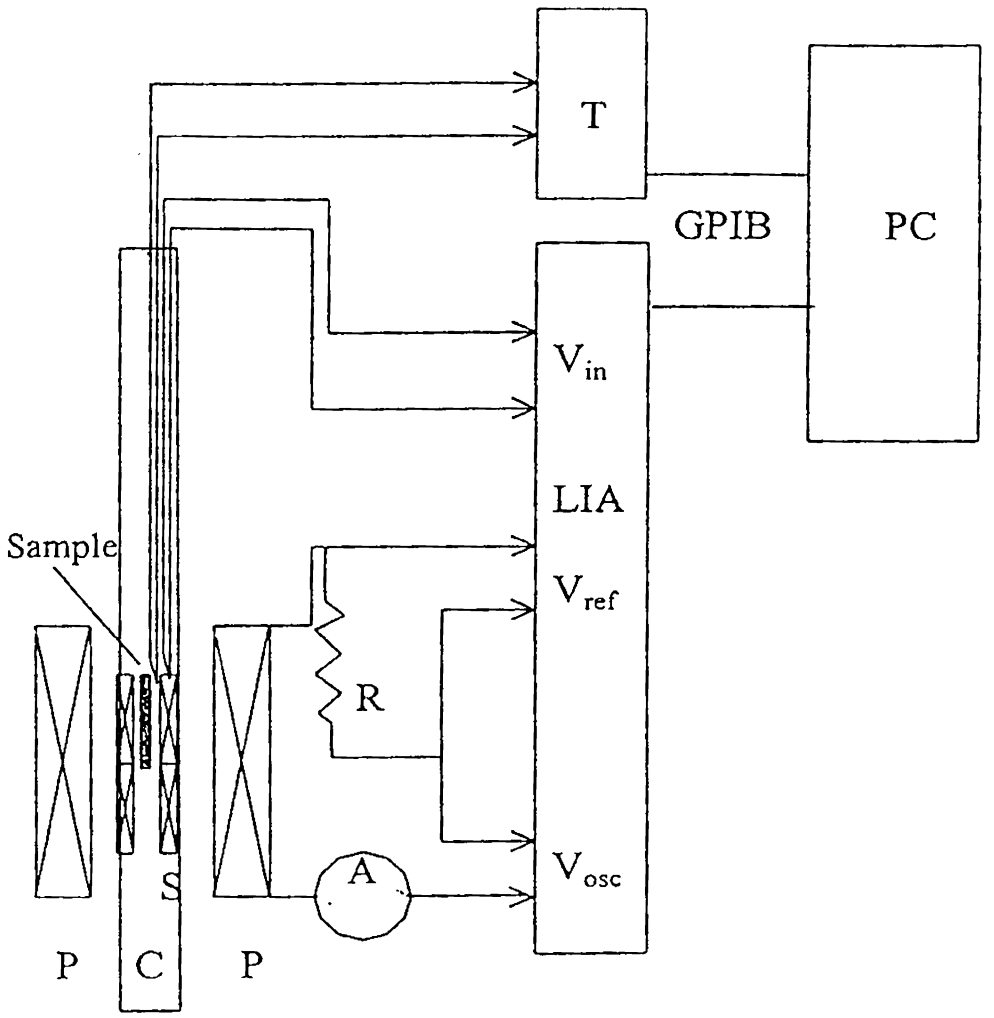

Fig. 2.6. AC Susceptibility measurement setup. Sample kept at the centre of one of the secondary coil pairs (S) and primary (P) is excited with built-in oscillator of the Lock-In-Amplifier, LIA (EG&G PAR 5210 Dual Phase LIA).In phase and quadrature signals as well as sample temperature being sent to PC through GPIB interface. Sample and secondary pairs are with in the low temperature zone of APD cryostat. T: low temperature controller (Scientific Instruments Inc.), A: ac ammete (Prema 6000 DVM), R: standard resistance, PC: 486 based personal computer (HCL-HP)

References

[1]. H. P. Klug and L. E. Alexander, "X-ray Diffraction Procedures", (John Wiley & Sons, New York, 2nd edn. 1974).

[2] W. W. Wendlandt, "Thermal Methods of Analysis", (Interscience Publishers, New York, 1964)

[3]. J. K.F.Yau, N.Savvides, and C.C.Sorrell, *Physica C* **266,** 233 (1996)

[4]. T. Onogi, T. Ichiguchi, and T. Aido, *Solid State Commun.* **69,** 991 (1989)

[5]. E. Evetts, and B. A. Gloacki, *Cryogenics* **28,** 641 (1988)

[6]. M. Ban, T. Ichiguchi and T. Onogi, *Phys. Rev. B* **40,** 4419(1989)

[7]. J.W. Ekin, H.R. Hart Jr. and A.R. Gaddipati, *J. Appl. Phys.* **68,** 2285(1990)

[8]. T. Fukami, T. Yamamoto, T. Nishisaki, Y. Horie, F. Ichikawa, T. Aomine, E. Halguin, and L. Rinderer, *Solid State Commun.* **83,** 605(1992)

[9]. R.B.Goldfarb, and J.V. Minervini, Rev. Sci. Instrum. **55,** 761(1984)

CHAPTER 3

PHASE EVOLUTION, MICROSTRUCTURE AND TRANSPORT PROPERTY OF (Bi, Pb)-2223/Ag TAPES PREPARED USING POWDERS OF VARYING PARTICLE SIZE DISTRIBUTION

3.1. Introduction

The conventional method of preparing ceramic materials by calcination of a reaction mixture prepared through dry or wet grinding of components oxides/carbonates has been replaced by wet chemical routes such as co-precipitation, metal alkoxide methods, freeze drying, sol gel methods etc. In all these methods, metal salts are dissolved in suitable solvents and mixed together so that atomic level mixing is obtained. On controlled removal of solvent, the mixing is retained by avoiding the precipitation of individual salts. The advantages of these methods include

i). Reduction of calcination temperature compared to the powder prepared by conventional ceramic route.
ii). Fine ceramic powder with better homogeneity.

So even though we obtain a fine and homogeneous powder in the beginning by adopting wet chemical methods, superconducting

properties of the tape again depends on the quality of the precursor powder (ie the powder we obtained after the calcination) and is governed by the phase assemblage and particle size distribution of the precursor powder. The effect of particle size distribution of the precursor powder on the superconducting properties of the tape has been under constant investigation over the last years by several authors [1-6] and all of them have a general view that the finer the precursor the more the reactivity is. Also when the particle size decreases the sintering temperature of the tape appears to decrease [2-4] due to the high surface area, large contact area and reduced diffusion distance among small 2212 and non-superconducting phases. But too fine a precursor will lead to early melting and formation of undesired phases, which cannot be recovered, on further heat treatment steps. This means that there must be an optimum particle size distribution for the precursor powder, which can have the best reactivity favouring the Bi-2223 formation with minimum impurity phases and that the tapes with precursors of different particle size have to be heat treated at different temperatures depending on the particle size of the precursors. There is little effort in this direction to study the performance of the tapes sintered at their optimum temperatures.

In the present chapter we systematically varied the particle size of the precursor using a planetary ball mill and investigated the effect of particle size distribution on superconducting properties. The results show that the particle size has a significant effect on reaction kinetics, ultimate phase fraction, microstructure and transport properties[■].

■ Published in Supercond. Sci. Technol. 14, 417 (2001)

3.2. Experimental

3.2.1. Synthesis of the Precursor Powder

A basic precursor with a stoichiometry of $Bi_{1.8}Pb_{0.4}Sr_2Ca_{2.2}Cu_{3.1}O_y$ was prepared by a sol-gel route as described in chapter 2. This was divided into five batches of 10g each and milled in a planetary ball mill for different duration using agate balls in acetone. After grinding for 15 min, 30 min, 60 min, 120 min and 240 min at a uniform speed, the powders were named as 0.25HP, 0.5HP, 1HP, 2HP and 4HP respectively. The phase assemblage and the change in crystallinity of these milled powders were analysed using a powder X-Ray diffractometer (PW1710) with CuKα radiation. SEM images of the precursor powders were observed using JEOL JSM 5600LV and samples for SEM were prepared by finely dispersing the powder in a suitable medium. The particle size distributions of the powders were determined by a particle size analyser (Micromeritics sedigraph 5100). The thermal behaviour of the ground powders were analysed using a differential thermal analyser (Shimadzu DTA 50).

3.2.2. Processing of Tapes

All the five precursor powders were filled into five different Ag tubes of identical dimensions (OD/ID: 10mm/8mm) with a packing density 3g/cc. The tubes were subsequently groove-rolled and then flat rolled down to a final thickness of 130μm and the tapes thus obtained were named as 0.25HT, 0.5HT, 1HT, 2HT, 4HT respectively.

3.2.3. Heat Treatment

The optimum temperatures for heat treatment were determined by a preliminary experiment by heat-treating all the tapes at temperatures from 823 to 837^{0}C with an interval of 2^{0}C (this range of temperature was selected on the basis of DTA). The total duration of heat treatment was 200h. After optimising the temperature, all the 5 batches of samples were heat treated in separate batches at 835^{0}C, 833^{0}C, 831^{0}C, 829^{0}C and 825^{0}C for 0.25HT, 0.5HT, 1HT, 2HT and 4HT respectively with same heat treatment schedule and rolling conditions. The heat treatment was done in a large muffle furnace with a flat temperature profile and with temperature stability and accuracy of ± 0.5^{0}C.

3.2.4. Characterization

The phase evolution of the tape samples during the heat treatment was studied using XRD by peeling off the sheath and grinding the core material taken from the tape. The volume percentage of the different phases were estimated from the integrated peak intensities of the respective phases such as Bi-2223 (2θ=24.05), Bi-2212 (2θ=23.1), Bi-2201 (2θ=29.8), Ca_2PbO_4 (2θ=17.8), CuO (2θ=38.8) and Ca_2CuO_3 (2θ=36.4). The four-probe method with a criterion of 1μV/cm was used to measure the critical current. The I_C dependence on magnetic field upto 3000 Gauss at 77K was studied using a home designed set-up as described in chapter 2.

3.3. Results and Discussion

3.3.1. Precursor Powder Characterization

X-Ray diffraction patterns of the differently ground precursors are shown in Fig. 3.1. It is clear from Fig.3.1 that by the extension of grinding time, the crystallinity of the 2212 and 2201 phases (especially *00l* plane) degrades and sharp peaks in the XRD pattern get broadened.

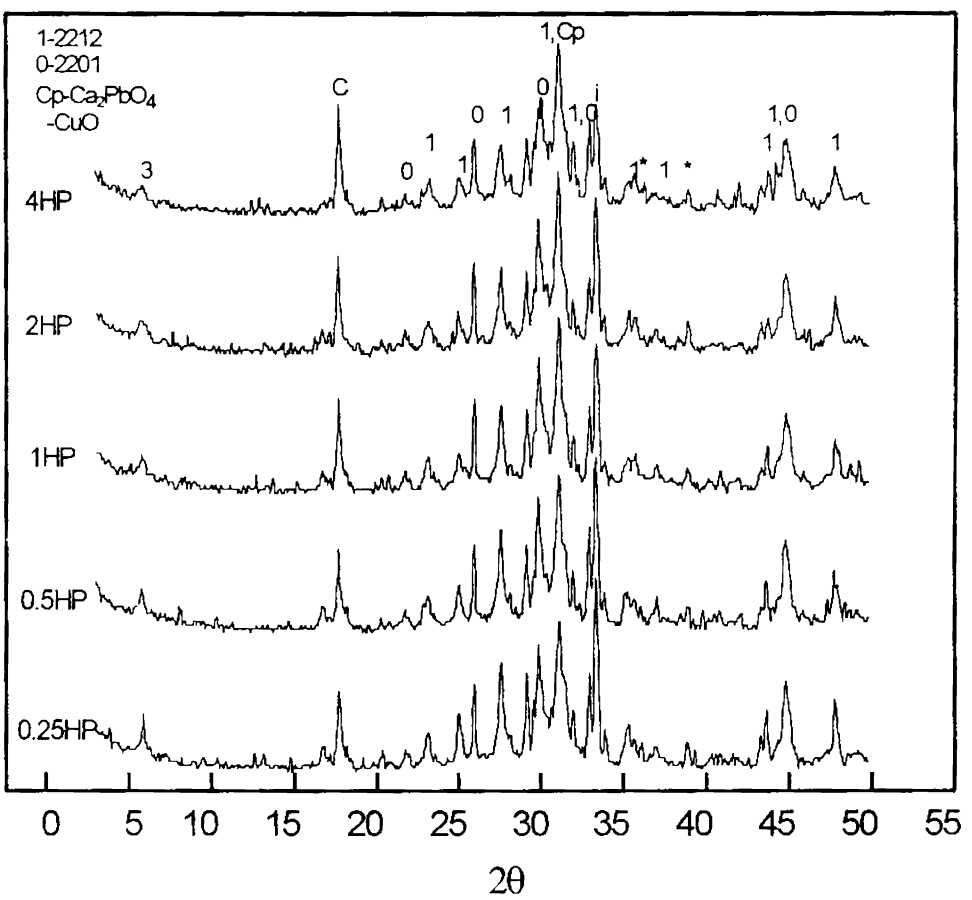

Fig. 3.1. X-Ray diffraction patterns of the precursor powders

The degradation is more prominent for *00l* plane because of the smaller distance between a pair of successive BiO layers compared to the ionic radius of Bi, and the weak vander Waals bond between them. [6-7] It is noteworthy that the crystallinity of Ca_2PbO_4 phase, which is the main ingredient supposed to be responsible for the liquid phase formation [8-9] during the heat treatment and thereby assists the growth of Bi-2223 phase, is not losing by the extension of grinding time.

3.3.2. Particle Size Distribution

Fig. 3.2 shows a typical graph showing the particle size distribution of the powder 0.25HP obtained from the particle size analyser. The particle size distribution of the precursors is given in Table.3.1 which gives the diameter of the particles in three weight fractions viz. 90%, 50% and 20% denoted by D90, D50 and D20 respectively. The average particle size is taken as D50. The average particle size of the precursors 0.25HP, 0.5HP, 1HP, 2HP and 4HP are found to be 6.5, 5.1, 3.2, 2.5 and 1.8μm respectively. SEM micrographs of the powders are shown in Fig.3.3.

3.3.3. Optimization of Sintering Temperature of the Tapes with Different Precursors.

Fig.3.4 shows the DTA plots of the different precursors. The DTA plots have been taken at a heating rate of 10^0C/min in static air atmosphere. The two endotherms visible in all the five precursors

Table 3.1. Particle size distribution for the precursor powders.

Powder	D90(μm)	D50(μm)	D20(μm)
0.25HP	11.7	6.5	2.5
0.5HP	9.8	5.1	1.8
1HP	8.1	3.2	1
2HP	6.4	2.5	0.8
4HP	4.2	1.8	0.7

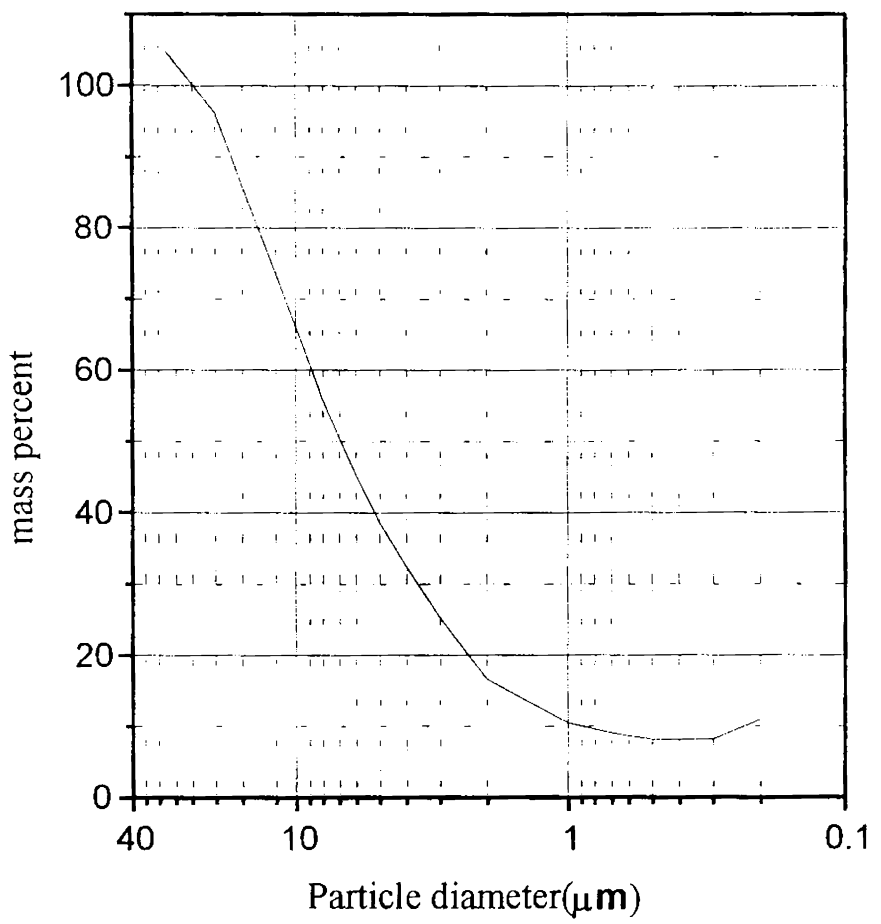

Fig. 3.2. A typical graph showing the particle size distribution.

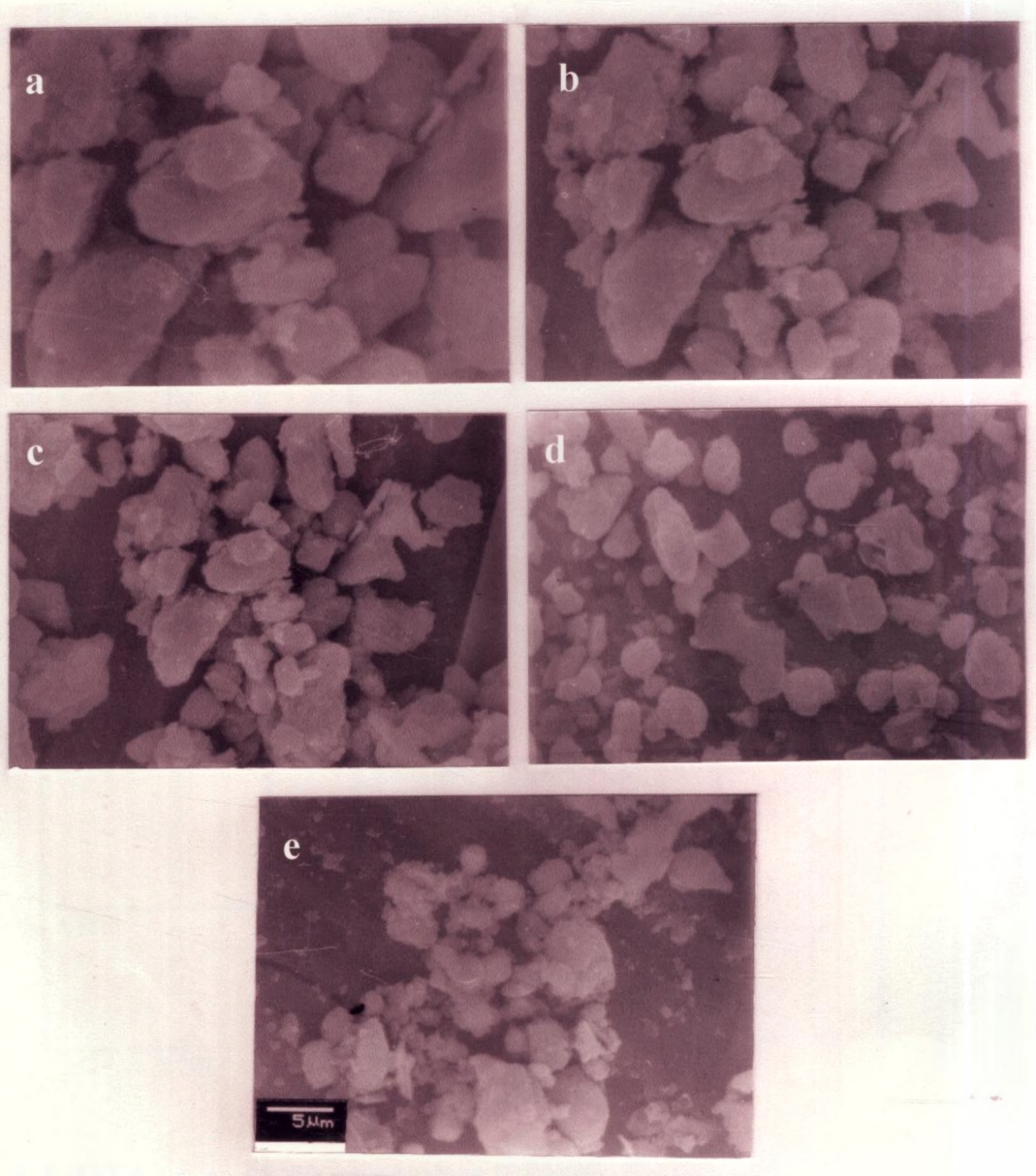

Fig. 3.3. SEM image of the precursor powders (a). 0.25HP, (b) 0.5HP, (c). 1HP, (d) 2HP and (e) 4HP

correspond to the formation of liquid phase and melting of the (Bi,Pb)-2212 phase [10-11]. These two endotherms are at temperatures of 863.5 and 876.9 for 0.25HP, 861.9 and 874.9 for 0.5HP, 859.6 and 872.4 for

1HP, 857.4 and 870.1 for 2HP and 853.3 and 866.4 for 4HP. From this it can be adjudged that the optimum reaction temperatures of the first four precursors (ie 0.25HP, 0.5HP, 1HP and 2HP) differ by about 2^0C between each other and that of 4HP powder is lesser by about 4^0C compared to 2HP powder.

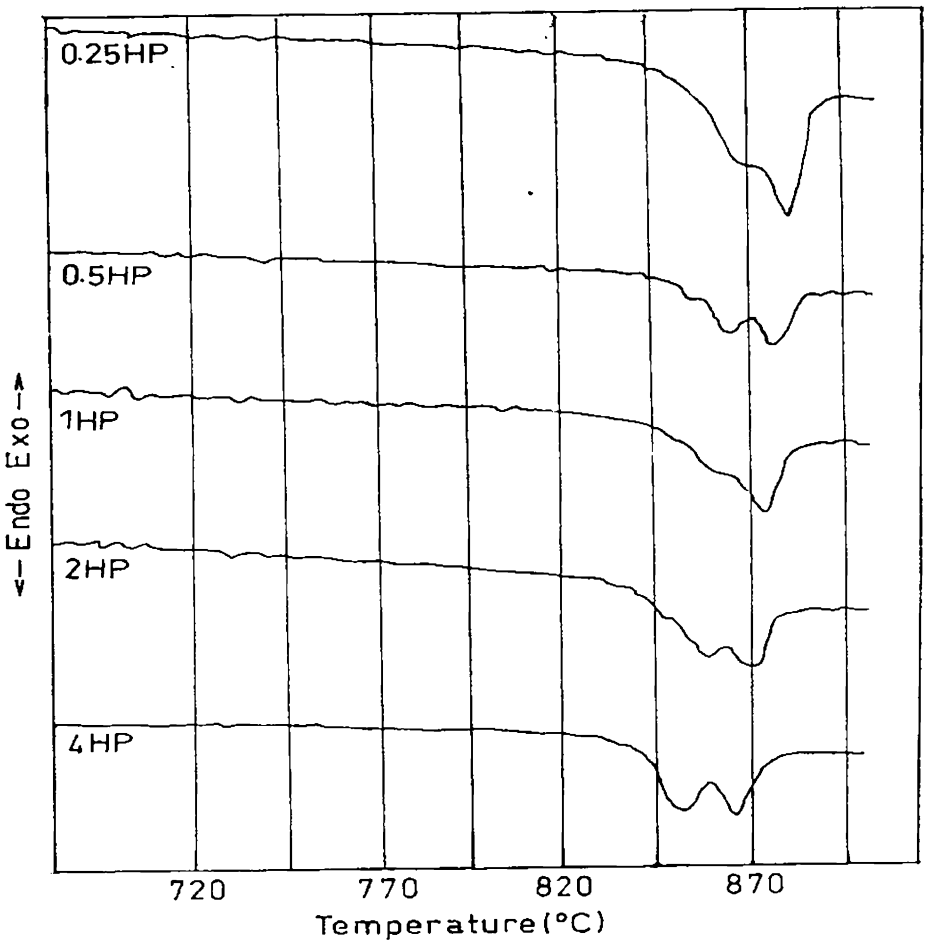

Fig. 3.4 DTA plots of the precursors 0.25HP, 0.5HP, 1HP, 2 HP, 4 HP

J_C values of the tapes (0.25HT, 0.5HT, 1HT, 2HT and 4HT) prepared from powders 0.25HP, 0.5HP, 1HP, 2HP and 4HP as a function of sintering temperature are plotted in Fig. 3.5. From the Fig. it is clear that the critical currents of the tapes with smaller particle size are more sensitive to sintering temperature and the optimum temperature

decreases with decrease in particle size. This is because smaller particles causes a reduction in the melting point of the sample due to reduced induction period [4,12], shorter interparticle distance, increased area of contact and reduced crystallinity.

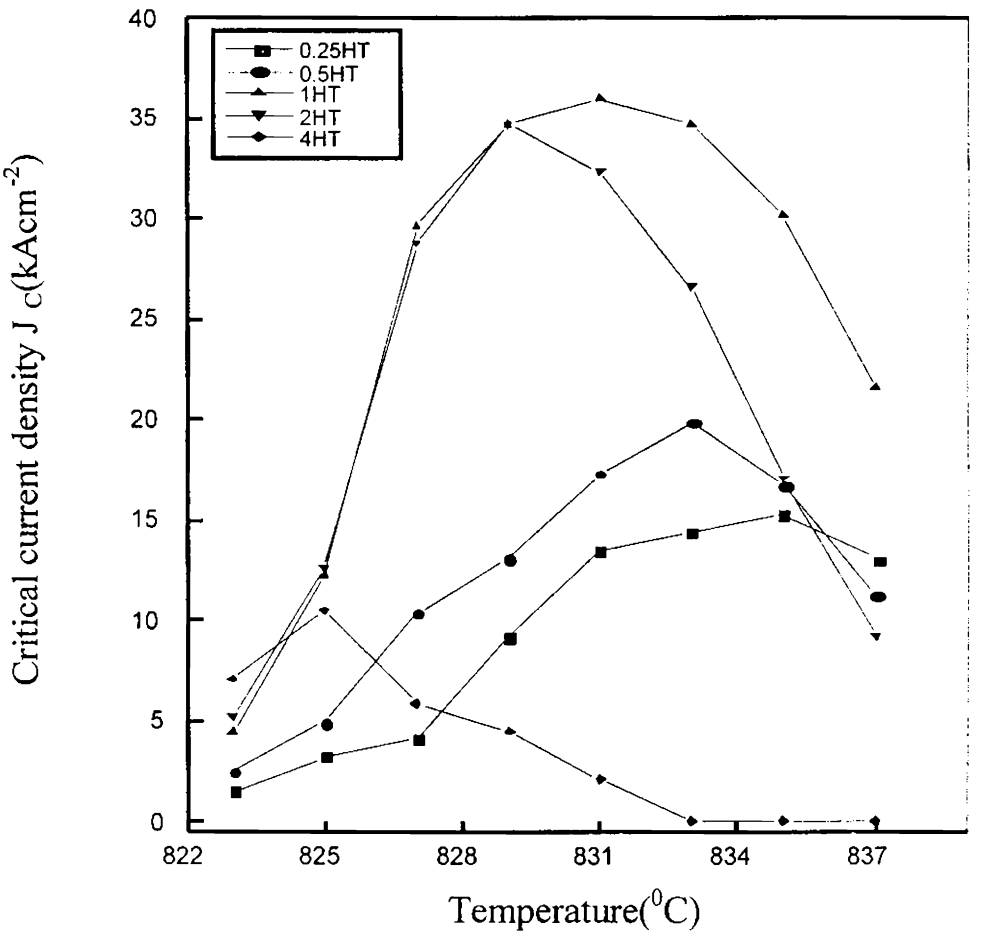

Fig . 3.5. Critical current density as a function of temperature for tapes after sintering in air for 200h.

3.3.4. Characterization of the Tapes

Table 3.2 gives the volume fraction of all the phases in the sintered (Bi, Pb)-2223/Ag tapes after different stages of heat treatment

at their respective optimum temperatures. The phases detected are Bi-2223, Bi-2212, Bi-2201, Ca_2PbO_4, CuO and Ca_2CuO_3. The phase fraction calculations are based on the relation $F_X=I_X/\Sigma I$ and the details are described in chapter 2.

After 60h of sintering it is found that the Bi-2223 fraction initially increases with grinding time, showing a maximum for 1HT and then decreases. At this stage the Bi-2223 phase fraction for 1HT is almost double (43.2%) compared to that of 0.25HT (18.1%) and 2HT (21.2%). While in the case of 4HT tape which contain the finest precursor; the formation rate of Bi-2223 is found to be extremely slow with a Bi-2223 fraction of only 1.4% after 60h. It contains relatively larger fraction of secondary phases, such as Bi-2201, Ca_2CuO_3 and CuO compared to the other tapes. The same trend more or less continued at the 90h stage also. Eventhough the rate of formation of 2223 phase was slower in 2HT sample in the first two stages; it attains a faster reaction rate after 90h of heat treatment. The large induction period observed in the 2HT sample may be due to the partial loss of crystallinity of the 2HP precursor. Bi-2212 grains being the primary ingredient for the formation of Bi-2223 [13], the amorphousisation of a portion of the Bi-2212 precursor causes a proportional decrease in Bi-2223 formation initially. However, during the induction period a fraction of the amorphous powder recrystallise into Bi-2212, which enables the reaction to proceed faster. After 140h, the fraction of Bi-2223 in 2HT tape is found to be 80.6%, which is close to that in 1HT (82.9). At this stage also the 4HT sample shows exceptionally low volume fraction of Bi-2223 phase (29.5 %). In 4HT sample the reaction sequence seem to have changed altogether due to high degree of degradation of crystallinity of the precursor.

Table. 3.2. Phase assemblage of (Bi, Pb)-2223/Ag tapes at different stages of heat treatment.

Samples	Phases	Volume fraction of different phases			
		Duration of heat treatment			
		60h	90h	140h	200h
0.25HT	Bi-2223	18.1	44.4	61.8	71.7
	Bi-2212	61.6	30.4	18.5	12.1
	Bi-2201	1.2	8.4	5.9	5.6
	Ca_2PbO_4	13.5	7.4	5.7	4.2
	CuO	1.2	5.2	5.1	4.8
	Ca_2CuO_3	4.4	4.2	3	1.6
0.5HT	Bi-2223	30.3	54.5	68.6	77.8
	Bi-2212	48.2	21.4	13.0	10.8
	Bi-2201	1.1	3.4	2.1	0
	Ca_2PbO_4	13.6	10.5	6.3	5.7
	CuO	2.8	5.9	5.9	4.1
	Ca_2CuO_3	4.0	4.3	4.1	1.6
1HT	Bi-2223	43.2	70.9	82.9	91.4
	Bi-2212	34.3	16.5	10.2	2.1
	Bi-2201	8.2	1.4	0	0
	Ca_2PbO_4	10.3	7.9	4.9	3.4
	CuO	2.5	2.3	2	3.1
	Ca_2CuO_3	1.5	1	0	0
2HT	Bi-2223	21.2	53.1	80.6	90.8
	Bi-2212	53	32	8.2	1.4
	Bi-2201	13.3	3.1	0	0
	Ca_2PbO_4	7.3	7	6.8	3.6
	CuO	2	1.9	1.7	2.1
	Ca_2CuO_3	3.2	2.9	2.7	2.1
4HT	Bi-2223	1.4	17.9	29.5	40.7
	Bi-2212	48.7	38.2	33.3	23.6
	Bi-2201	23.2	15.4	11.1	8.5
	Ca_2PbO_4	7.1	8.5	8.2	8.8
	CuO	9.3	9.9	9.8	11.8
	Ca_2CuO_3	10.3	10.1	8.1	6.6

Large fractions of secondary phases are found (Table.3.2) in 4HT sample after final stage of heat treatment. This may be due to the smaller activation energy required to form the secondary phases, makes them kinetically favoured in the early stages of heat treatment, they grow to large size and will obviously be hard to consume in subsequent reaction to form the 2223 phase even if long time reaction and multiple deformation cycles are given. Upto the final stage of heat treatment (200h) the same trend continued i.e. the 1HT yielding the highest volume fraction of Bi-2223 phase (91.4%), 2HT: 90.8%, 0.5HT: 77.8%, 0.25HT: 73.4% and 4HT: 40.7%. The XRD patterns of the fully processed tapes are given in Fig.3.6, which show that in 1HT and 2HT tapes, the 2212 phase is almost completely converted into 2223 phase and these are highly textured.

The SEM micrographs of the surface of oxide core are shown in Fig.3.7. It is seen that the surface morphologies are different for samples prepared using powders of different particle size distribution. The tape 4HT prepared using the finest powder shows an entirely different morphology from all other samples with so many impurity phases along with randomly oriented high T_C grains. Large flaky grains highly aligned parallel to the tape surface are seen in the 1HT tape sintered for 200h. Smaller grains with lower grain alignment and voids are observed in the 0.25HT tape. The grain size increases from 0.25HT to 1HT and in 1HT the grains are continuous and densely packed without much voids. In 2HT the grains are not so uniform and contain relatively larger number of smaller grains compared to 1HT.

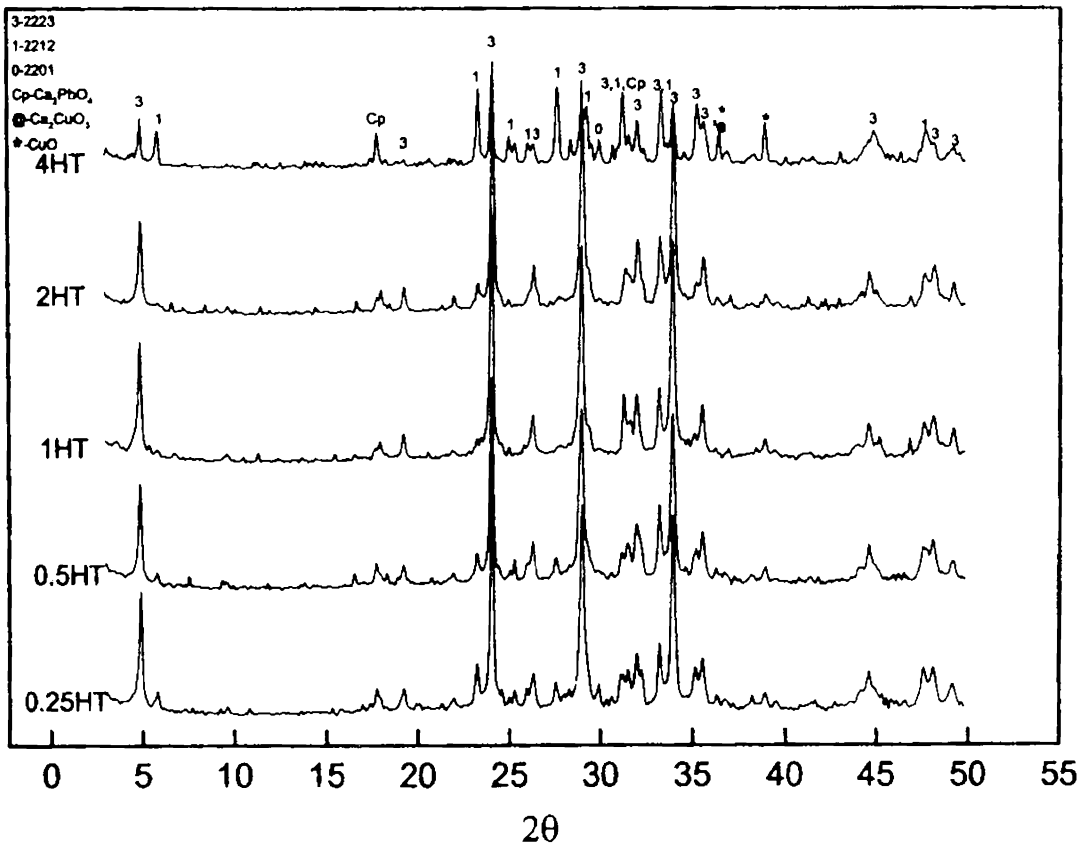

Fig. 3.6. XRD patterns of the fully processed tapes

The critical current density of the tapes at different stages of heat treatment is shown in Fig.3.8. In the first and second stages of heat treatment J_C increases with increase in precursor fineness from 0.25HT to 1HT and then decreases with further grinding. Among all the samples 1HT shows the highest J_C. As the particle size of the 2212 phase reduces, the diffusion distance between Bi-2212 and secondary particles, which is known to play an important role in the formation of aligned 2223 phase reduces and the reaction kinetics increases. The increased reactivity results in higher formation of Bi-2223, larger grain growth and better connectivity between the grains and hence J_C

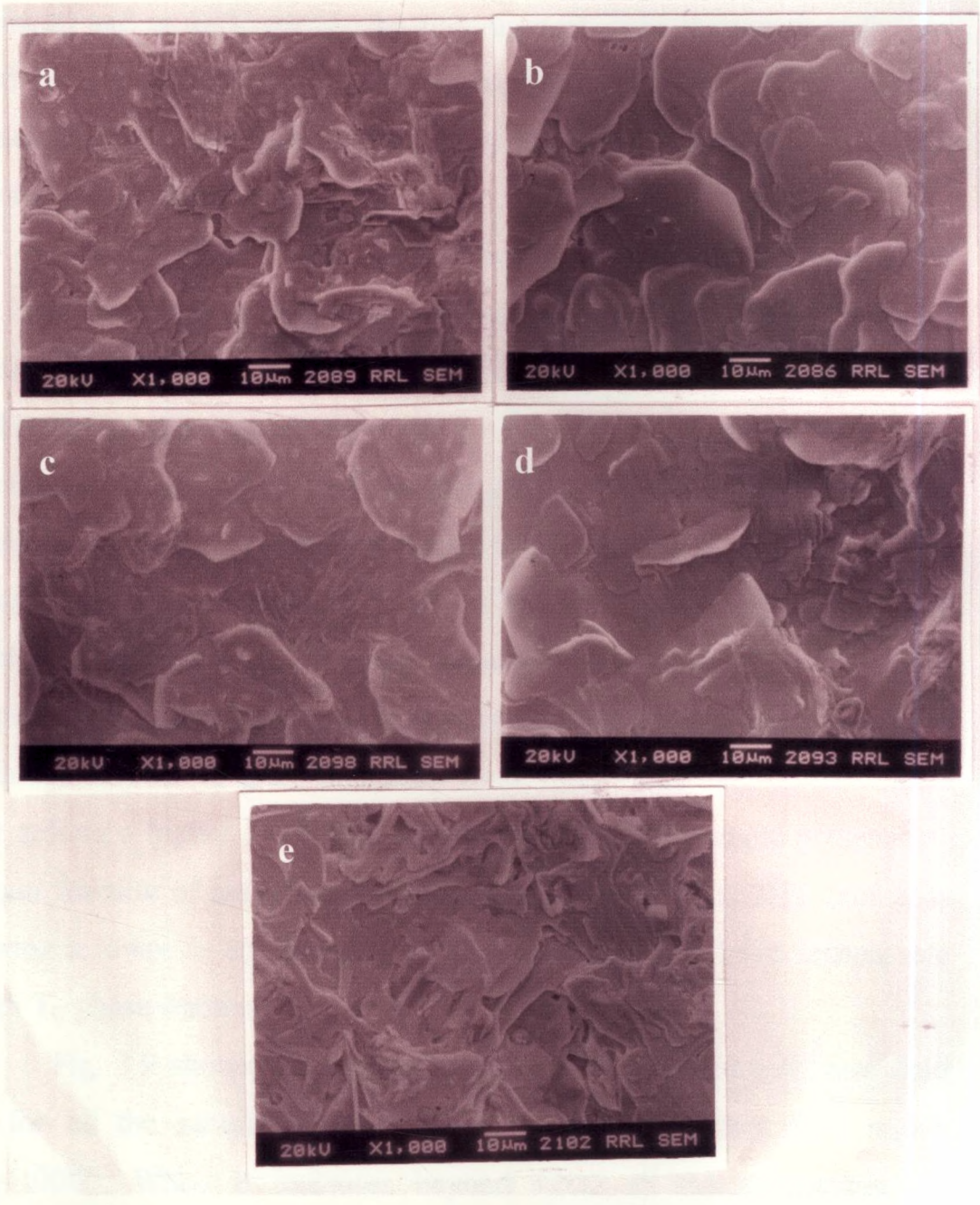

Fig. 3.7. The SEM image showing the surface structure of the etched tapes. (a). 0.25HT, (b) 0.5HT, (c). 1HT, (d) 2HT and (e) 4HT

increases with increase in precursor fineness. However, in 2HT and 4HT eventhough the particle size distribution is smaller than 1HT their

J_C is found to be lower than 1HT. Here the formation of 2223 phase is delayed and in 4HT sample the formation of 2223 is exceptionally low and its J_C is zero even after the second stage of heat treatment. This can be attributed to the degradation of crystallinity of the precursor due to prolonged grinding.

After third and fourth stage of heat treatment the trend of 0.25HT to 1HT continues as before and their J_C and Bi-2223 phase fraction in these tapes continue to increase with increase in precursor fineness and 1HT attains the highest value of J_C 34.4 $kAcm^{-2}$ after 200h of heat treatment. However, in 2HT sample eventhough the reaction rate was slow in the first two stages, it attains a faster reaction rate after 90h of heat treatment and attains a J_C of 30 $kAcm^{-2}$. The critical current will increase with increase in grain alignment and large plate like grain growth will improve the electrical connectivity between the grains with reduced number of grain boundary weak links. This may be the reason for getting a higher J_C in 1HT sample while in 2HT sample presence of larger fraction of smaller grains will reduce the J_C. Thus 2HT sample is having a lower J_C compared to 1HT eventhough both have comparable high T_C phase fraction.

Fig. 3.9 shows the I_C-B characteristics normalised with zero field I_C for all the samples. The I_C drops mainly in the low field region (B<100G). When B increases beyond 100G all the curves become almost parallel to each other, which suggest that main difference between the tapes is their intergranular connectivity, rather than flux pinning. The 1HT sample shows the best I_C-B behaviour among all the tapes and the 4HT sample shows the maximum degradation with a steep reduction beyond 1000G. It can be seen from Fig. 3.9 and Table 3.2 that the I_C-B variation with respect to different sample is related to the

quantity of the secondary phases present in them. For instance, the sample which show the best I_C-B dependence (1HT) has the minimum amount of secondary phase (6.5% excluding 2212) while the one which show the maximum degradation (4HT) has the maximum amount of

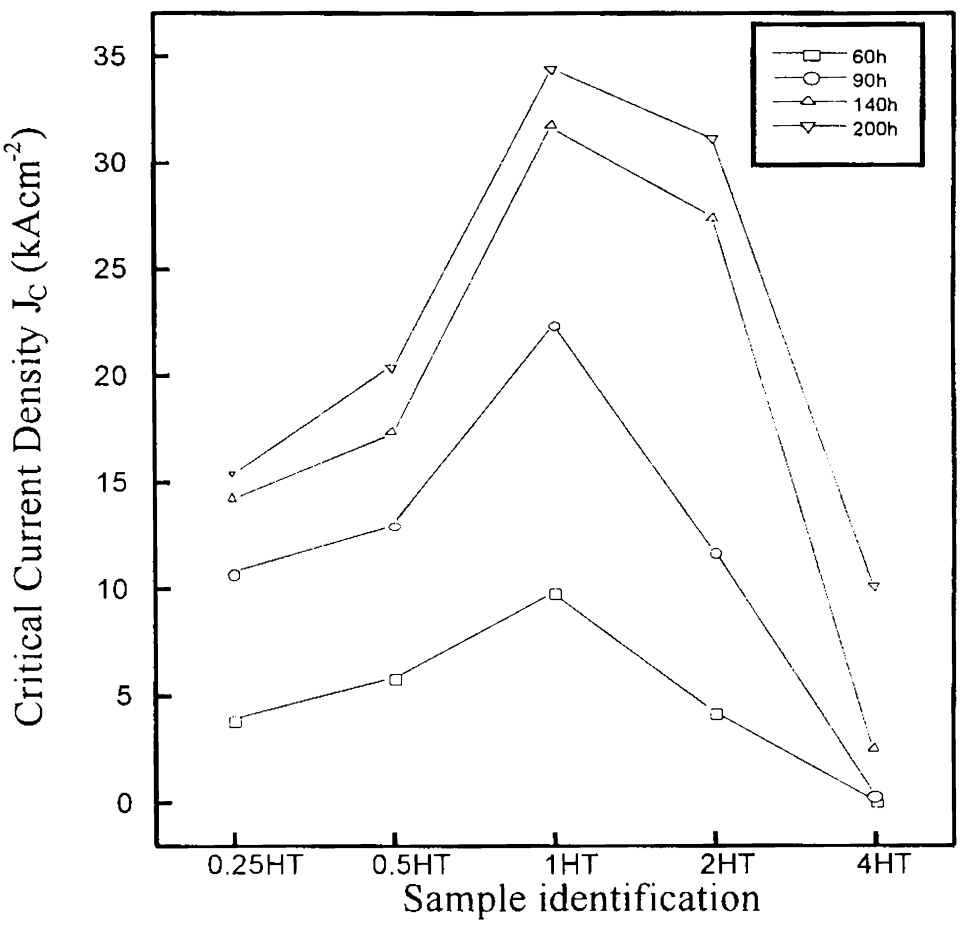

Fig. 3.8. Critical current density (J_C)at 77K of Ag/Bi-2223 tapes prepared using powders of different particle size distribution.

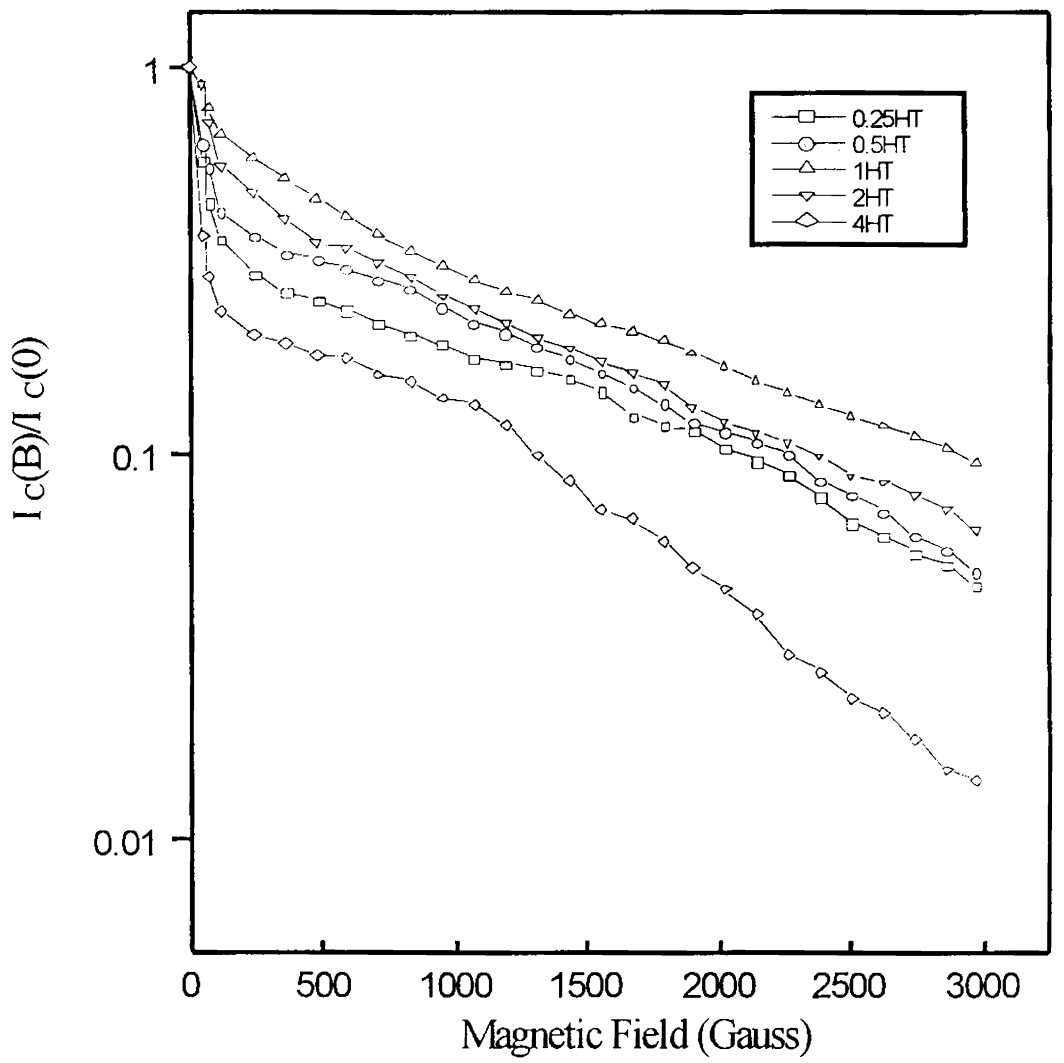

Fig. 3.9. The normalised I_C at 77 K for the fully processed tapes with the applied field parallel to the c-axis

secondary phase (35.7% excluding Bi-2212). The residual secondary phase will remain either as independent grain between the high T_C grains or segregate at the grain boundaries. While the former one directly blocks the supercurrent flow, the latter acts as weak links between the superconducting grains along the a-b plane. Therefore,

when the quantity of secondary phase increases it not only reduces the critical current but also leads to poor J_C-B characteristics.

3.4. Conclusions

Investigations on (Bi,Pb)-2223/Ag superconducting tapes prepared from powders with different particle size distribution have shown that:

(i) Particle size distribution of the precursor is a crucial parameter, which affects the reaction temperature, phase evolution, microstructure, J_C and J_C-B characteristics.

(ii) Increased precursor fineness not only improves the reaction kinetics but also reduces the sintering temperature of the tape. However, size reduction below a certain limit (average 2.5μm) degrades the crystallinity of the precursor, which further reduces the sintering temperature significantly. Such precursors yield tapes with very low high T_C phase fraction and poor J_C.

(iii) Tapes prepared using precursors with average particle size in the range 3 to 4μm yield the best result in respect of high T_C phase fraction, microstructure, J_C and J_C-B characteristics.

References

[1] K Sato, T Hikata, H Mukai, M Ueyama, N Shibuto, T Kalo, T Masuda, M Nagata, k Iwata and T Mitsui *IEEE Trans. On Magnetics* **27(2),**1231(1991)

[2] Q Li, K Brodersen, H A Hjuler and T Fretoft 1993 *Physica C* **217,** 360 (1993)

[3] Weon-Ju Kim, Sun-Chill kwon, Ho Jin Lee, Hei-Gyoun Lee , Gye-Won Hong and II- Hyun kuk *Physica C* **294,** 147 (1998)

[4] Xiao- Dong Su, Jai- Moo Yoo, Jai-Wong Ko, Hai-Doo Kim, Hyung- Sik Chung, Z Q Yang and Gui-We Qiao *Physica C* **331,** 285 (2000)

[5] J Jiang and J S Abell *Physica C* **296,**13 (1998)

[6] Tsuneyuki Kanai, Tomoichi Kamo and Shin-Pei Matsuda *Jap.J of Applied Physics* **29(3),** L412 (1990)

[7] J S Luo, H G Lee and S N Sinha *J. Mater. Res* **9,** 297 (1994)

[8] J S Lue, N Merchant, E J Escorcia-Aparicio, V A Maroni and B S Tani *J.Mater. Res.* **9,** 3059 (1994)

[9] A Jeremie and R Flukiger *Physica C* **267,** 10 (1996)

[10] T Hatano, K Aota, S Ikeda, K Nakamura and K Ogawa *Jpn. J. Appl.Phys.* **27** L2055 (1988)

[11] J C Grivel, A Jeremie, B Hensel and R Flukiger *Supercond. Sci. Technol.* **6,** 725(1993)

[12] Y L Wang , W Bian , Y Zhu, Z X Cai, D O Welch, R L Sabalini, M Suenaga and T R Thurston *Appl.Phys. Letters* **69**,580 (1996)

[13] Kin C G and J Ho Je *Physica C* **203**, 385 (1992)

CHAPTER 4

PHASE EVOLUTION IN Ag, Ag_2O AND $AgNO_3$ ADDED (Bi,Pb)-2223 SUPERCONDUCTOR

4.1. Introduction

Most of the HTSC cuprates contain relatively large number of cations. The reactivity of these cuprates with other metals and oxides is of significant importance because of the need for nonoxidising normal metals in composite wire fabrication, non poisonous substrate or diffusion barrier materials for thin or thick film devices and to strengthen the brittle ceramic core without affecting the superconducting properties and the processing temperature. Unfortunately all these ceramics, particularly BPSCCO react with nearly every metal with which they come into contact.

Silver has been found to be the most appropriate metal for fabricating BPSCCO superconductor tapes. Apart from the mechanical workability and high electrical and thermal conductivity, the properties, which isolate silver as the option, include its non-poisoning nature and compatibility at the processing temperature. So it is not surprising that much attention has been paid to the study of role of silver in BPSCCO/Ag composites and to utilize these unique properties for improving the superconducting properties essential for applications.

The beneficial and detrimental effects of Ag addition in Bi(Pb)-Sr-Ca-Cu-O (BPSCCO) system have been studied by several groups. Ag is known to promote the formation of (Bi,Pb)-2223 phase and improve c-axis texture, mechanical ductility and J_C [1-8]. Conflicting results such as deterioration of J_C and degradation of T_C have also been reported. [8-9] In most of these studies Ag is added to the system in the form of Ag powder, Ag_2O or $AgNO_3$. The widely varying or conflicting results call for a detailed study on the relative effect of these additives particularly on the phase evolution of BPSCCO system, which has not been addressed so far.

In this chapter, a detailed study was carried out on the relative effect of Ag powder, Ag_2O and $AgNO_3$ (0-25 wt% Ag) on the sequence of phase evolution, kinetics of (Bi,Pb)-2223 formation, density variation and finally the transport current in BPSCCO system. The study has shown that Ag addition in BPSCCO accelerates the Bi-2223 phase formation and the rate formation strongly depends on the form of Ag additive. It is also found that Ag_2O and $AgNO_3$ are much effective in promoting the phase formation as well as J_C than Ag powder◙.

4.2. Experimental

The precursor with a nominal cation ratio Bi:Pb:Sr:Ca:Cu = 1.8:0.4:2:2.2:3.2 was prepared by solid state synthesis route using high purity (>99.99%) Bi_2O_3, PbO, $SrCO_3$, $CaCO_3$ and CuO. After an initial calcination step (at 800°C for 12 h) the powder was divided into ten

---

◙ Part of this work is published in Physica C **307**, 277 (1998)

batches of which one was taken as the pure sample. High purity (99.99%) Ag powder (average particle size 40 μm), Ag_2O (average particle size 2 μm) and $AgNO_3$ crystals were added and thoroughly mixed in acetone medium to the other nine batches in three different weight percentage viz. 10, 18, 25. After a second stage calcination step (at 820°C for 50 h) the powders were further ground in acetone medium, dried and pressed into bar shaped pellets of typical dimension 20x4x2 mm^3 at a pressure of about 30 MPa and heat treated in air at temperatures in the range 835-840°C for a total of 200 h with three intermediate grinding and pressing. The heat treatment of all the samples were carried out in the same batch in a large volume muffle furnace in order to ensure uniform temperature to all the samples.

The phase evolution of the samples at different stages of heat treatment, microstructural examination of the Ag added samples, density measurements, J_C measurements etc were done using the same procedures as described in chapter 2.

Sample identification

We label P (pure sample 0 wt% Ag), A10, A18, A25 for samples having 10, 18, 25 wt% of Ag powder respectively. Similarly O10, O18, O25 for Ag_2O and N10, N18, N25 for $AgNO_3$ added samples.

4.3. Results and Discussion

The volume percentage of different phases viz. Bi-2223, Bi-2212, Bi-2201, Ca_2PbO_4 and CuO present in pure and Ag, Ag_2O and $AgNO_3$ added BPSCCO samples after different stages of heat treatment are given in Table 4.1. Here, the phase assemblages shown at 0 h refer to those available in different samples after the calcination or prior to the

heat treatment. The sequence of phase changes occurring in the different types of BPSCCO samples with respect to time can be better understood and discussed separately with the help of comparative plots (Figs.4.1 to 4.3) as shown in the succeeding sections.

4.3.1. Effect of Ag Powder

In Fig.4.1, the rate of formation of Bi-2223 and the consequent depletion of Bi-2212 with respect to time in the Ag powder added BPSCCO samples are compared with pure sample. The rate of formation in all the Ag powder added samples are much higher than that in the pure sample for a period upto 100 h, the highest being in 10% Ag sample. Thereafter, the rate becomes very slow in Ag added samples upto 150 h, whereas it sharply increases in pure BPSCCO. Subsequently, Bi-2223 phase begins to deteriorate in Ag added samples, and after a period of 200 h, the Bi-2223 fraction in the pure sample (83.4%) exceeds that in all the Ag added samples (10% Ag – 71.2%, 18% Ag – 60.9% and 25% Ag – 52.9%). In the case of 25 wt% Ag sample a significant quantity of Ca_2CuO_3 (18.8%) is detected apart from unusually high percentages of Bi-2212 (23.0%), CuO (10.6%) and low Ca_2PbO_4 (2.8%). Another important observation was the segregation of Ag during heat treatment of the Ag added samples. Part of the silver in the Ag added sample was found to settle down at the bottom of the pellet as a separate layer after every stage of sintering. Since the layer was porous and friable, this was again ground along with the bulk pellet and was used for XRD analysis and subsequent heat treatment. The segregation behavior was more pronounced at higher wt% Ag powder added sample.

Table 4.1: The volume percentage of Bi-2223,Bi-2212,Bi-2201,Ca_2PbO_4 and CuO at different stages of heat treatment.

Samples	VOLUME PERCENTAGE OF DIFFERENT PHASES																								
	Bi-2223 Duration of heat treatment (h)					**Bi-2212** Duration of heat treatment (h)					**Bi-2201** Duration of heat treatment (h)					**Ca_2PbO_4** Duration of heat treatment (h)					**CuO** Duration of heat treatment (h)				
	0	50	100	150	200	0	50	100	150	200	0	50	100	150	200	0	50	100	150	200	0	50	100	150	200
Pure	5	11.2	26.2	70.2	83.4	34	53.4	56.7	19.4	8.2	31.1	18.2	2.3	1.0	1.7	14.1	9.4	9.5	6.3	3.3	15.8	7.8	8.3	2.1	3.4
A10	11.5	47.5	64.2	72.3	71.2	42.2	25.5	9.8	7.1	2.9	15.9	9.2	9.1	4.0	10.4	18.0	12.6	13.2	11.4	11.6	12.1	5.2	3.7	5.2	3.8
A18	8.2	42.2	52.6	60.9	58.0	40.4	29.6	11.4	6.8	5.1	14.1	8.8	16.3	10.7	16.5	22.5	13.9	15.8	16.4	16.5	14.8	5.5	4.0	5.2	3.9
A25*	7.1	36.9	52.6	52.9	29.5	45.3	35.7	7.9	9.9	23.0	13.6	7.0	16.4	15.3	15.2	19.6	14.7	18.1	16.7	2.8	14.5	5.7	5.0	5.2	10.6
O10	4.2	27.6	70.7	72.3	79.5	50.6	59.1	15.8	7.3	4.2	18.4	1.0	3.7	2.1	6.0	12.6	10.9	6.9	15.1	7.9	14.2	1.4	2.9	3.2	2.3
O18	9.4	36.9	74.0	78.8	79.9	48.5	45.1	9.1	6.1	4.3	15.2	2.9	4.6	2.3	5.6	13.6	10.8	9.2	10.0	7.3	13.3	4.3	3.1	2.8	2.9
O25	14.6	48.0	82.0	79.2	78.8	49.5	36.7	4.6	5.6	3.8	12.7	3.9	4.1	2.7	8.0	9.7	9.0	6.6	9.7	6.6	13.5	2.4	2.7	2.8	2.8
N10	6.3	40.8	59.7	77.6	78.9	57.9	43.4	27.7	5.3	4.0	12.6	2.3	2.1	1.7	6.4	10.5	11.1	7.9	12.8	7.0	12.7	2.4	2.6	2.6	3.4
N18	6.6	37.4	50.0	79.6	78.9	58.7	45.3	37.7	6.1	5.6	11.8	2.2	1.9	2.1	5.6	17.3	11.4	8.0	10.1	7.3	11.6	3.7	2.4	2.1	2.6
N25	9.0	37.1	48.1	81.5	84.5	59.1	48.4	39.8	5.0	2.4	7.6	1.8	2.3	1.3	4.4	13.7	9.4	7.4	8.9	4.9	10.6	3.3	2.3	3.3	3.7

*Ca_2PbO_4 – 18.

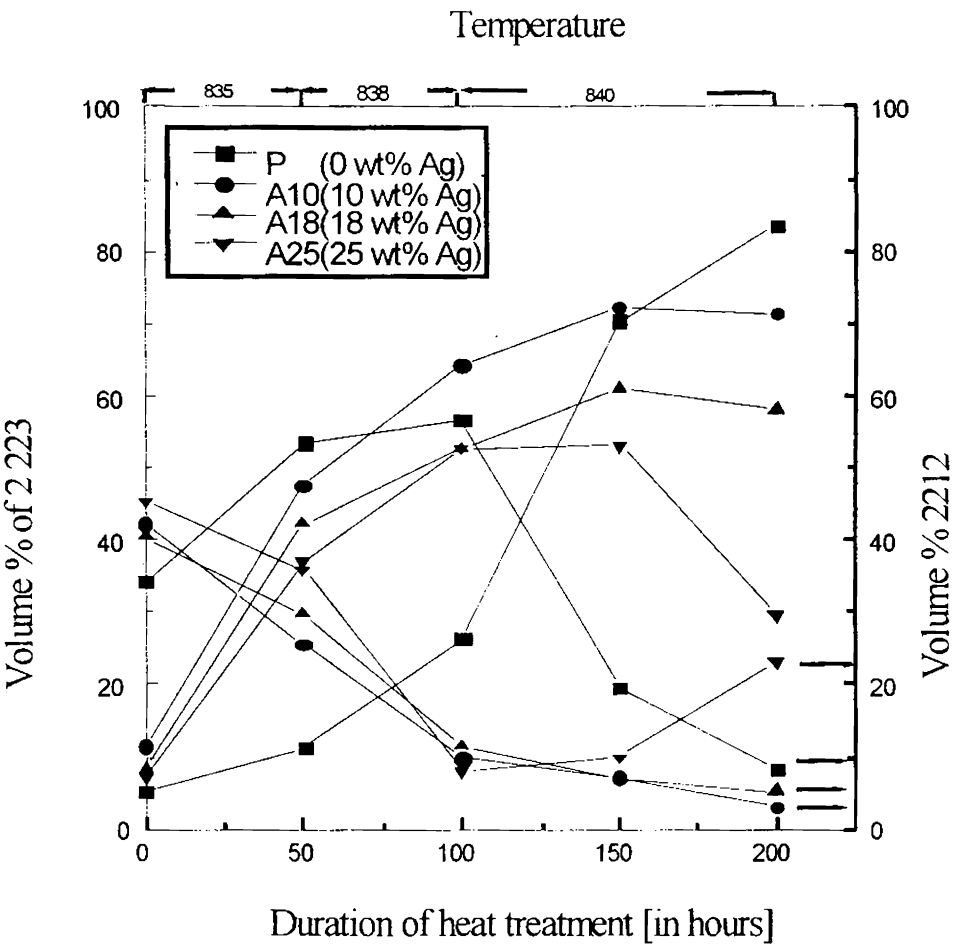

Fig 4.1. Variation of B i-2223 and B i-2212 phase fractions in Ag powder (0-25 wt%) added BPSCCO samples

4.3.2. Effect of Ag_2O Powder

The rate of change of Bi-2223 and Bi-2212 phase fractions in Ag_2O added and pure BPSCCO samples with respect to duration of heat treatment is shown in Fig.4.2. It can be seen that the Bi-2223 phase fraction in the Ag_2O added samples reach their maximum values within a period of

100 h with a formation rate much higher than that of pure

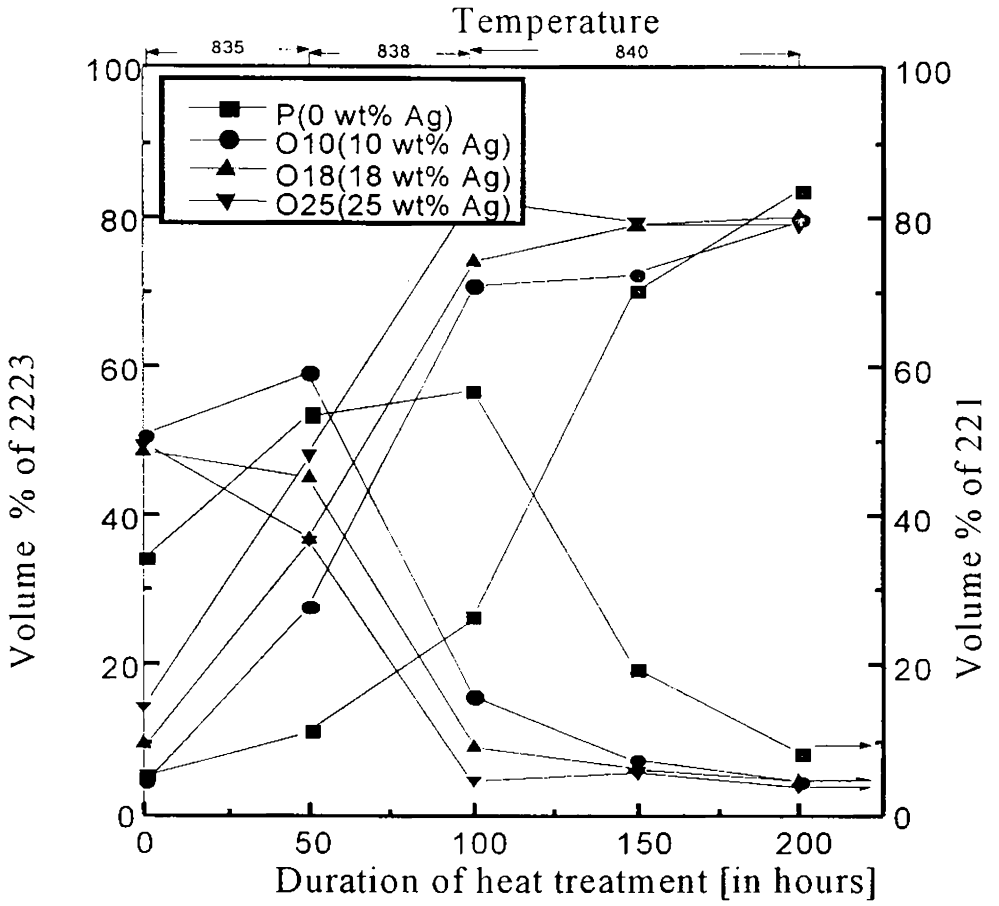

Fig. 4.2. Variation of Bi-2223 and Bi-2212 phase fraction in Ag_2O (0-25 wt%) added BPSCCO sample

sample. Unlike in the case of Ag powder added sample, the volume fraction of Bi-2223 increases with increase in Ag percentage for the Ag_2O added samples. However, after 200 h of heat treatment the Bi-2223 fraction in all the Ag added samples reaches almost the same value of about 80% which is 3-4% less than that in pure sample.

4.3.3. Effect of $AgNO_3$

The variation of Bi-2223 and Bi-2212 phase in pure and $AgNO_3$ added BPSCCO samples with respect to heat treatment duration is shown in Fig.4.3. Here again, the Bi-2223 formation rates in $AgNO_3$ added samples are much higher than the pure sample. However, the Bi-2223 phase in the $AgNO_3$ added samples saturates only after a period of about 150 h and the saturation values do not have much influence on the $AgNO_3$ content. However, after 200 h, the Bi-2223 phase fraction in the 25% $AgNO_3$ sample attains a maximum of about 85% which is higher than that in 10% and 18% $AgNO_3$ samples (both 78.9%) but comparable with the Bi-2223 fraction in pure sample (83.4%).

4.3.4. SEM Microstructure

SEM microstructure of the Ag powder, Ag_2O and $AgNO_3$ added (18% Ag each) BPSCCO samples under an identical magnification of 1000x is shown in Fig.4.4. It is seen that the morphology of the Ag powder added sample is distinctly different from that of the Ag_2O and $AgNO_3$ added samples. The latter two samples (Figs.4.4b and 4.4c) show characteristic Bi-2223 flakes wherein very fine silver particles are homogeneously distributed. On the other hand, Ag powder added sample (Fig.4.4a) comprises large bar shaped grains with rounded or fractured surface distributed with large intergrain pores indicating partial melting of the sample. Traces of partially molten Ag can be seen sticking to the grains.

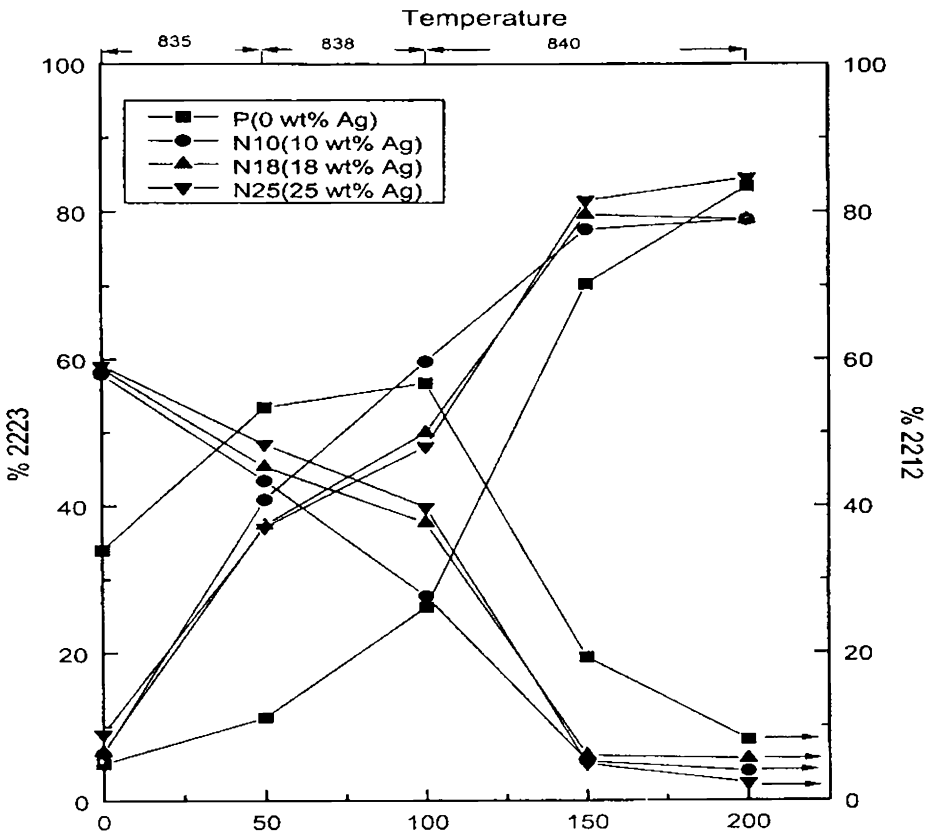

Fig. 4.3. Variation of Bi-2223 and Bi-2212 phase fraction in $AgNO_3$ (0 to 25 wt%) added BPSCCO sample

4.3.5. Density Measurements

Fig. 4.5 gives the density variations of pure and Ag added pellets. Effect of Ag on density (% of theoretical density) of BPSCCO before (green density) and after sintering (200 h) is reported. It can be seen from the Fig. that green density is almost same for all the samples. But the sintered density increases with increase in Ag content

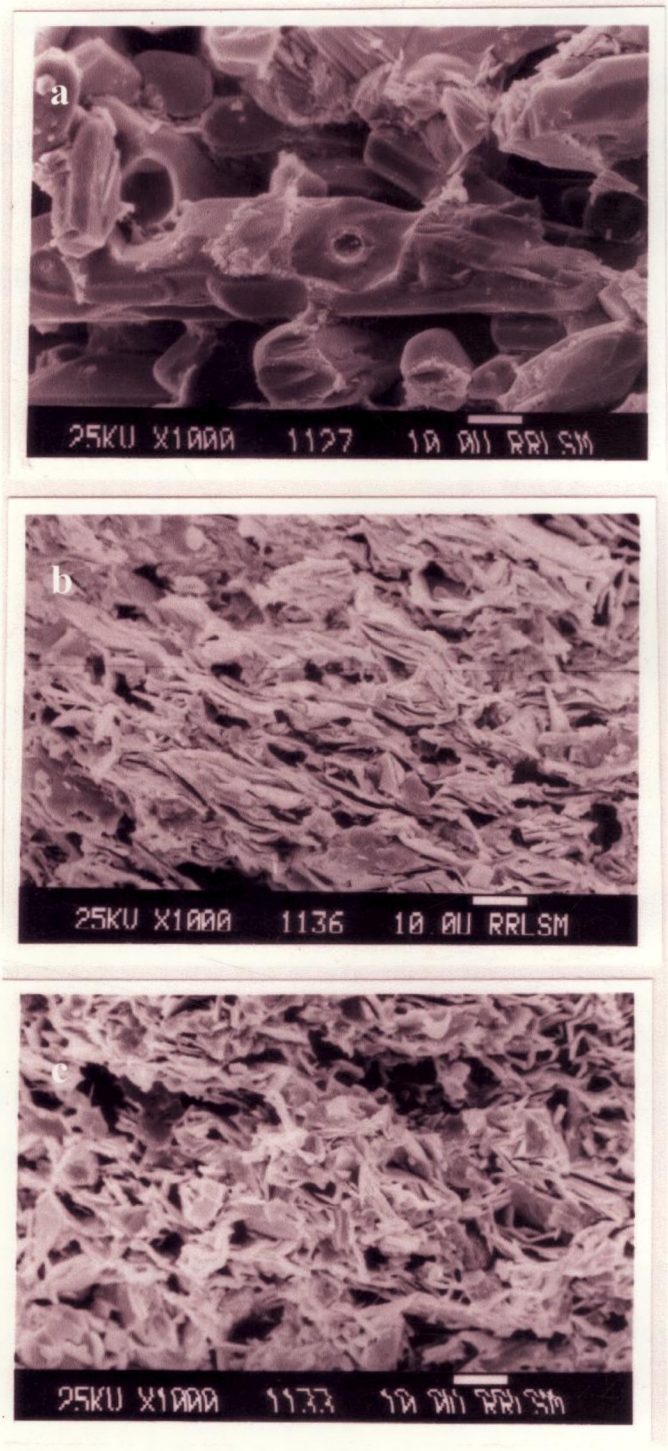

Fig. 4.4. SEM Microstructures of Ag added BPSCCO sample (18 wt% Ag each).(a). Ag powder, (b).Ag_2O (c). $AgNO_3$

in the case of Ag_2O and $AgNO_3$ added samples. But in Ag powder added sample density decreases with increase in Ag content. This is due to the segregation and consequent loss of silver rich liquid phase in Ag powder added samples. A detailed discussion on this aspect is given in the subsequent sections of this chapter.

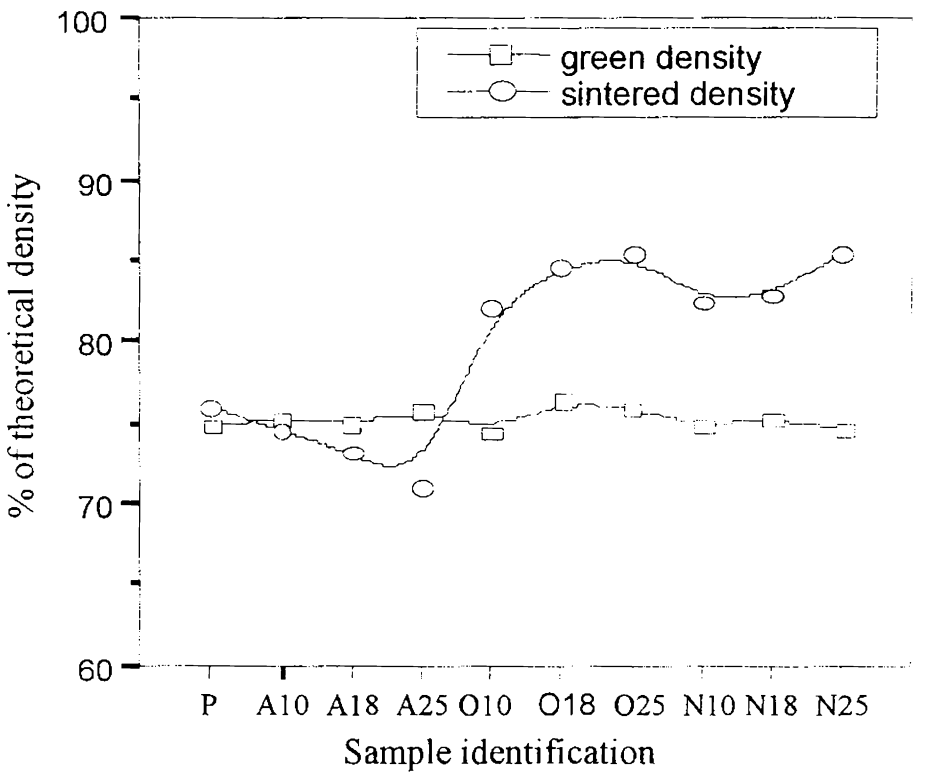

Fig. 4.5. Variation of relative density of the BPSCCO core with respect to silver addition

4.3.6. Comparison of Phase Evolution

The experimental results (Fig.4.1-4.3) conclusively show that the Bi-2223 formation rates in Ag added BPSCCO samples depend on the form of Ag additives. The Ag_2O added samples show a much faster formation rate than both Ag powder and $AgNO_3$ added sample upto a heat treatment period of 100 h. During this period the volume fraction of Bi-2223 phase in Ag_2O added sample reaches values as high as 82% compared to 26.2%, 52.6% and 48.1% in pure as well as Ag powder and $AgNO_3$ added samples respectively (Table 4.1). Beyond 100 h the rate of formation of Bi-2223 phase slows down in Ag powder and Ag_2O added samples while it sharply increases in $AgNO_3$ added samples upto a period of about 150 h. At this stage, the fractions of Bi-2223 formed in Ag_2O and $AgNO_3$ added samples are found to be higher for higher percentage of Ag whereas in Ag powder added samples the Bi-2223 fraction decreases with increase in Ag content. Subsequent heat treatment beyond 150h deteriorates the Bi-2223 phase in Ag powder added samples whereas it levels off in Ag_2O and $AgNO_3$ added samples. However, in pure sample the Bi-2223 formation rate monotonically increases till the maximum period of heat treatment carried out in this study. As a result, the Bi-2223 phase fractions in pure as well as Ag_2O and $AgNO_3$ added samples attain comparable values while in Ag powder added samples the phase fraction is much lower.

It has been widely accepted that Ag addition in BPSCCO reduces the partial melting temperature of the system and thereby accelerates the formation rate of Bi-2223 phase [6,10]. Among the Ag additives used in this study, Ag powder was having a larger particle size (average particle size:

40 μm) compared to the Ag powders produced as a result of dissociation of fine Ag_2O particles (average particle size of Ag_2O is 2 μm) and $AgNO_3$ crystals. During heating Ag_2O starts dissociating at 100°C and at around 300°C it completely dissociates into its elements. $AgNO_3$ crystals, on the other hand, melts at 212°C to a yellow liquid and decompose at 440°C to metallic silver, nitrogen and nitrogen oxides. Since the additions are done prior to the second calcination stage, the evolved gases go out freely. Uniform dispersion of the very fine silver particles is ensured by wet-mixing/grinding done before the second stage calcination. The larger surface area of the fine and freshly produced Ag particles in the Ag_2O and $AgNO_3$ added samples may be responsible for the higher rate of formation of Bi-2223 phase on these samples. Scanning electron micrographs of these samples (Figs.4.4b and 4.4c) confirm the fine nature of the Ag particle and their homogeneous distribution and further show that addition of Ag_2O and $AgNO_3$ do not affect the flaky morphology of Bi-2223 grains. The relatively large Ag particles available in the Ag powder added samples especially at higher percentages are likely to soften and agglomerate to form still large Ag droplets in presence of the liquid phase [8-9] formed in BPSCCO during prolonged sintering. This will not only lead to the segregation of part of the molten silver together with the liquid phase towards the bottom of the pellets due to gravity, but also cause large grain growth, changes in stoichiometry and reaction sequence. The distinctly different morphology of BPSCCO with very large grains and intergranular pores observed in the Ag powder added sample (Fig.4.4a) very well supports the above argument. The observation of significant quantities of Ca_2CuO_3 and unusually high Bi-2212, CuO and low Ca_2PbO_4 phases in the

25% Ag powder samples (Table 4.1) is also a consequence of the segregation of liquid phase. Ca_2CuO_3 can grow out of the segregated liquid phase [4,9,10] as it constitutes mainly Ca^{2+}, Cu^{2+} and Pb^{2+} ions [11]. At the same time, Bi-2223 formation in the other parts of the samples ceases due to the deficiency of liquid phase, which is considered to be a reservoir of Ca^{2+} and Cu^{2-} in the formation of Bi-2223. The deterioration of Bi-2223 phase may be attributed to the large difference in activation energies of formation of Ca_2CuO_3 (ΔH =300 KJ/mol) and Bi-2223 phase (ΔH = 1.5 MJ/mol) [12]. It would mean that the reaction taking place at the interface between the liquid phase and the remaining part of the pellet highly favours the formation of Ca_2CuO_3 which is presumed to occur even at the expense of Bi-2223 leading to increased volume fractions of 2212 and CuO.

4.3.7. Critical Current Density

The results of transport critical current density measurements of pure as well as Ag added samples after the final sintering are shown in Fig. 4.6. The critical current density of 10-wt% silver added sample is comparable with that of pure sample except for Ag powder added sample, followed by a marked decrease in current density as the silver concentration increases. Silver powder added samples were showing the least J_C values among all the batches. This can be attributed to the lower fraction of Bi-2223 phase and poor microstructure. Even though samples with higher silver fraction have similar high T_C fraction compared to that of pure sample, they have relatively lower J_C values because the nonsuperconducting silver particles obstruct the passage of supercurrent through the superconducting matrix.

The studies show that approximately 10-wt% is the optimal Ag content for maintaining the J_C.

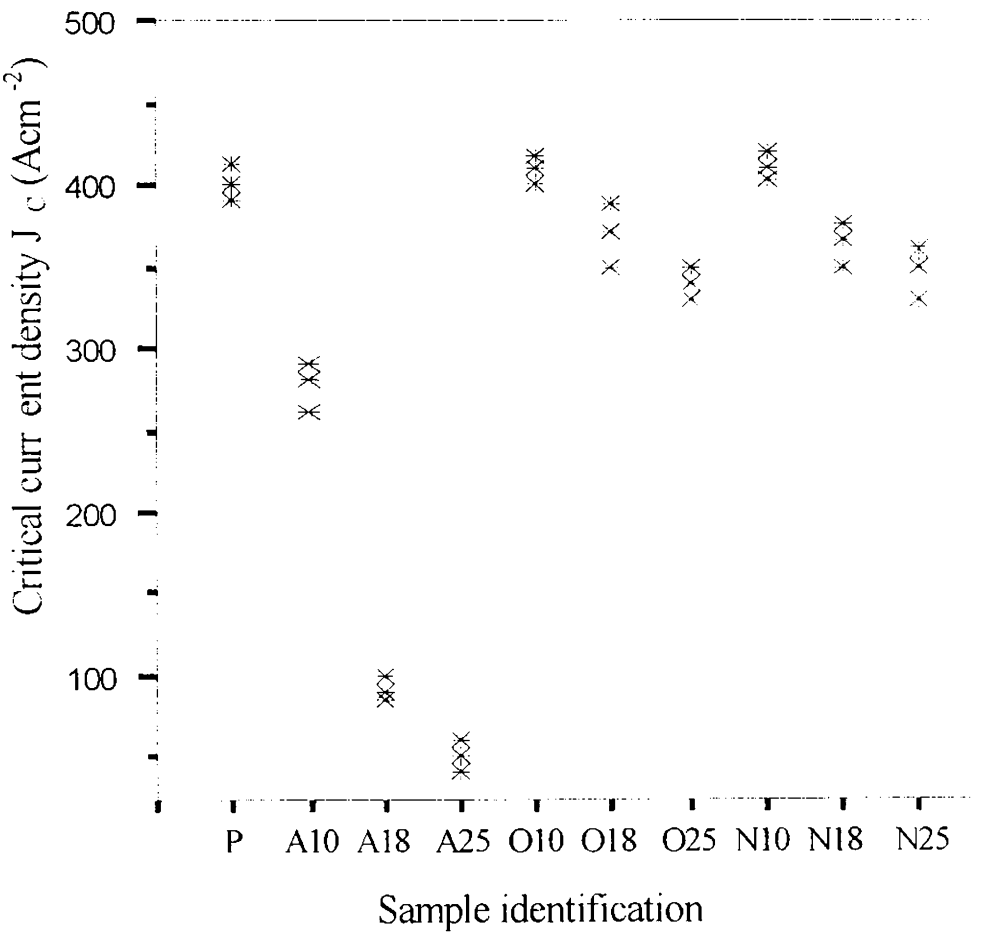

Fig. 4.6. Critical current density of Ag added BPSCCO samples

4.4. Conclusions

(i) Ag addition in BPSCCO accelerates the Bi-2223 phase formation. However the rate of formation strongly depends on the form of Ag additive.

(ii) Ag_2O and $AgNO_3$ are found to be much effective in promoting the Bi-2223 phase formation and J_C than Ag powder.

(iii) Addition of higher percentages of Ag powder with larger particle size leads to segregation of Ag in bulk BPSCCO pellets.

(iv) No significant increase in the ultimate volume fraction of Bi-2223 phase / J_C can be made by the addition of Ag in any form (Ag powder, Ag_2O or $AgNO_3$).

(v) Sintered BPSCCO pellets with theoretical density as high as 90% and critical current density about 400 Acm^{-2} can be prepared by addition of around 10 wt% Ag to the superconductor either in the form of Ag_2O or $AgNO_3$.

(vi) The result could be of great use in designing the precursor composition for the development of dense BPSCCO bodies in bulk form and Ag/BPSCCO-2223 tapes with high J_C.

References

[1] T.E.Jones, W.C. McGinnis, E.W. Jacobs, R.D.Boss, P.M.Thibado, J.S. Briggs, W.E. Glad, *Physica C* **201**, 279 (1992)

[2] Y. Maksomoto, J. Hombo, Y. Yamaguchi, T. Mitsunaga, *Mat.Res. Bull.* **24**,1469(1989)

[3] R. Zhou, W.L. Hutts, J. F. Bingert, J.Y. Coulter, E. J. Peterson, J.L.Smith, *Physica C* **249**, 166(1995)

[4] W.Gao, S.C.Li, D.A.Rudman, J.B.Vander Sande, *Physica C* **167,** 395(1990)

[5] H. Comert, M. Altunbas, T.D. Dzhafarov, T.Kucukomeroglu, Y.G. Asadov, H.Karal, *Supercond. Sci. Techno.* **7,** 824(1994)

[6] Y.D. Chiu, C.H. Kao, T.S. Lei, M.K. Wu, *Physica C* **235-240,** 485(1994)

[7] R. Zhou, W.L. Hutts, R.J. Sebring, J. F. Bingert, J.Y. Coulter, J. O. Willis, J.L.Smith, *Physica C* **255**, 275(1995)

[8] Y.C. Guo, H.K. Liu, S.X. Dou, *Physica C* **215,** 291(1993)

[9] S.X. Dou, K.H. Song, H.K.Liu, C.C. Sorrell, M.H. Apperley, N. Savvides, *Appl. Phys. Lett.* **56,** 493(1990)

[10] P.Majewski, A. Sotelo, H. Szillat, S. Kaesche, F. Aldinger, *Physica C* **275**, 47(1997)

[11] Y.L. Chen, R. Stevens, *J. Am. Ceram. Soc.* 75 (5) 1150

[12] Y.E. High, Y. Feng, Y.S. Sung, E.E. Hellstrom, D.C. Labalestier, *Physica C* **220**, 81(1994)

CHAPTER 5

EFFECTS OF SILVER ON SUPERCONDUCTING AND MECHANICAL PROPERIES OF (Bi,Pb)-2223/Ag POWDER-IN-TUBE TAPES

5.1. Introduction

The results of the studies conducted by adding silver on bulk pellets as described in the previous chapter cannot be directly applied for silver sheathed tapes because in the case of tapes, silver is already present in the form of sheath. Even though silver does not seem to get into the structure of the phases present in the system, its presence in the form of sheath causes nonuniform phase formation with in the oxide core. This means an increased grain alignment near the Ag/BPSCCO interface compared to the centre of the tapes. Thus the homogenisation that can be imparted to the powder inside the silver sheath is a big practical limitation and this restriction can affect the 2223 phase formation as well as critical current densities in various ways. Again the critical current densities in tapes are intimately connected with the c-axis texturing that can be imparted to the 2223 grains. Addition of Ag to the BPSCCO core will increase the Ag/BPSCCO interface area. It is also expected that the Ag particle will

align the grains longitudinally during thermo mechanical treatment while processing the tape by PIT technique.

In addition to high critical current density J_C , practical applications of these superconductors (such as coils, motors and generators) also require high strain tolerance. Strain tolerance is the ability of a superconductor to retain its critical current when subjected to strains. Strain tolerance of BPSCCO tapes in both tensile and bending modes were studied by several authors and observed that the response of the tapes to applied strain depends on the mode of strain applied i.e. uniaxial tension or bending. The strain is more uniform throughout the tape in tension than in bending. In bending there is a distribution of strain across the cross section with maximum compressive and tensile strains experienced by the outer most layers. This sets up a strain gradient, and the effective strain experienced by the core is lower than the applied bend strain. Crack development in the ceramic core of the superconductor is the main cause for the degradation of I_C due to applied strain. The cores in the PIT tapes often neck, sausage or crack due to large difference in the mechanical properties between the Ag sheath and the brittle ceramic superconductor. This mismatch in mechanical properties can be minimised by adding silver in the core.

In view of these aspects, there has been many reports in the literature which addressed the effect of Ag on J_C, T_C, microstructure, texture, mechanical property etc. [1-5] The purpose of the present study is to fabricate Ag sheathed Bi-2223 tapes with various Ag additives in the BPSCCO core and systematically evaluate relative effect of Ag additives on phase formation, microstructure, transport and mechanical properties of (Bi,Pb)-2223 tapes. The chapter is divided into two parts. The first part

which comprises the study on the effect of different kinds of silver additives on phase evolution, microstructure and critical current density in silver sheathed (Bi,Pb)2223 tapes is presented in section 5.2. In section 5.3, the result of strain tolerance and tensile strength of varying percentage of silver added mono and multifilament tapes are discussed.

5.2. Effects of Ag, Ag_2O and $AgNO_3$ Additions in (Bi,Pb)-2223/Ag Powder-In-Tube Tapes

In Ag sheathed BPSCCO tapes; addition of Ag to the precursor can lead to results different from bulk samples especially on phase evolution and J_C in view of the presence of Ag sheath. Therefore, the objective of the present work was to study effect of Ag powder, Ag_2O and $AgNO_3$ on the phase evolution, microstructure and critical current density in BPSCCO-2223/Ag tapes[◙].

5.2.1. Experimental

The calcined 2212 rich sol-gel derived powder having a nominal cation ratio of Bi:Pb:Sr:Ca:Cu = 1.8:0.4:2.0:2.2:3.2 was used as the precursor for the PIT tapes. The details of the powder preparation have been discussed in chapter 2. Requisite wt.% of Ag powder (average particle size 10 μm), Ag_2O (average particle size 2μm) and $AgNO_3$

◙ Published in Physica C **316**, 63 (1999)

crystals were added separately to the precursor and thoroughly mixed in acetone medium. In the case of $AgNO_3$ the mixture was given a short duration (2h) heat treatment at 800°C in air in order to effect the dissociation of $AgNO_3$ and the evolved gases to go out. The uniformly dispersed Ag added precursor together with one batch of pure BPSCCO precursor were analysed by DTA (Shimadzu DTA-50) in static air at 10^0C/min .The powders were then filled into Ag tubes of OD 10.0 mm and ID 7.5 mm with a uniform packing density of 2.7 gcm^{-3}. The powder filled tubes were initially groove-rolled repeatedly into wires of 1.6 mm and then flat-rolled into tapes of 300 μm thickness.

The tapes were sintered initially at temperatures in the range 824 to 837^0C for determining the optimum sintering temperature and then all the samples were sintered at a common optimum temperature of (827 ± 1°C) for a total period of 240 h with three intermediate rolling. The final thickness of the tapes was in the range 150-160 μm .

Characterization such as phase evolution of the tape core at different stages of heat treatment, microstructural examination of polished section of the heat treated tapes, critical current measurements etc were conducted by using the same procedures as described in chapter 2.

5.2.2. Results and Discussion

The DTA curves obtained for pure as well as Ag, Ag_2O and $AgNO_3$ added precursors (10 wt% each) are shown in Fig.5.1. The two endothermic peaks seen in all these curves between 840 and 870^0C correspond to the formation of the liquid phase (first peak) and the melting

of the 2212 phase (second peak) . In pure sample these peaks appear at 848.4^{0}Cand 865.9^{0}C whereas in the Ag added samples they shift downward by 3.6 to 4.6^{0}C (first peak) and 6.4 to 8.8^{0}C (second peak) depending on the type of Ag additive. This means that Ag addition in BPSCCO lowers

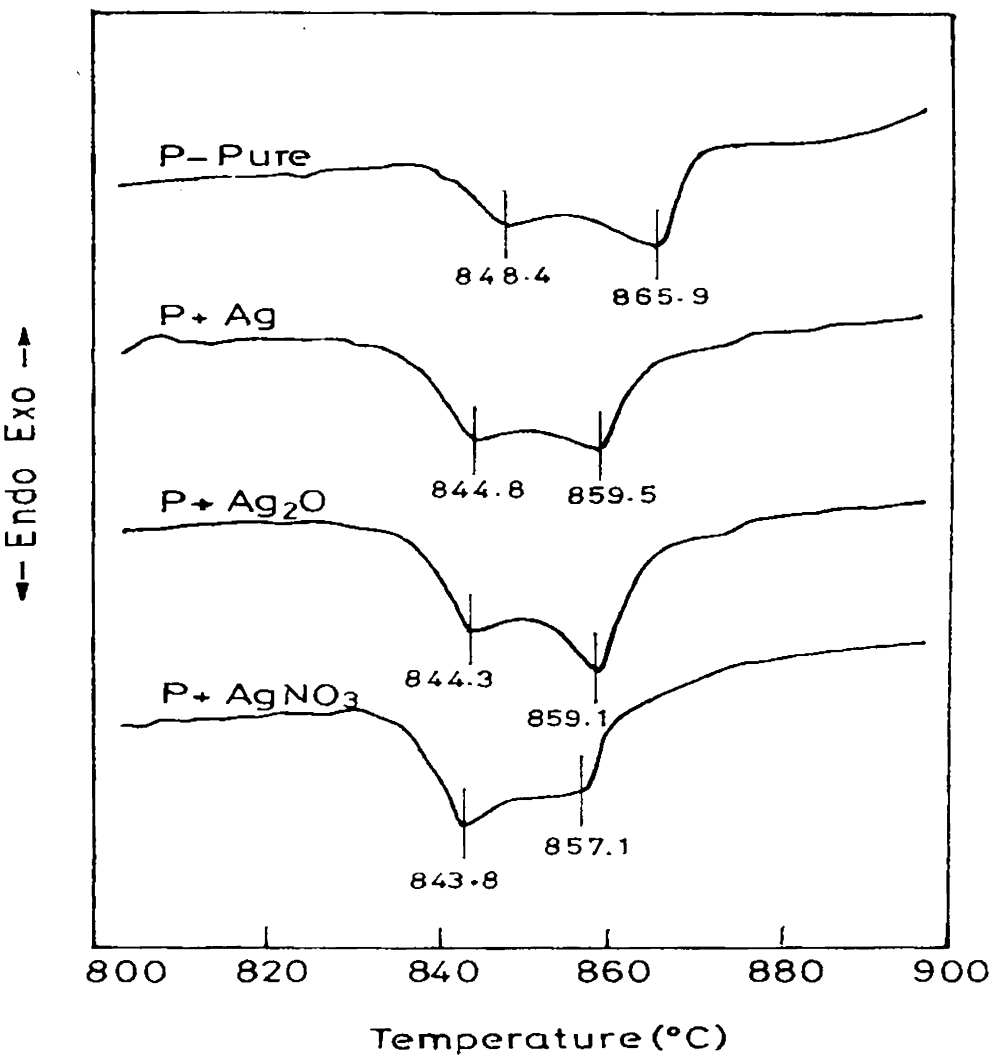

Fig. 5.1. DTA curves of the pure as well as Ag, Ag_2O and $AgNO_3$ added (10 wt% each) precursors

the temperature of liquid phase formation only to a lesser extent compared to the reduction in the melting point of 2212. Since the sintering temperature of BPSCCO is related to the temperature of the liquid phase formation, the optimum temperatures of the Ag added samples will be 3.6-4.6^{0}C lesser than that of the pure sample. In order to determine the optimum sintering temperature, pure BPSCCO/Ag tapes are initially heat treated at temperatures ranging from 824 to 837^{0}C for an overall period of 200h and the I_C values averaged over three samples are plotted as a function of sintering temperature (Fig. .5.2). Here, the samples sintered at 830^{0}C give the best results which indicate that the optimum sintering temperature for pure BPSCCO/Ag tape is close to 830^{0}C. This finding together with the DTA results enabled us to choose a temperature of 827±1^{0}C as a common optimum for sintering both the pure and the Ag added tapes in the remaining studies for a meaningful comparison of the phase evolution and J_C.

The rates of change of the high T_C (Bi-2223) and low T_C (Bi-2212) phases of pure as well as Ag powder, Ag_2O and $AgNO_3$ added (10 wt% each) BPSCCO /Ag tapes with respect to the heat treatment (827°C) duration are shown in Fig.5.3. (Variations of other minor phases such as 2201, Ca_2PbO_4 and CuO are not considered here for discussion and are not presented.) In contrast to the results reported in the previous chapter on bulk pellets, the plots in Fig.5.3 show that Ag addition considerably reduces the rate Bi-2223 formation in Ag sheathed tapes irrespective of the form of additive. It is clear from Fig.5.3 that the tape loaded with pure BPSCCO shows the highest rate of Bi-2223 formation, especially during

the initial stages of heat treatment compared to all the Ag added BPSCCO tapes. The ultimate Bi-2223 phase fraction in pure BPSCCO/Ag tapes is

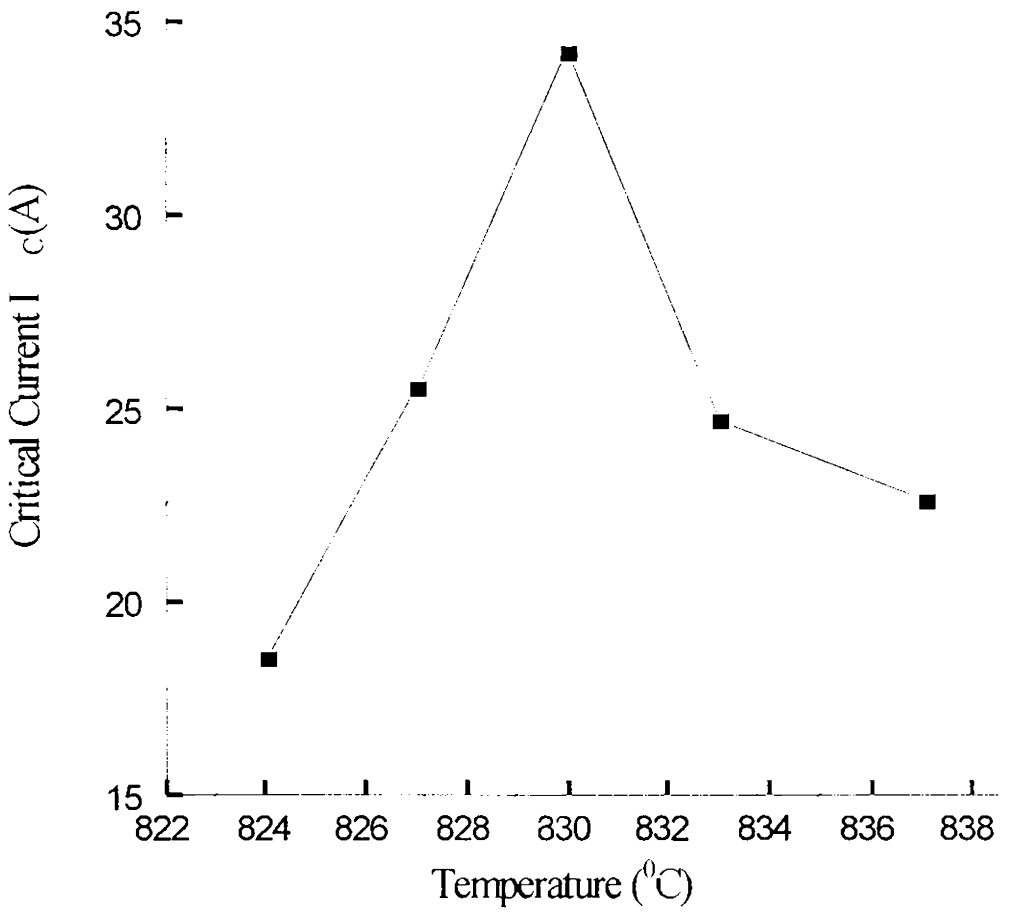

Fig. 5.2. Critical current (I_C) at 77K as a function of heat treatment temperature for pure BPSCCO tape after 200h

found to be 86.3 vol% after a heat treatment duration of 240 h. Among the Ag added tapes, $AgNO_3$ added one shows a distinctly higher rate of Bi-2223 formation throughout the whole range of heat treatment duration

which ultimately leads to 85.1 vol% of Bi-2223 phase. In the cases of Ag powder and Ag_2O added tapes the Bi-2223 formation rates are significantly lower and the ultimate phase fractions are only 70.1 and 75.4 vol% respectively.

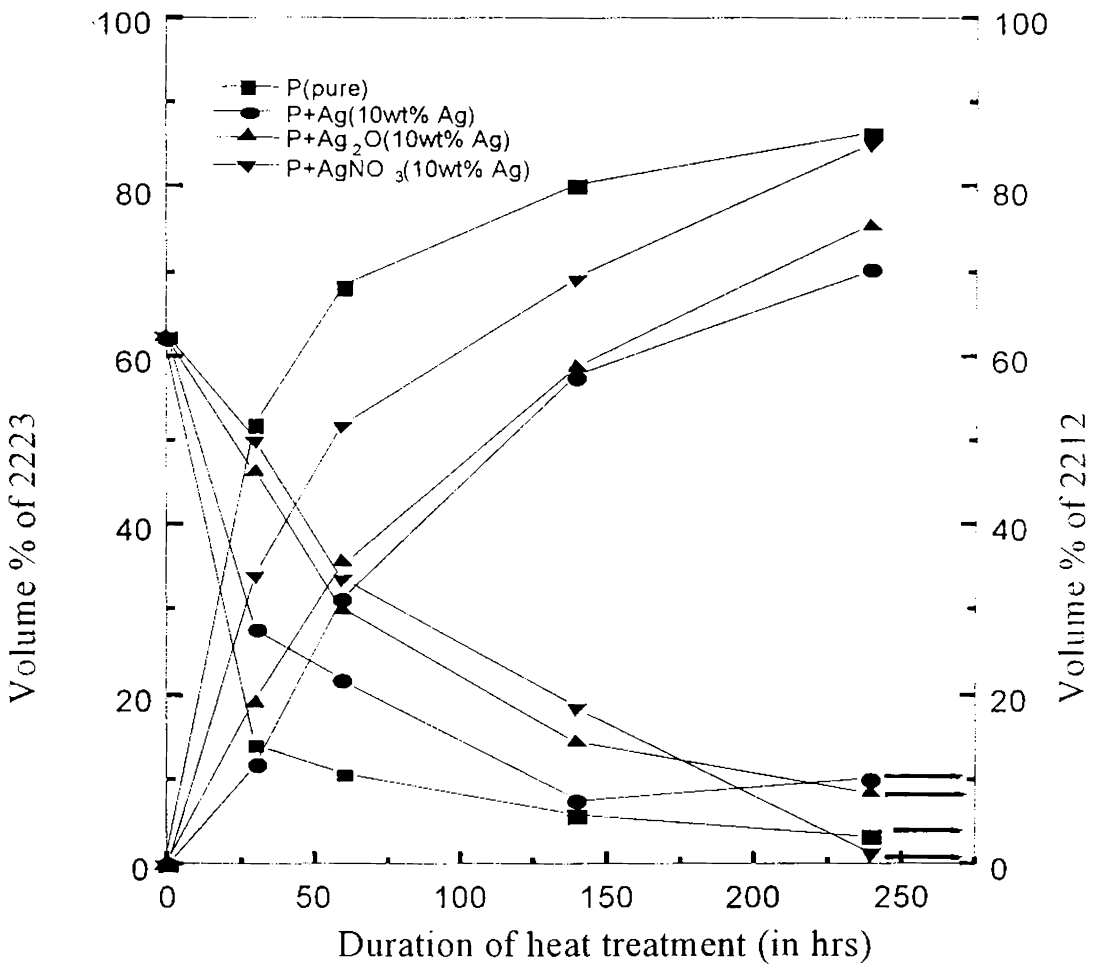

Fig. 5.3. Variation of Bi-2223 and Bi-2212 phase fractions after different durations of heat treatment for pure and Ag added tapes.

The slower rates of formation of the high T_C phase in all the Ag added BPSCCO/Ag tapes, a result contrary to that in bulk BPSCCO sample, can be attributed to the presence of Ag available in tapes in the form of sheath. Studies on bulk BPSCCO samples have shown that an optimum Ag content which depends on the form of Ag additive (viz. Ag powder, Ag_2O or $AgNO_3$) can only yield the best result in promoting the Bi-2223 formation. The present result, therefore, indicates that addition of 10 wt% Ag in any of the above forms apart from the Ag sheath exceeds the optimum limit of Ag. In other words, pure BPSCCO/Ag tape probably has an effective silver content closer to the optimum requirement.

Optical micrographs of the polished sections of pure as well as Ag powder, Ag_2O and $AgNO_3$ added tapes under an identical magnification of 500X are shown in Fig.5.4. The distribution of isolated Ag particles in a matrix of Bi-2223 flakes can be seen in all the Ag added samples wherein the size of the Ag particles is found to depend on the size and form of the Ag additive. The size is largest in Ag powder added samples and smallest in $AgNO_3$ added samples. The microstructures also show a larger grain growth of the high T_C phase in all the Ag added samples compared to the pure sample. This may be due to greater availability of liquid phase in the Ag added samples produced as a result of excessive Ag content.

The critical current densities (J_C) at 77K and self field of pure and Ag added tapes after different heat treatment durations (50,100, 150 and 240 h) are plotted in Fig.5.5. (the J_C values plotted here are the average values of J_C measured over three samples processed in the same batch), It is seen that the J_C values of all the Ag added tapes are lower than those of the pure sample. This is mainly due to the lower volume fractions of the high T_C

phase content in the Ag added tapes. The undesirable microstructure of th Ag added tape core caused by the Ag particles can also obstruct the

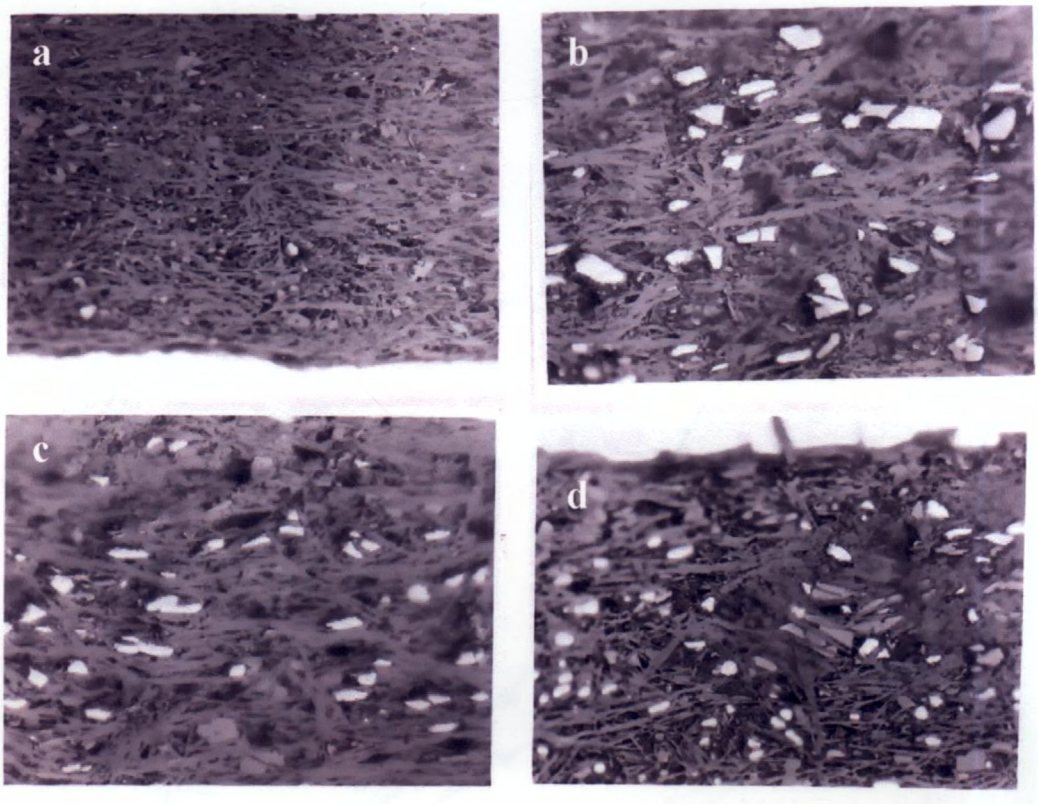

Fig. 5.4. Optical micrograph of the transverse sections of the tape core: (a). pure, (b). Ag powder added, (c). Ag_2O added and (d), $AgNO_3$ added . Magnification: A11 500X

transport current to a considerable extent. This will be clear if we analys the J_C and high T_C fraction results particularly for the pure and AgNO

added tapes after a heat treatment duration of 240 h [Figs.5.3 and 5.5]. Both these samples have comparable high T_C fractions of 86.3 vol% for pure and 85.1 vol% for $AgNO_3$ added samples. However, their J_C values are 31.7 $kAcm^{-2}$ for pure and 18.4 $kAcm^{-2}$ for $AgNO_3$ added samples. This

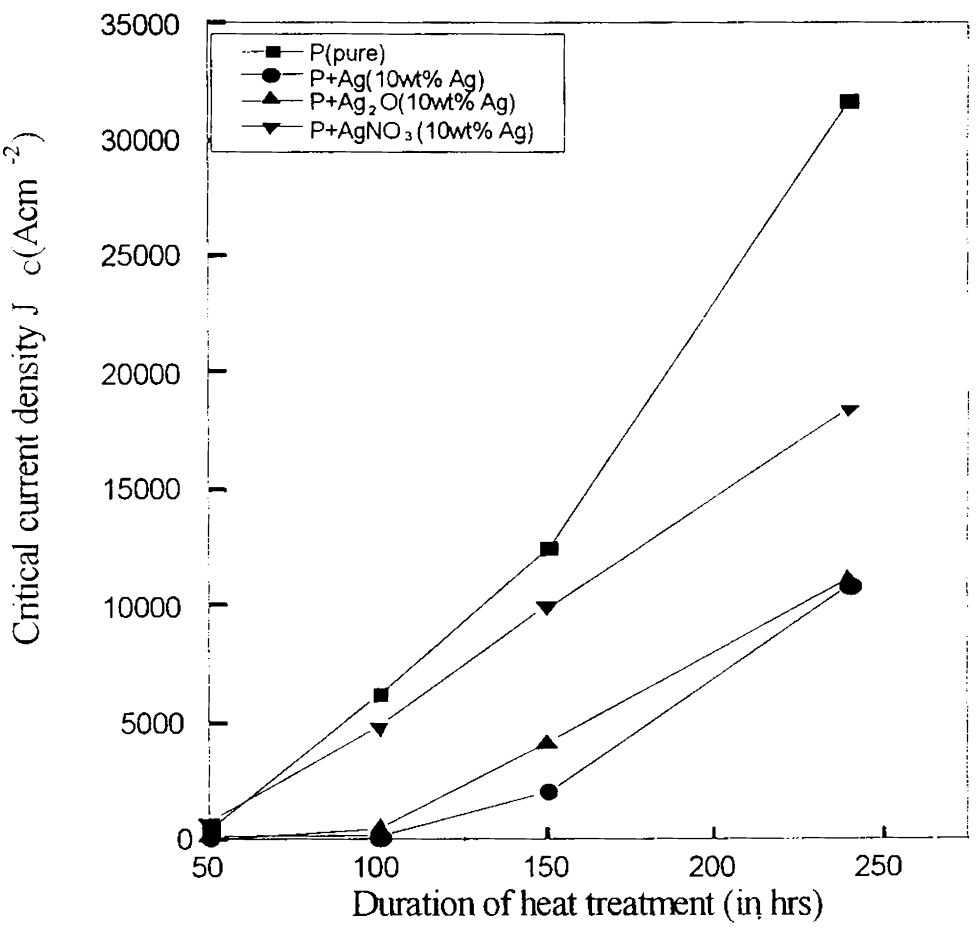

Fig. 5.5. Critical current density (J_C) at 77K as a function of heat treatment duration for pure and Ag added tapes

large difference in J_C can only be attributed to the undesirable morphology of the $AgNO_3$ added tapes since all the tapes are prepared under exactly identical conditions and composition except for the addition of Ag.

Having found that $AgNO_3$ addition has a better effect both on phase formation and J_C among all the Ag additives (Ag content 10 wt%), further studies were conducted on $AgNO_3$ addition with smaller fractions of Ag

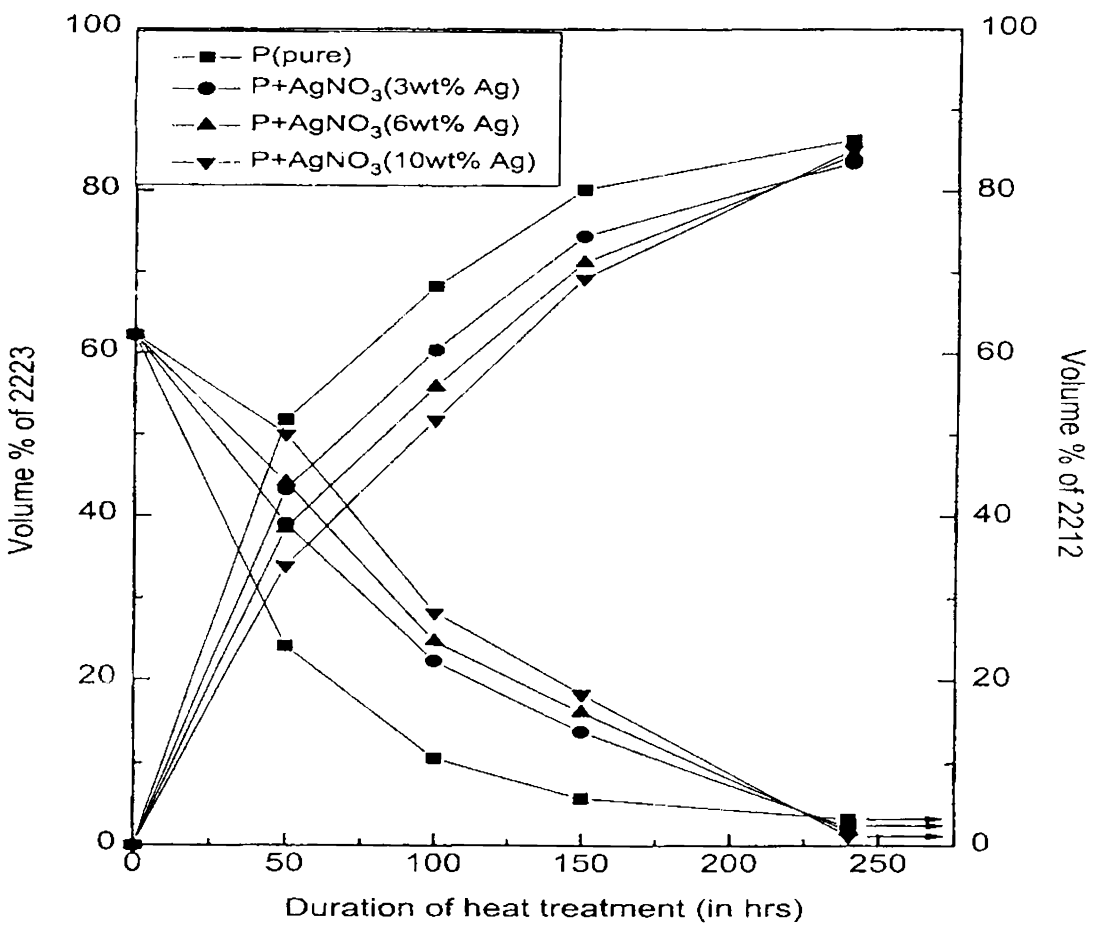

Fig. 5.6. Variation of Bi-2223 and Bi-2212 phase fractions with respect to heat treatment duration for varying percentage of $AgNO_3$ added tapes

(Ag content 0,3, 6 and 10 wt%) with an objective to determine the optimum Ag content for achieving the best results. The variations of Bi-2223 and Bi-2212 phases with respect to the heat treatment duration for these samples are shown in Fig.5.6 and their J_c corresponding to each stage

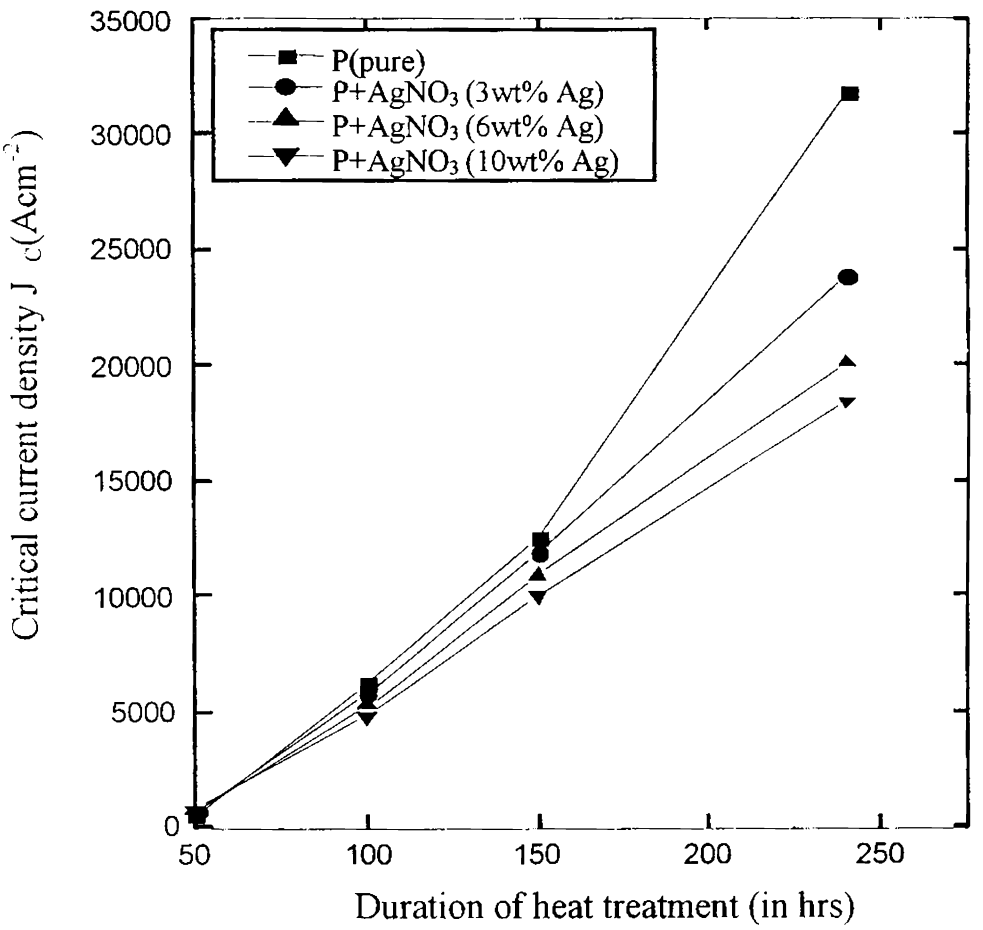

Fig. 5.7. Critical current density (J_C) at 77K and self field as a function of heat treatment duration for varying percentage of $AgNO_3$ added tapes

is plotted in Fig.5.7. It is seen that the rate of high T_c phase formation and the J_C are the highest for pure BPSCCO/Ag tapes and these values decrease with increase in Ag content right from 3 wt% Ag onwards. The result clearly shows that in the PIT processing of BPSCCO -2223 /Ag tapes, the Ag available in the form of sheath is sufficient to impart the beneficial effects of Ag addition found in bulk BPSCCO system and addition of Ag to the precursor in any form apart from the sheath only reduces the high T_c phase and J_c in BPSCCO-2223/Ag PIT tapes.

5.3. Strain Tolerance And Tensile Strength Of Ag Added Mono And Multifilamentary (Bi,Pb)-2223/Ag Tapes

The mechanical properties of (Bi,Pb)-2223/Ag tapes are intrinsically poor since the composite consists of a brittle ceramic core embedded in a ductile metal matrix. The tapes can be utilized for large scale applications such as in magnets, motors, cables etc only if they have sufficient mechanical strength to withstand the mechanical/Lorenz force experienced during processing and service. Several approaches have been investigated to increase the strain tolerance of the BPSCCO tape [6-7]. The strain tolerance/ tensile stress limit of (Bi,Pb)-2223 tape can be improved by adding Ag in different forms [8-11] to the superconducting core, by making the tape in multifilamentary form [12-14] and by alloying and reinforcement of the sheath material [15-16].

The effect of Ag addition in bulk as well as in tape has shown that $AgNO_3$ addition has a better effect on phase formation and J_c compared to

other Ag additives viz. Ag powder and Ag_2O, though there is a marginal reduction in the superconducting properties in general for the Ag added tapes. As a continuation of the above investigations we have carried out a systematic study on the effect of $AgNO_3$ addition on strain tolerance as well as tensile stress of (Bi,Pb)-2223/Ag mono and multifilamentary tapes◙ and the results are reported in this section.

5.3.1. Experimental

(Bi,Pb)-2223/Ag composite tapes were fabricated by the powder-in-tube (PIT) technique .The precursor powder with a composition of $Bi_{1.8}Pb_{0.4}Sr_2Ca_{2.2}Cu_{3.1}O_x$ was well mixed with $AgNO_3$ crystals (Ag:0-7wt%) following the same procedure as we described earlier. Four types of precursor powders were prepared with varying percentage of $AgNO_3$ viz. 0,1,4,7 wt % and filled in Ag tubes of ID/OD 8/10 mm and groove rolled down to ∅ 1.45 mm with intermittent annealing at 500^0C. The groove rolled wires was cut into pieces. One long piece each from all the 4 batches were flat rolled to obtain monofilamentary tapes. The remaining cut pieces of the wires were repacked into another set of tubes of ID/OD 9/10 mm and again grove rolled repeatedly into wires and then flat rolled to make multifilamentary tapes. The heat treatment temperature (830± 1^0C), schedule (30+60+ 100h) and the rolling procedure were same for all the 8 batches. The final thickness of the tapes were 150 μm and 330 μm for

---

◙ Published in Supercond. Sci. Technol. **13**, 1487 (2000)

mono and multifilamentary tapes respectively. Bending mode measurements and Tensile mode measurement in liquid nitrogen was carried out according to the procedures as described in chapter 2.

5.3.2. Results and discussion

5.3.2.1. Bend Strain Tolerance

Figs 5.8(a) and 5.8(b) show the normalized curve I_C (bend)/I_C (0) verses bend strain (%) of pure as well as $AgNO_3$ added mono and multifilamentary tapes. It is clear from the Figs that in all the samples there is no degradation of I_C upto a certain strain limit. This limit, known as irreversible strain limit (ε_{irr}), increases with increasing percentage of Ag.

ε_{irr} of pure monofilamentary tape is 0.175±0.025% and the corresponding bending diameter is 43±6 mm. The ε_{irr} value observed here agrees with generally observed values [6, 8]. By the addition of 1 wt% Ag the ε_{irr} increases from 0.175 to 0.225%. Similar improvement is observed in 4 wt% as well as 7 wt% $AgNO_3$ added samples. ε_{irr} of 7 wt% $AgNO_3$ added tape is found to be two times higher than that of pure, i.e. strain tolerance has improved from 0.175 to 0.36%. Bend strain limit and bending radius for 100% and 90% I_C retention and corresponding standard errors are given table 5.1.

Microstuctural studies [Fig. 5.4] have shown that addition of Ag increases the grain size of the high T_C phase due to the presence of higher fraction of liquid phase formed during sintering. Ag also reduces the porosity of the microcomposite specimen and the uniform distribution of

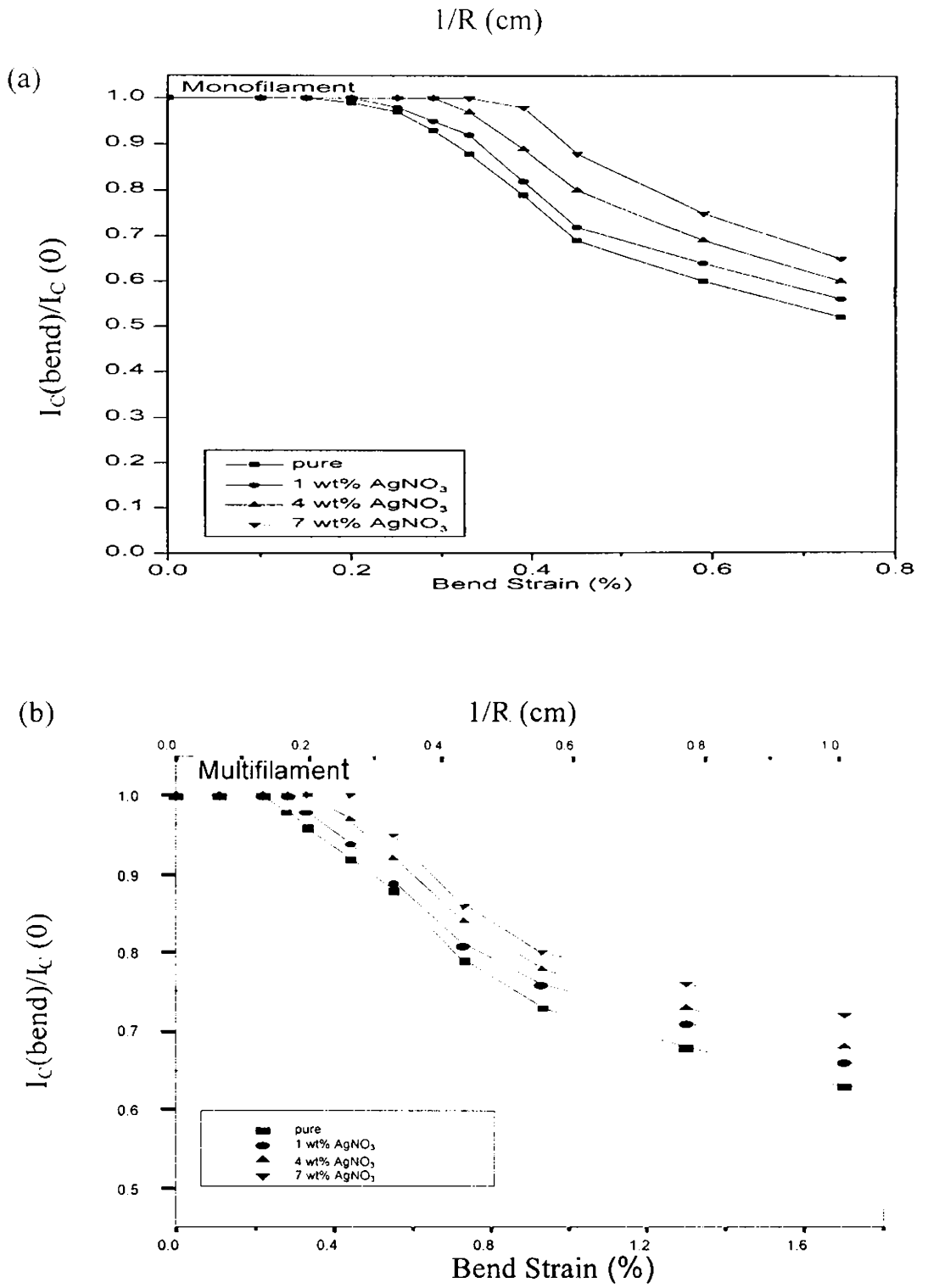

Fig. 5. 8 .Normalized I_C as a function of bend strain for varying % Ag added (a) Mono, (b) Multifilamentary Bi-2223/Ag tapes

the ductile silver particles in the matrix can relax the stress resulting from the expansion anisotropy of the grains and provide increased resistance to crack propagation by pinning the propagating crack and thereby increases the strain tolerance of the matrix.

The strain tolerance of the multifilamentary tape is found to be more than two times of that of monofilamentary tape (Fig. 5.8b & Table 5.1). ε_{irr} of the 25 filament multifilamentary tape is 0.39 ± 0.015% and the corresponding bending radius is 45±2mm. Similar to the monofilamentary tapes, in multifilamentary tapes also strain tolerance increases with

Table 5.1. Bend strain limits for pure and Ag added (Bi,Pb)-2223/Ag mono and multifilamentary tapes

Tape Specification	Strain limit (%)		Bending radius (mm)	
	100% I_C retention	90% I_C retention	100% I_C retention	90% I_C retention
MONO				
Pure	0.175±0.025	0.295±0.020	43±6	25±2
1 wt% $AgNO_3$	0.225±0.025	0.360±0.030	33±4	21±2
4 wt% $AgNO_3$	0.310±0.020	0.390±0.010	24±3	19±.5
7wt% $AgNO_3$	0.360±0.030	0.420±0.030	21±2	18±1
MULTI (25 filaments)				
Pure	0.390±0.015	0.640±0.010	45±2.0	27±0.5
1wt% $AgNO_3$	0.420±0.015	0.710±0.020	42±1.5	24±0.7
4wt% $AgNO_3$	0.490±0.015	0.780±0.010	36±1.0	22±0.3
7wt% $AgNO_3$	0.580±0.015	0.860±0.025	30±2.0	20±0.6

increasing percentage of Ag. The remarkably high ε_{irr} values observed in the multifilamentary tapes can be attributed to the following reasons. Here, the brittle ceramic core is subdivided into thinner filaments, each of which is embedded in the ductile silver matrix. Similarly, the area of the Ag-superconductor interface, a very thin layer through which most of the supercurrent flows, is more in multifilamentary tapes than in monofilamentary tapes.

5.3.2.2. Tensile Stress Tolerance

I_C (load) /I_C (0) verses tensile stress plots of mono and multifilamentary tapes are shown in Fig. 5.9 (a) and 5.9 (b). The tolerable stress for 100% and 90% I_C retention in respect of mono and multifilamentary tapes are given in Table 5.2. It can be seen that multifilamentary tapes show better stress tolerance than monofilamentary tapes. The tolerable stress for 100% and 90% I_C retention in respect of pure samples of mono and multifilamentary tapes are 38 ± 2.5 MPa and 54±1 MPa respectively. The higher stress tolerance observed in multifilamentary tapes is obviously due to the higher fraction of Ag content available in multifilamentary tapes. Addition of Ag also increases the stress tolerance of both mono and multifilamentary tapes almost in an identical manner. 7 wt% Ag addition improves the stress tolerance from 38±2.5 MPa to 54±2.5 MPa in monofilamentary tapes and from 54±1 MPa to 74±1 MPa in multifilamentary tapes. The higher stress tolerance observed in the Ag

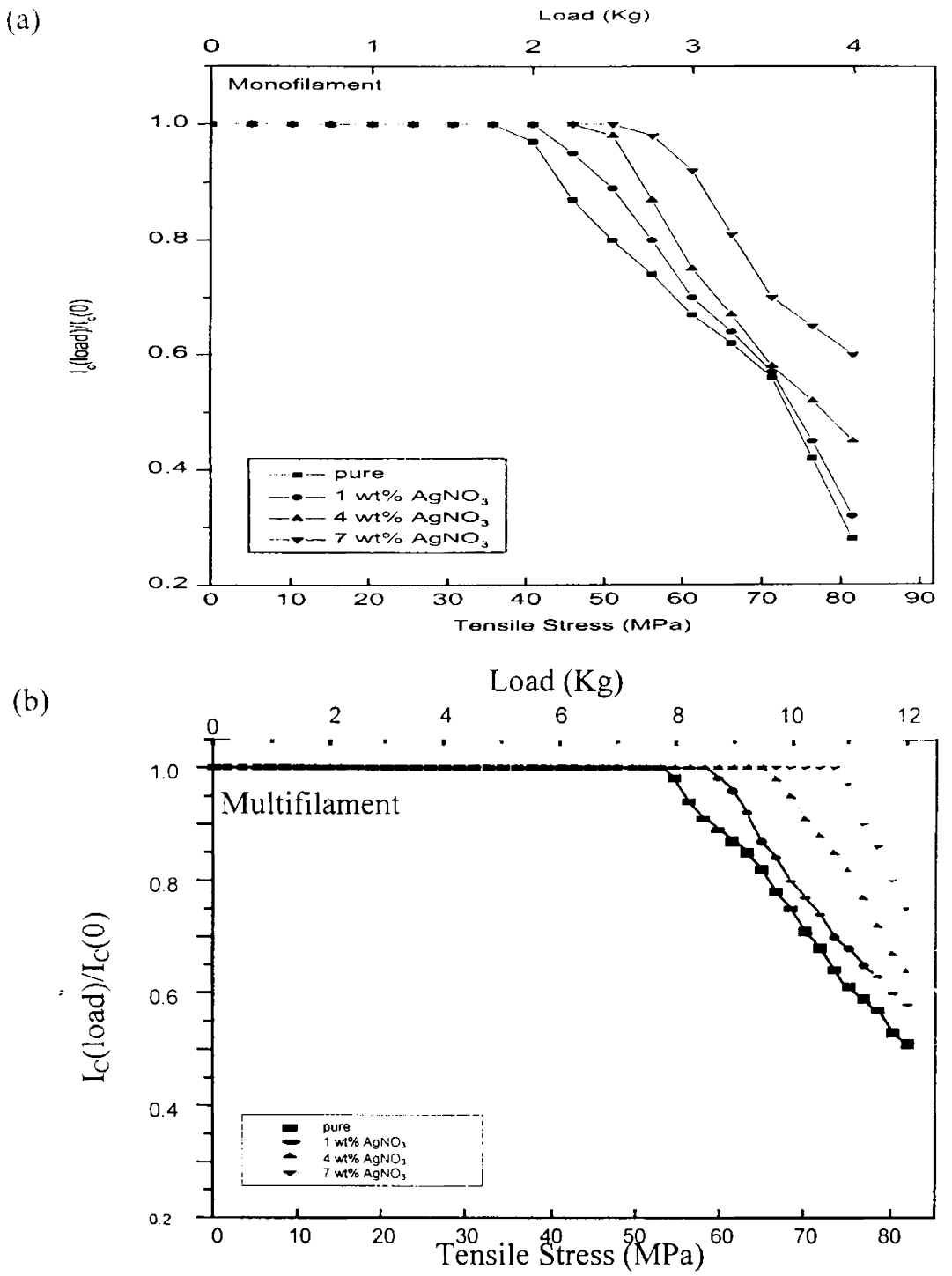

Fig. 5.9. Normalized I_C as a function of tensile stress for varying % Ag added (a) mono and (b) multifilamentary Ag/(Bi,Pb)-2223 tapes

added tapes can be attributed to the improved microstructure of the superconductor core due to Ag addition as explained under strain tolerance.

Table 5.2. Tensile stress limits for pure and Ag added (Bi,Pb)-2223/Ag mono and multifilamentary tapes

Tape specification	Tolerable stress (MPa)	
	100% I_C retention	90% I_C retention
MONO		
Pure	38±2.5	43±2.5
1wt% $AgNO_3$	43±2.5	48±2.5
4wt% $AgNO_3$	48±2.5	54±2.5
7wt% $AgNO_3$	54±2.5	64+2.5
MULTI (25 filaments)		
Pure	54±1	59±1
1wt% $AgNO_3$	59±1	64±1
4wt% $AgNO_3$	66±1	71±1
7wt% $AgNO_3$	74±1	78±1

5.4. Conclusions

(i) In contrast to the results reported for bulk BPSCCO, Ag addition in(Bi,Pb)- 2223 /Ag tapes reduces the rate of high T_c phase formation , ultimate high T_c phase fraction and J_c to different extents depending on the form of Ag additive viz. Ag powder, Ag_2O and $AgNO_3$.

(ii) In Ag powder and Ag_2O added tapes the reduction in the above properties are significant while in $AgNO_3$ added samples the reduction is only to a lesser extent.

(iii) Microstructural examination shows all forms of Ag additive cause larger grain growth of the high T_c grain . The Ag particle size distribution depends on the size and form of the Ag additive.

(iv) The lower J_C values observed in the Ag added tapes are found to be mainly due to the lower volume fractions of the ultimate high T_C phase content and the undesirable morphology of the Ag added tape core.

(v) The bend strain tolerance and tensile stress tolerance of (Bi,Pb)-2223/Ag tapes are found to improve remarkably as the Ag content in the matrix increases. The improvement in mechanical properties of the Ag added tapes is attributed to the improved microstructure of the tape core

(vi) Multifilament tape can withstand higher strain and stress than monofilament due to higher content of Ag fraction in the sheath and larger Ag- superconductor area

(vii) The irreversible strain limit of the monofilamentary tapes (0.175 ±0.025%) increases by about two fold (0.360±0.030%) by the addition of 7 wt% Ag and more than two fold by fabricating them in multifilamentary conFig.uration.

(viii) An overall assessment of the results shows that the marginal reduction of J_C can be well tolerated on account of the substantial increase in their strain limit and stress tolerance.

References

[1] S.X. Dou, Y.C. Guo,R.K. Wang, M. Ionescu, H.K.Liu, *Appl. Phys. Lett.***56,** 493(1990)

[2] Y. Ishida, J. Matsuzaki, T. Kizuka and H. Ichinose, *Physica C*, **190**, 67 (1991)

[3] A. Oota, T. Horio, K. Ohba and K. Iwasaki, *J. Appl. Phys.* , **71** , 5997 (1992)

[4] A.K.Sarker, I. Maartense, and T.L. Peterson, *J. Mater. Res.*, **7,** 1672(1992)

[5] I. Kusevic, E. Babic, M. Prester, S.X.Dou, and H. K. Liu, *Solid State Commun.* **88**, 241 (1993).

[6] K.Sato,T.Hikata,H.Mukai,M.Ueyama,N.Shibuta,T.Kato,T.Masuda , M.Nagata,K.Iwata, and T.Mitsui *IEEE Tran .Magnetics* **27(2)** 1231-1238 (1991)

[7] S.Ochiai, K.Hayashi and O.Samira, *Cryogenics* **31,** 954(1991)

[8] S.Salib and Vipulanandan *Mater.Res.Bull* Vol **32** No.10 1333(1997)

[9] Singh J.P , J .Joo, N.Vasanthasundaram and R.B. Poeppel. *J.Mater. Res.* **8,** 2458(1993)

[10] R. Zhou, W.L. Hults, J.F. Bingert, J.Y. Coulter, E.J. Peterson, J.L.Smith *Physica C* **249**,166(1995)

[11] M.Polak ,J.A. Parrell ,A.A. Polyanaskii, A.E.Pashitski and D.C. Larbelestier, *Appl.Phys.Leit.***70,** 8 (1997)

[12] M.T.Malachevsky, D.A. Esparza *Physica C* **324,** 153(1999)

[13] Gherardi L,Ceracino P,Metra P, Vellego G, Published in "Processing of Long Length of Superconductor" edited by

U.Balachandran et al 147 (1994)

[14] L.R.Motowidlo, P. Haldar, S.Jin, and N.D. Spencer, *IEEE Trans. Appl. Supercond.* **3,** 942(1993)

[15] J.K Sykulski, K. F Goddard and R. L. Stoll, Proceedings of ICEM 1998 Istanbul Turkey ,pp 971-975 ISBM 975-429-1252-4 Sept (1998)

[16] C.King, K.Herd, T.Laskaris, A.Mantone, *Advances in Cryogenic Engineering* **42** 855-861(1996)

CHAPTER 6

PROPERTIES OF Ag SHEATHED (Bi,Pb)-2223-Ag NANOCOMPOSITE PREPARED BY SOL-GEL METHOD

6.1. Introduction

We have found from the previous chapter that even though silver addition improves the mechanical properties of the tape considerably, it slightly reduces the critical current density. Improved critical current density is also equally important for the utilization of high temperature superconductor in electric power application. In Bi-2223 superconductors one of the main problems on the way to better conductors is the insufficient understanding of the different mechanisms limiting the J_C. However, it is known that an improved of grain connectivity accompanied by both grain alignment and densification will strengthen the transport current. [1-4]

We have seen from the microstructure of silver added tapes in the previous chapter (Fig. 5.4) that the silver particles are much thicker than the plate like high T_C (2223) grains. Again, the plate like high T_C grains are formed through a very slow process of the crystal growth, silver particles tend to reduce their surface area during the sintering because silver has a very large surface tension. For the same reason small silver particles tend to agglomerate into larger particles which adversely affect the grain

connectivity, grain alignment, densification and flux pinning strength and there by reduces the J_C.

In all the experiments carried out so far, silver was added to the calcined precursor and was mixed mechanically before putting it directly into the silver tube. Due to the limitations of mechanical mixing, the distribution of silver may not be uniform and the tendency for agglomeration may also be higher. Moreover, the wider particle size distribution of silver severely affects the performance of the ceramic composite. Precursor with well-dispersed ultra fine silver particles is therefore essential for development tapes with good superconducting and mechanical properties. An attempt is made here to synthesis such precursor by wet chemical methods so as to introduce silver at the molecular level. Bi-2223-Ag nanocomposites are prepared using these precursors with an intension to utilize the super plasticity of fine grain structure where the well-dispersed fine silver grains can resist grain coarsening as well. Since silver is introduced at the molecular level, very fine Ag mixed ceramic powder can be obtained on calcinations. Smaller silver grains can also act as pinning sites of the magnetic flux and thus improve the critical current density. The results of the studies on the preparation and characterization of Ag/Bi-2223-Ag nanocomposite tapes and optimisation of silver required for improving the transport property in mono and multifilamentary tapes are presented in this chapter. It has been found that silver addition in molecular level enhances the phase formation and J_C compared to other forms of additives.

6.2. Experimental

The powder for calcinations was synthesised from freshly prepared nitrate solutions of Bi, Pb, Sr, Ca, Cu and Ag by sol- gel method via an acrylate route as described in chapter 2. The initial cation stoichiometry was $Bi_{1.8}Pb_{0.4}Sr_2Ca_{2.2}Cu_{3.1}Ag_xO_y$ (x-> 0,1,3,6 wt%). After calcinations all the four precursor were filled into four different Ag tubes of identical dimensions (OD/ID : 10/8mm, length 10cm) with a packing density of 3g/cc. For the monofilamentary tapes the powder filled tubes were groove rolled to ϕ1.45 mm and then flat rolled to a thickness of 280 μm. For the multifilamentary tapes pure Ag sheathed wires of ϕ 1.45 were filled into another Ag tube of OD/ID : 10/8.5mm, which were further groove rolled to ϕ 2.8 mm and then flat rolled to a thickness of 450 μm. Filament count for the multifilamentary tape was 25. Heat treatment was performed in three stages at 830^{0}C with two rolling steps in between for a total duration of 190h. The final thickness of the monofilamentary tape was150 μm and that of multifilamentary tape was 300 μm. Mono and multifilamentary tapes were characterized by XRD, SEM, and the transport current measurement with and without the application of the field using the same procedure as described in chapter 2.

6.3. Results and discussion

Table 6.1 gives the volume fraction of all the phases at different stages of heat treatment. The phases detected are Bi-2223, Bi-2212, Bi-

2201, Ca_2PbO_4, CuO and Ca_2CuO_3. The details of phase fraction calculations are described in chapter2.

Here the volume fraction at 0h represents the phases available in different samples after the calcination stage. The volume percentage of Bi-2212, which is the main ingredient for the formation of Bi-2223, and the Bi-2201 are found to be marginally lower in Ag added precursor compared to the pure one. But the impurity phases such as Ca_2PbO_4 and Ca_2CuO_3, which are the main ingredients for the liquid phase, are more in Ag added precursors. As the Ag content increases the fraction of Bi-2212 and Bi-2201 decreases while Ca_2PbO_4, Ca_2CuO_3 increases. CuO is found to be very less in Ag added precursors and it is below the detectable limit in 3 wt% and 6 wt% Ag added precursors.

The volume fraction of Bi-2223 after 90 h of sintering (Table 6.1) increases with increase in silver percentage upto 3 wt% and then it decreases. Till the final stage of heat treatment the same trend continues and the sample AN3 yields highest volume fraction of Bi-2223 phase (90.1 %) and AN1 with 89.7 %. The least volume fraction of Bi-2223 is yielded by the 6 wt% Ag added sample (86.4 %), which is close to the pure sample (87.1 %). The results show that even in Ag sheathed tapes, it is possible to increase the formation rate and the final phase content of bi-2223 by incorporating Ag into the system at the molecular level. In the case of bulk pellets it is easier to achieve better reaction kinetics through the introduction of Ag by ordinary methods like mechanical mixing as described in chapter 4.The increased formation of 2223 phase in silver added tape is due to the increased reaction kinetics in presence of Ag as it reduces the partial melting point of the system. The lower melting point

Table. 6.1. Phase assemblage of (Bi, Pb)-2223/Ag tapes at different stages of heat treatment

Samples	Phases	Volume fraction of different phases			
		Duration of heat treatment			
		0h	90h	140h	190h
AN0	Bi-2223	0	53.2	68.7	87.1
	Bi-2212	66.1	18.1	11.8	2.8
	Bi-2201	3.8	2.7	1	0
	Ca_2PbO_4	23.6	20.3	14	7
	CuO	2.6	3.7	2.3	1.2
	Ca_2CuO_3	2.9	2	2.2	1.9
AN1	Bi-2223	0	59.5	73.1	89.7
	Bi-2212	65.9	15.8	8.6	2
	Bi-2201	3.4	3.8	1.8	1
	Ca_2PbO_4	25.8	16.6	13.1	5.1
	CuO	2.2	1.7	1	.7
	Ca_2CuO_3	3.7	2.6	2.4	1.5
AN3	Bi-2223	0	67.2	80.7	90.1
	Bi-2212	63.6	6.1	2.1	1.5
	Bi-2201	3.1	6.5	3.2	1
	Ca_2PbO_4	28.9	15	10.9	5.8
	CuO	0	2.8	1.2	.5
	Ca_2CuO_3	4.4	2.4	1.9	1.1
AN6	Bi-2223	0	51.2	65.8	86.4
	Bi-2212	62.6	6.7	4.7	1.7
	Bi-2201	2.6	10.9	7.1	1
	Ca_2PbO_4	30.2	23.3	16.7	9.1
	CuO	0	5.2	3.9	1.1
	Ca_2CuO_3	4.6	2.7	1.8	.7

along with uniform distribution of very fine Ag particles results in an increased interaction between silver and the ceramic core through out the whole cross section. This is consistent with the finding [5] that the phase conversion is largest at the sheath core interface. However greater percentage of silver, can lead to agglomeration due to closer interparticle distance. The present experiment shows that the maximum limit of silver that can be added to the system with favourable superconducting properties lies between 3 wt% and 6 wt%. It is noted already in the previous chapter that Ag additions even as low as 3 wt% only reduces the high T_C phase formation in the Ag sheathed tapes if added to the precursor by physical means.

SEM Micrograph of the transverse section of different percentage of Ag added samples taken in the back-scattered mode is shown in Fig. 6.1. Samples for SEM analysis were prepared by etching the sheath metal off by a solution containing 50 vol% H_2O_2 and 50 vol % NH_4OH . Sectional morphology shows that the connectivity, relative density as well as grain size are improving with increase in Ag content in the matrix upto 3 wt%. We can see from the Fig. that silver particles are distributed uniformly in the core in 1 wt% and 3wt% Ag added sections. But higher Ag content will cause a agglomeration of Ag particles during heat treatment and leads to weak links at grain boundaries as well as voids. These large particles also hinder the path of the transport current.

The critical current density of mono and multifilamentary tapes at different stages of heat treatment is shown in Fig. 6.2(a) and 6.2(b) respectively. In all the stages of heat treatment J_C increases with increase in silver content upto 3 wt% in both mono and multifilamentary tape and then

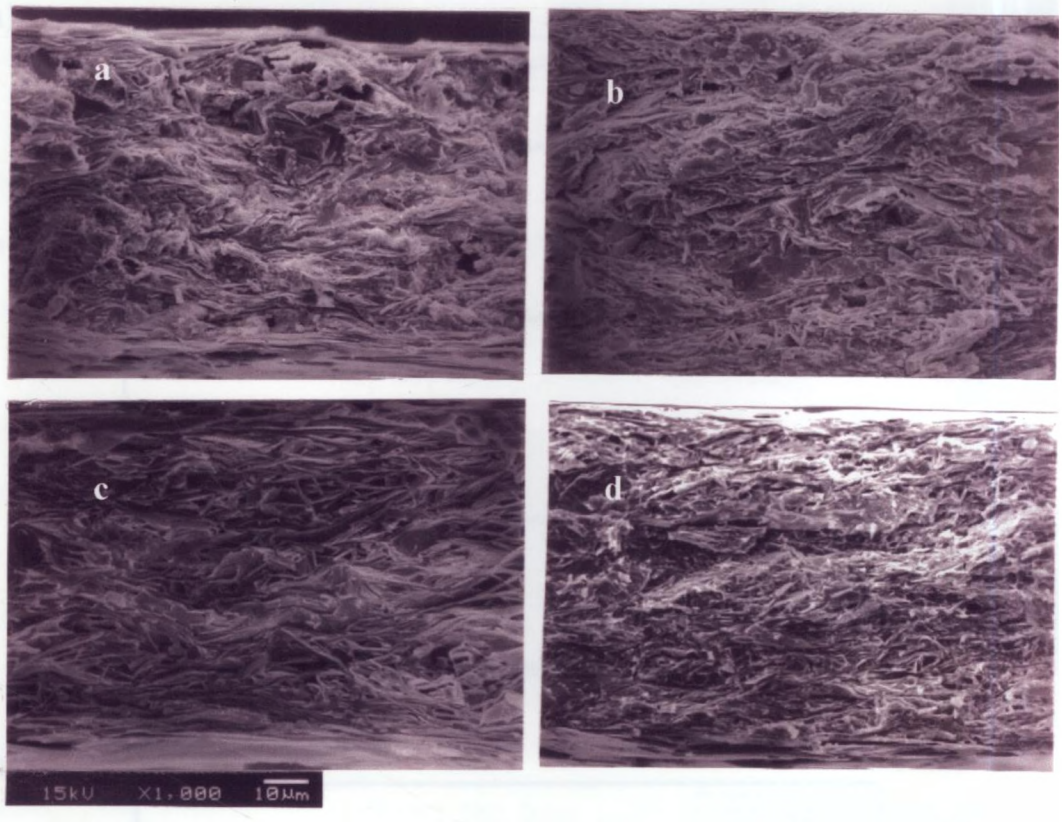

Fig. 6.1. SEM Micrograph of the transverse section of Ag added samples (a). AN0, (b). AN1, (c). AN3 and (d). AN6.

decrease with further addition. Among all the samples AN3 and MAN show the highest J_C values for the mono and multifilamentary tape respectively. As discussed earlier the increase in J_C is attributed to th increased Bi-2223 fraction, larger grain growth, and better connectivit between the grains as a result of Ag addition in molecular level. Eve though the rate of formation of Bi-2223 phase in pure sample and th highest silver doped sample are comparable, the J_C value has a margina difference. Silver improves the intergranular properties of ceramics by

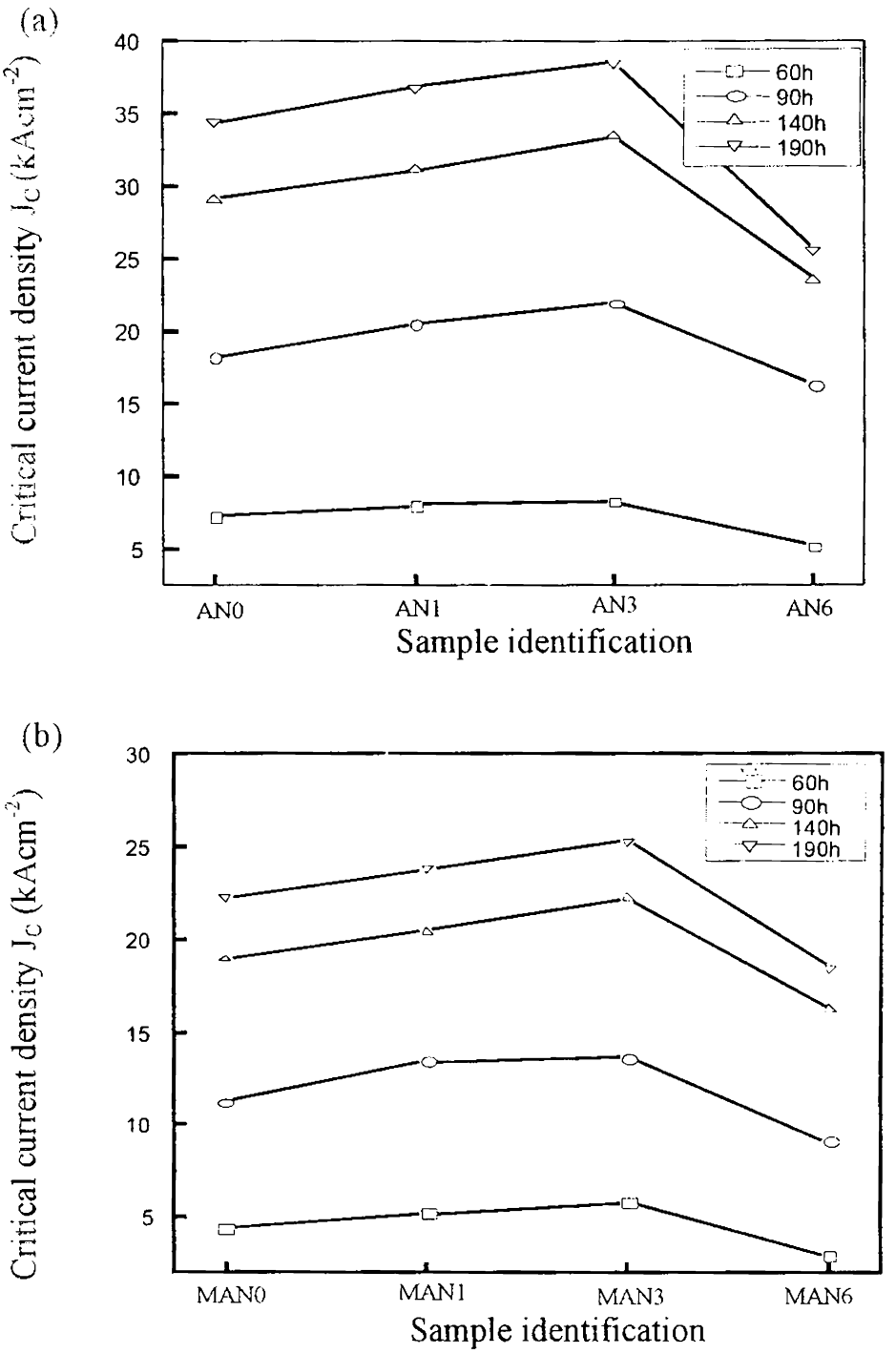

Fig. 6.2. Critical current density (77K) of (0-6 wt%) Bi-2223/Ag tapes: (a) mono and (b) multi.

filling the voids, reducing the cracks, diminishing the normal resistivity between the grains and preventing the intergranular flux creep etc. In turn, the increase of silver content above the optimum limit results in substitution of SNS-type for SIS type junction in doped materials. As a result, the heavily doped samples (AN6 and MAN6) have shown the least J_C in all stages.

The critical current (I_C) dependence on magnetic field was measured to investigate the effect of silver doping on the I_C behaviour in magnetic field. Fig. 6.3(a) and 6.3(b) show the I_C-B characteristics normalized with zero field I_C for all the mono and multifilamentary tapes. Sharp drop in I_C for small fields reflects the presence of weak links. This effect is smallest in AN3 and largest for AN6. In the higher field region (>100G) the weak links substantially decrease and the strongest current links are present in samples. The sample AN3 shows the best I_C-B behaviour among all the tapes and the sample AN6 shows maximum degradation with unusual reduction at higher fields. The performance of a superconductor materials in a magnetic field mainly depends upon the degree of grain alignment, grain connectivity and flux pinning [6-7]. Ag addition improves the weak links between the grains of the high T_C phase, which strengthen the transport path, and it helps to heal the cracks in a more effective manner during sintering. More than that small Ag can act as flux pinners. But higher silver addition causes agglomeration of silver grains leading to grain misorientations and this becomes more pronounced with increasing silver content. This may be the reason for slight improvement of J_C-magnetic field characteristics observed in the AN3 tape compared to pure sample,

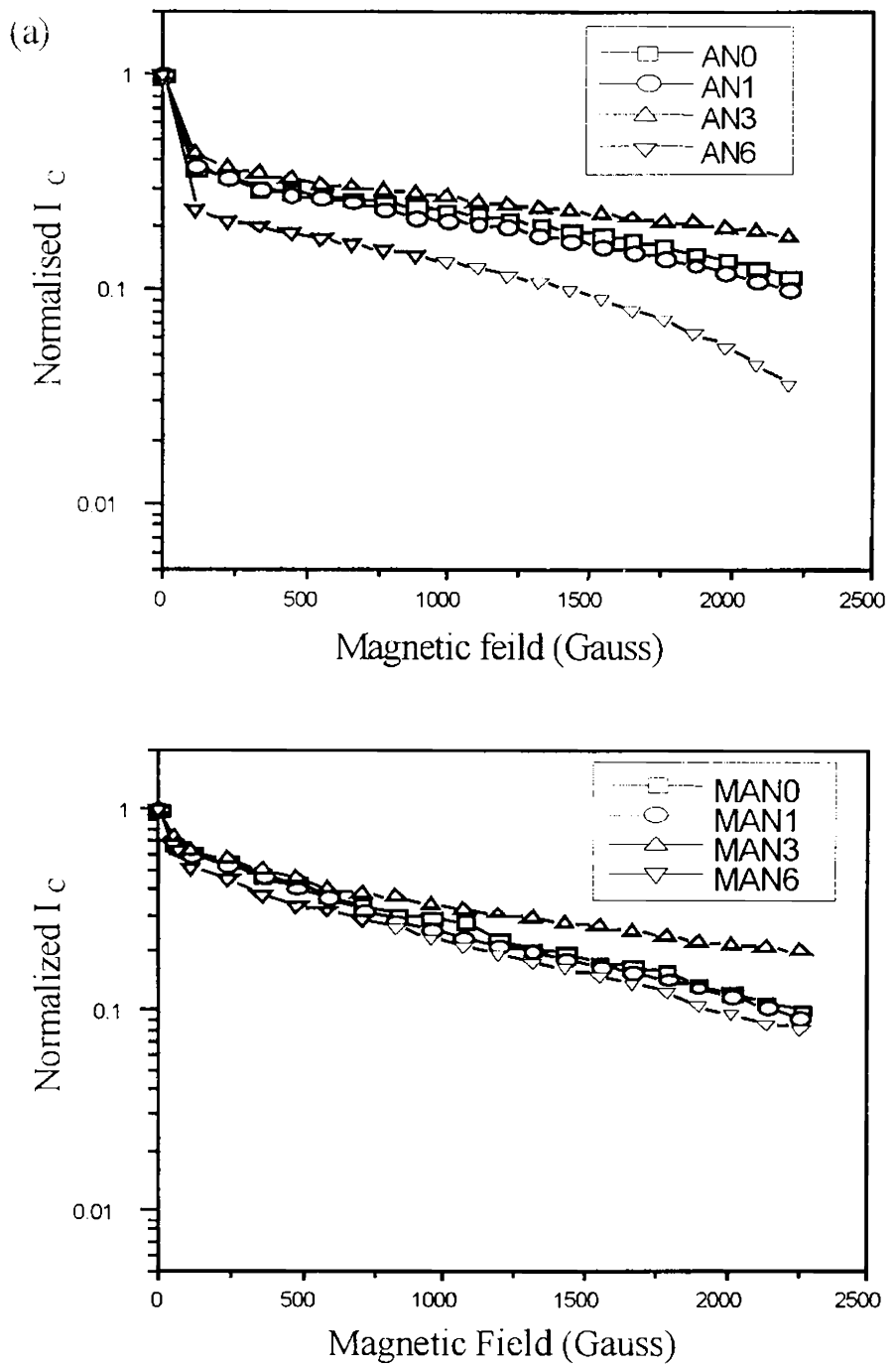

Fig. 6.3. Normalized I_C at 77K for the fully processed (a). Mono and (b). Multifilamentray tapes with the applied field parallel to the c-axis.

while a degradation is observed in AN6 tape. In multifilamentray tapes also, 3 wt % silver added tape shows a slight improvement in J_C –B characteristics while the pure sample as well as higher percentage of silver added tape show almost identical characteristics.

6.4. Conclusions

(i) Silver addition in molecular level enhances the phase formation as well as J_C of (Bi,Pb)-2223/Ag tapes compared to other forms of addition.

(ii) Even though the ultimate phase fraction of Bi-2223 in Ag added samples are not far different from those of pure sample, the J_C of the Ag added samples show definite improvement over the pure sample.

(iii) Critical current density of 1wt% and 3 wt% Ag added samples are higher than the pure sample of which 3 wt% Ag added sample show the highest J_C. Higher Ag addition (6 wt%) causes agglomeration of Ag particles leading to grain misorientation and reduced J_C.

(iv) 3 wt% silver added tape shows improvement in J_C-B characteristics and all the other samples show more or less same behaviour, except for the 6 wt% silver added monofilament tape in which the reduction of J_C is higher.

References

[1]. J. Jiang, X. Y. Cai, A. A. Polyanskii, L. A. Schwartzkopf, D. C. Larbalestier, R. D. Parrella, Q. Li, M. W. Rupich and G. N. Riley Jr, *Supercondct. Sci.Technol.* **14,** 548 (2001).

[2]. L. A. Schwartzkopf, J. Jiang, X. Y. Cai,D. Apodaca, and D. C. Larbalestier, *Appl. Phys. Lett.* **75**, 3168 (1999)

[3] J. A. Parrell, D. C. Larbalestier, G. N. Riley Jr, Q. Li, W. L. Carter, R. D. Parrella, and M. Tepliski *J. Mater. Res.* **12**, 2997 (1997)

[4] Q.Li, K.Brodersen, H. A. Hjuler, T. Freltoft, Physica C**217,** 360 (1993)

[5] Z. Li, L. Law, S. Fisher, C. Beduz, Y. Yang, R. Scurloc, *Physica C* **254,** 193(1995)

[6] Y. C. Guo, H.K. Liu, and S. X. Dou, *Appl. Supercond.* **1-2,** 25(1993)

[7] M.P. Maley, *J. Appl. Phys.* **70,** 6189(1991)

CHAPTER 7

PREPARATION AND CHARACTERIZATION OF LONG MULTIFILAMENTARY Ag/(Bi, Pb)-2223-Ag COMPOSITE SUPERCONDUCTING TAPES

7.1. Introduction

Significant progress has been made in producing long lengths of high temperature superconductors in the form of silver sheathed mono and multifilament tape [1-5]. However several technological requirements need to be overcome in order to use these novel materials in commercial applications. The incorporation of Bi-2223 tape conductors in power applications such as motors, generators, transformers, and high field magnets still require improvements in the following properties.

- The composite should carry high levels of overall current density.
- The ceramic superconductors should also have significant tolerance to strain effects usually encountered during coil winding and /or Lorenz forces during operation.

Work described in the previous chapters was mainly concentrated on finding out the optimum particle size, suitable form and optimum

percentage of silver to be added to the system for better superconducting and mechanical properties in short length tape. [6] The main purpose of undertaking these elementary studies has been to gather information useful for making long length Ag/BPSCCO composite superconducting tapes. At the present time monocore tapes have a strain tolerance below the required values for most applications. [7-9] Thus multifilamentary configuration is a need for large-scale applications. Multifilamentary configuration has several other advantages also such as

- Parallel electrical conduction to serve as a bypass in case of local failure
- Better heat sink
- Improved strain tolerance and mechanical strength
- Reduced ac losses and
- Better protection from atmospheric environment

However, a major part of the work presented in the previous chapters is on short length monofilamentary tapes. But the crucial aspects that have been clarified in monofilamentary short length tape can be utilized in multifilament tape also. These can be summarized as,

- Tapes prepared using precursor with average particle size in the range 3- 4 μm yield the best result in respect of high T_C phase fraction, microstructure, J_C and J_C-B characteristics.

- Ag addition slightly reduces high T_C phase fraction and the J_C in (Bi,Pb)-2223/Ag tapes when Ag is added to the precursor.
- Among the Ag additives $AgNO_3$ gives the best results with respect to phase formation and transport J_C.
- Strain tolerance and tensile strength are improved a lot with Ag addition and they increase with increase in concentration of Ag.
- Molecular level Ag addition enhances both the phase formation and J_C compared to other forms of addition.

In other words, the work reported in the previous chapters helped in preparing precursor powder which meet the requirement like the particle size, type and form of Ag additive, optimum percentage of silver etc for better transport and mechanical properties. Therefore the aim of the studies reported in the present chapter is to in corporate better tape processing schedule also so as to fabricate long multifilamentary Ag/BPSCCO composite tape and pancake coils with good superconducting and mechanical properties.

The present chapter deals with the preparation and characterization of long multifilamentary Ag/BSCCO composite superconducting tapes. First of all, optimum wire diameter in the first and second stages, filament number, and final tape thickness were identified in short length multifilamentary tapes. Next, the results of the studies on processing and characterization of long multifilamentary Ag/BPSCCO composite tapes by incorporating the comprehensive process optimization are presented. Finally, we showed the technical feasibility of making pancake coils by using the long multifilamentary tapes. Both 'react and wind' and 'wind and

react' approaches are used to fabricate these coils and the results of the characterization studies are reported.

7.2. Optimization in Short Length Multifilamentary Tapes

The objective of the studies reported here is to find out the optimum parameters such as wire diameter in the first and second stages, filament number, final tape thickness etc. The experiments involved are mainly on preparation of precursor powder and processing of multifilamentary tapes. Tapes were characterized by J_C measurements and dependence of J_C on applied strain.

7.2.1. Experimental

7.2.1.1. Synthesis of the precursor powder.

The precursor powder for the tape fabrication was synthesized by sol-gel technique as described in chapter 2. The initial stoichiometry was chosen as $Bi_{1.8}Pb_{0.4}Sr_2Ca_{2.2}Cu_{3.1}O_y$ – (x) Ag (x-> 3 wt% Ag in the form of $AgNO_3$). Silver is added in the molecular level as described under section 6.2. Dynamic vacuum calcination under oxygen partial pressure at 750^0C for 12 h was used. The powder was then wet ground in acetone and further calcined in free flowing oxygen at 800^0C for (12+12)h with one intermediate grinding. The resulting powder was found to be highly reactive, rich in (Bi,Pb)-2212 phase and free from carbon.

7.2.1.2. Processing of Multifilamentary Tapes

Various stages of processing of multifilamentary Ag/BPSCCO composite tape is described in chapter 2. Monocore Ag sheathed wires were initially prepared by PIT process. Monocore wires with different diameters ranging from 0.8 to 2.2 mm were cut into pieces and packed into different Ag tubes of OD/ID: 10 mm/8.5 mm. The wire filled tubes were then subjected to a second stage of groove rolling to yield multicore wires of diameters from 2.2 mm to 4.5 mm. These wires were flat rolled using a specially designed flat rolling machine which had provision for rolling tapes upto a length of 15 m under desired front and back tension and speed. Multifilamentary tapes with thickness in the range 0.2 mm to 0.45 mm were prepared by intermittent rolling and heat treatments at temperatures in the range 830 ± 1^{0}C for an overall duration of 190h.

7.2.1.3. Characterization

Stereomicroscope was used to study the morphology of the tape sections, estimation of the superconductor area for calculation of J_C and measurement of filament thickness. Transport critical current measurements at 77K were conducted by four-probe method using 1μV/cm criterion. J_C dependence on the bending strain was studied by bending the samples onto different cylindrical mandrels of predetermined radius and measuring the I_C in the bent state.

7.2.2. Results and Discussion

Fig. 7.1 shows the variation of J_C with respect to the final tape thickness for different values of filament number and final wire diameter. It can be seen that J_C is more influenced by the final tape thickness and to a lesser extent by the final wire diameter. The number of filaments have still lesser role in deciding the maximum J_C. It is clear from the Fig. that tapes

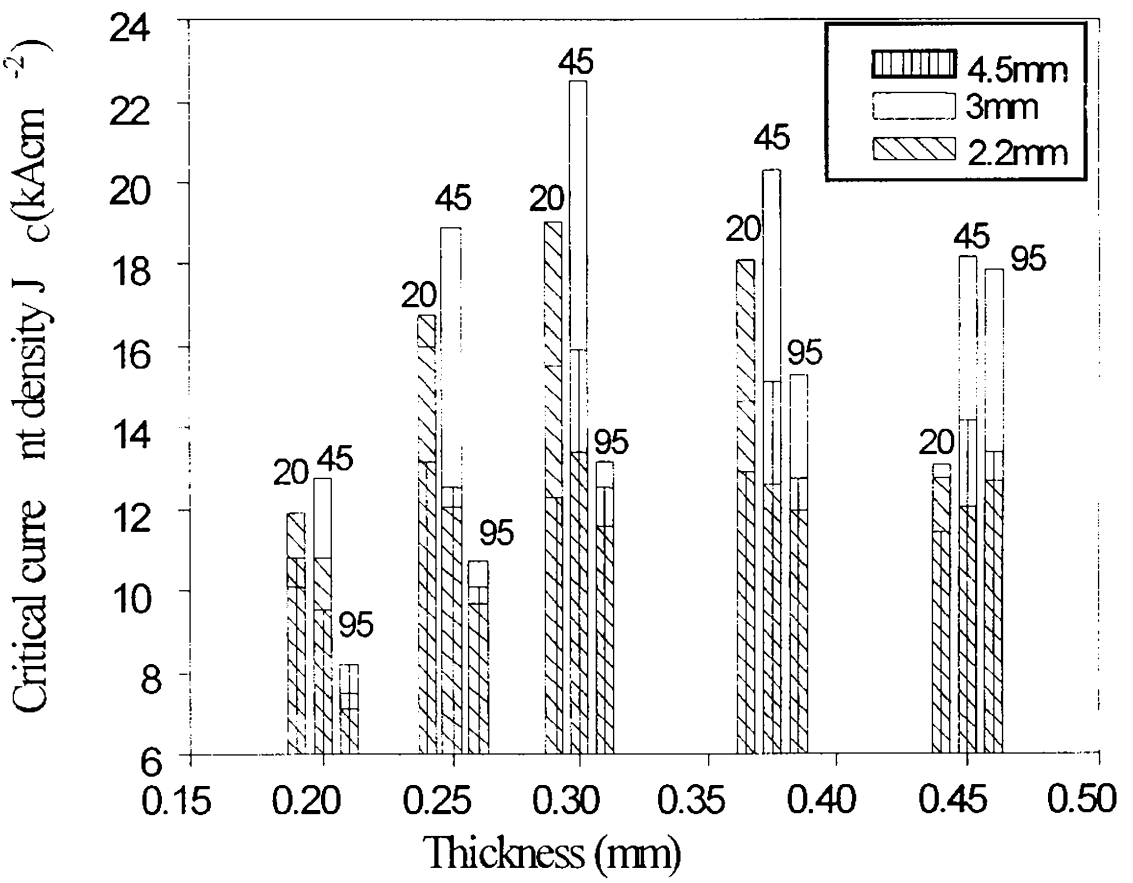

Fig. 7.1. Variation of J_C with respect to thickness of multifilamentray tapes for different wire diameters and filament numbers.

with a thickness of around 0.3 mm shows the maximum J_C, irrespective of the final wire diameter in cases where 20 and 45 filaments are used. But for 95 filament tape, J_C (max) is observed in thicker tapes of around 0.45 mm. The highest J_C of 22.5 kA/cm^2 is observed in a tapes having thickness of 0.3 mm, filament number 45, and final wire diameter 3.0 mm. For specific values of tape thickness and final wire diameter , the filament number is inversly related to the individual filament thickness. For obtaining the best J_C the individual filament thickness has to be maintained at an optimum value. Therefore , when the number of filaments are increased, the J_C (max) will occur at higher tape thickness for a given value of wire diameter.

Fig. 7.2 shows the normalised J_C verses bend strain for tapes with different number of filaments. It is seen that, the critical strain for all the Ag added tape is higher than that of pure sample. The critical strain of pure 45 filament tape is 0.45 % while the critical bend strains of Ag added 20,45,95 filament tapes are 0.51%, 0.67%, 0.67% respectively.The normalized J_C drops very slowly with increasing bend strain for the 45 and 95 filament tape. Sato et al[10] reported that the bendstrain increases from .1% to 0.7% when the number of filaments in the tape increased from 1 to 1296. But in our case bend strain of 45 and 95 filament tape was showing almost same value. Eventhough we obtain a similar improvement in critical bend strain for 45 and 95 filament tapes, 95 filament tape is of less significance for applications due to reduced fill factor and lower critical current compared to 45 filament tape.

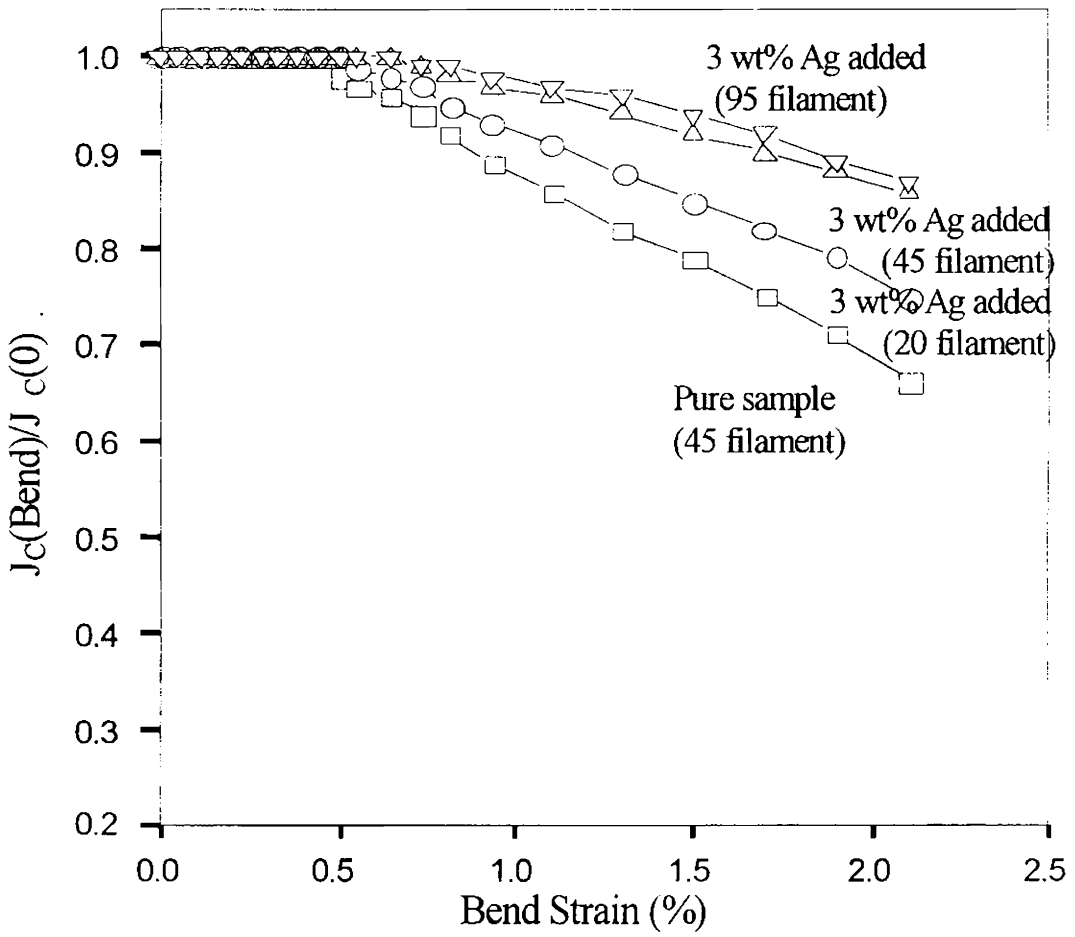

Fig. 7.2. Normalised critical current density verses bend strain for pure and Ag added multifilamentary tapes

Table 7.1 gives the optimum parameters for achieving the best J_C value and higher mechanical strength.

Table 7.1. Optimum parameters for preparation of multifilamentray tapes		
1	Initial stoichiometry	$Bi_{1.8}Pb_{0.4}Sr_2Ca_{2.2}Cu_{3.1}O_y$-(x)Ag (x->3 wt% Ag)
2	Tube dimentions for the first stage (PIT)	O.D-10 mm; I.D. – 8 mm
3	Tube dimention for second stage (WIT)	O.D-10 mm; I.D. – 8.5 mm
4	Wire diameter –first stage	0.9 - 1.1 mm
5	Wire diameter –second stage	2.9-3.1 mm
6	Number of filaments	40-50
7	Final Tape thickness	280-300 μm
8	Final tape width	4.6-5 mm
9	Average filament thickness	10-12 μm
10	Fill factor	23-25
11	Heat treatment temperature	830 ± 1^0C

7.3. Preparation and Characterization of Long Multifilamentary Ag/(Bi, Pb)- 2223-Ag Composite Superconducting Tapes

Many of the applications require long and high J_C superconducting wires and tapes with improved strain tolerance. The results obtained so far show that this could be made possible by adopting three important outcome of the present work viz. thermo-mechanical processing with optimum particle size, silver addition and multifilamentray technique. Optimum particle size with controlled thermo-mechanical technique could make

dense, well-aligned and strong bonded grains, small percentage of silver will improve the mechanical as well as superconducting property and multifilamentray technique could make flexible tapes. Studies on processing and characterization of long multifilamentary Ag/Bi-2223-Ag composite tapes are presented in this section.

7.3.1. Tape Fabrication and Measurement

Precursor powders of the optimized composition derived by sol-gel method were loaded into a silver tube as described in the experimental part of section 7.2.1. Silver sheathed BPSCCO/Ag composite tapes of 45-50 filaments were fabricated from single core wires and these tapes were heat treated at 830 ± 1^{0}C with intermediate rolling to final dimension of about 0.3 mm thickness and 4.7 mm width.

Studies on long length tapes have been conducted in three phases, i.e. studies on 1 m, 5 m and 10 m long tapes. The tapes were heat-treated by winding them helically on mullite mandrels of diameters varying from 10 to 15 cm. In order to measure the distribution of the critical current along the tape length, up to 25 voltage tabs were placed on the turns of the tape wound on ceramic tubes. Critical current measurements were performed at 77K as well as 64K by immersing the mandrels along with the tape in liquid nitrogen with and without the application of vaccum. The tapes were characterized by XRD, J_C, J_C-B and susceptibility measurements according to the procedures described in chapter 2.

7.3.2. Results and Discussion.

All the tapes were heat-treated for 190 h and the characterization has been conducted at 77 K as well as 64 K. Critical current density measurements were done over the entire length of the tape and the results are given in the table 7.2. The wire dimension and the core cross sectional areas are determined by metallography combined with image analysis. The sectional views of the polished sections of a typical multifilament wire and tape are shown in Fig. 7.3. The filaments are of uniform size and are uniformly distributed.

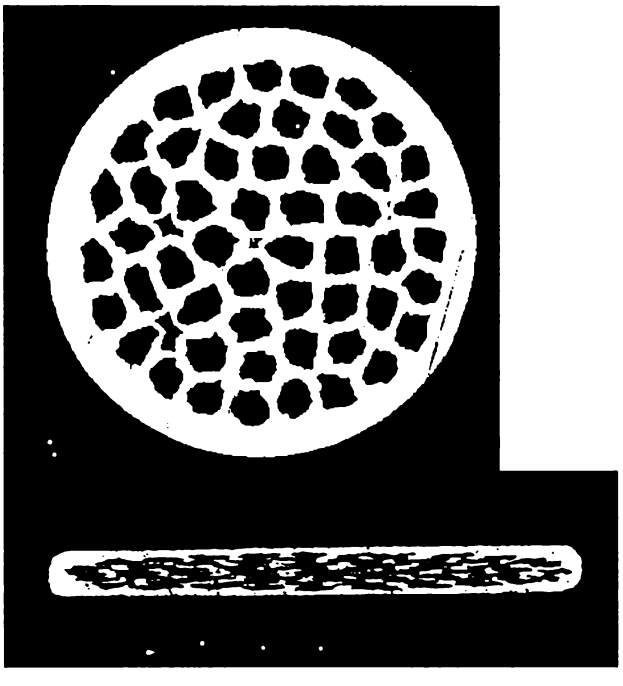

Fig. 7.3. Cross sectional views of the multifilament wire and tape

Examination of the segment along the length of the tape did not show any discontinuities or large voids in the filament. The individual filament in the 45-filament tape has a thickness of 10-12μm and is uniformly elongated within the tape.

Table 7.2. Typical whole-length Jc values measured in 1 m, 5 m and 10 m long multifilamentary tapes in helical coil form

Sample Code	No. of filaments	Length (m)	Whole length J_C (77 K, 0T) ($kAcm^{-2}$)	Whole length J_C (77 K, 0T) ($kAcm^{-2}$)
MFT1	45	0.95	19.2	36.57
MFT2	45	1.10	18.5	34.91
MFT3	45	1.30	19.0	36.1
MFT4	49	5.20	16.0	30.5
MFT5	49	5.50	17.5	34.1
MFT6	49	5.30	17.0	33.5
MFT7	47	10.50	14.8	28.5
MFT8	47	9.90	15.5	29.8
MFT9	47	10.70	16.3	30.8

A number of factors affect the electrical performance of the finished tape such as internal defects as well as wire handling during processing etc. The performance uniformity over the entire length of the tape is shown in Fig. 7.4. The maximum dispersion of J_C is estimated to be within ± 3 % for

1m, and 5m long tapes and within ± 6% for 10m long tapes. Although temperature fluctuation along the length during the heat treatment is much higher than that for treating the short tapes, the reproducibility of the long tape is good because of the high thermal conductivity of the silver used in

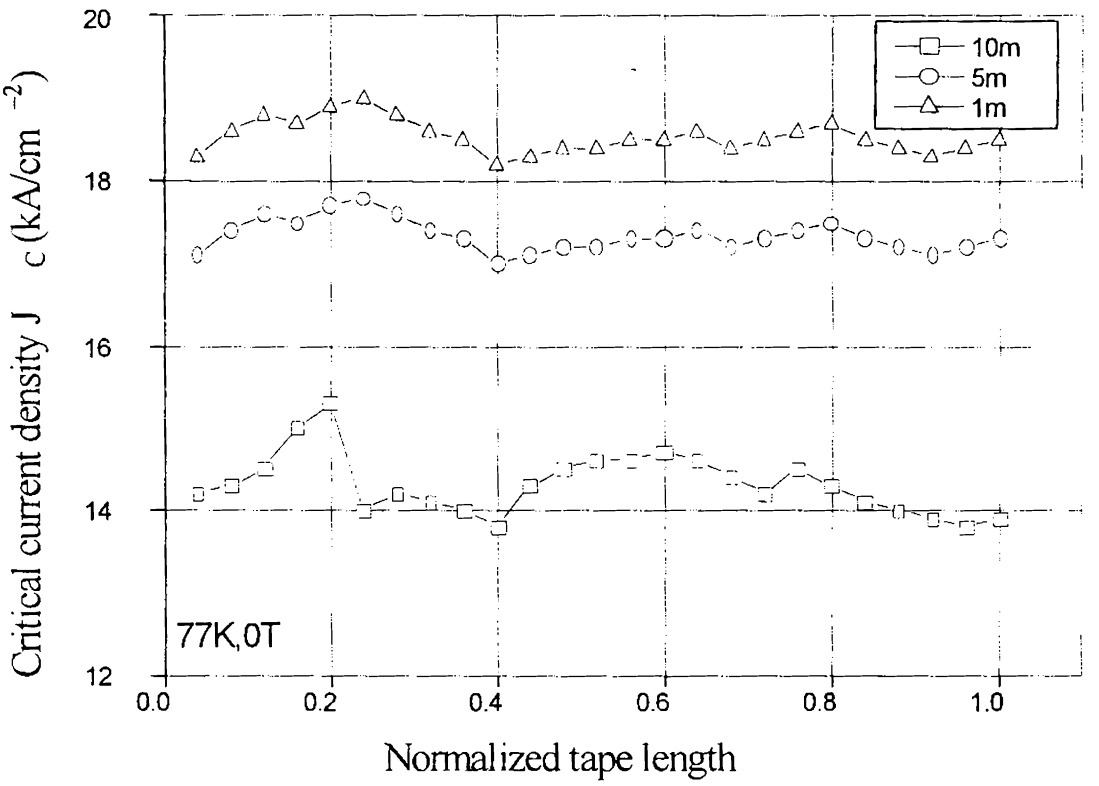

Fig. 7.4. Distribution of J_C values along the length of a 1m, 5m and 10m long Bi-2223/Ag tapes at 77K.

the form of sheath as well as additive. A typical tape from all the 3 batches was used to determine the distribution of critical current density at 77K.

Small particle size of the precursor, large grain size and good alignment are important to achieve homogeneity and high J_C over the long tape.

Fig. 7. 5 . Shows the dispersion of thickness and width over 10 m length. The maximum variation for both thickness and width over the 10 m length is found to be as low as ±2%.

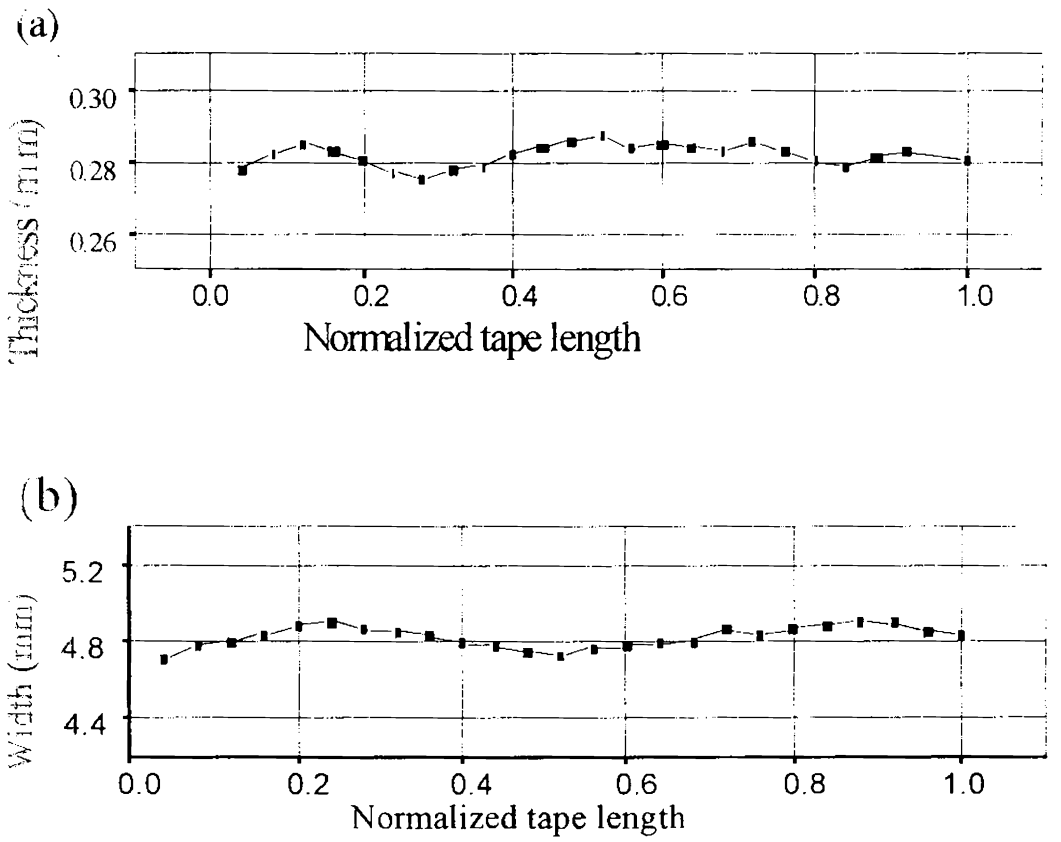

Fig. 7. 5. Dispersion of (a) thickness and (b) width over 10 m length.

Fig. 7. 6 show a typical XRD pattern of the fully processed multifilamentary tape. It can be seen that the core contains mainly the high

T_C phase with very little quantities of secondary phases such as Bi-2212 and Ca_2PbO_4.

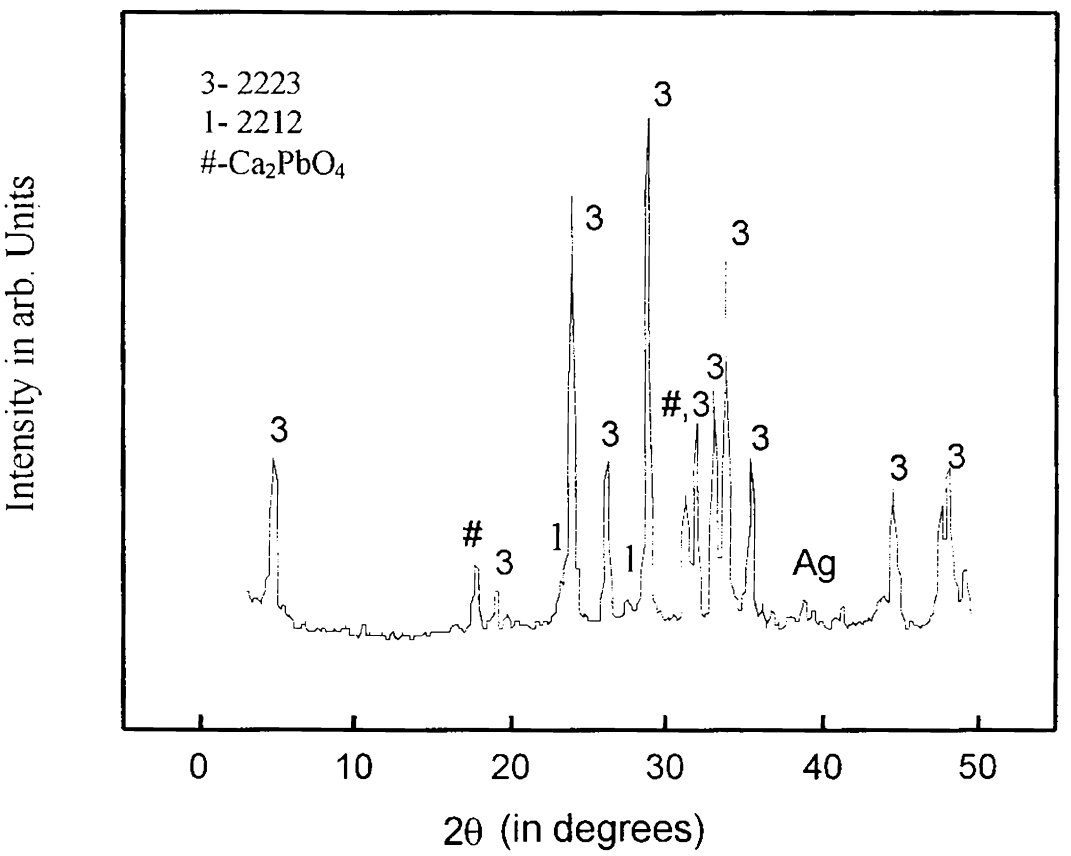

Fig. 7.6. XRD pattern of the fully processed tape

AC susceptibility measurements performed on a typical multifilamentary tape with temperature indicate a sharp single step transition (Fig.7.7). The

T_C onset from the plot is found to be 109.5^{0}C. The single step transition once again show the high level of high T_C phase purity.

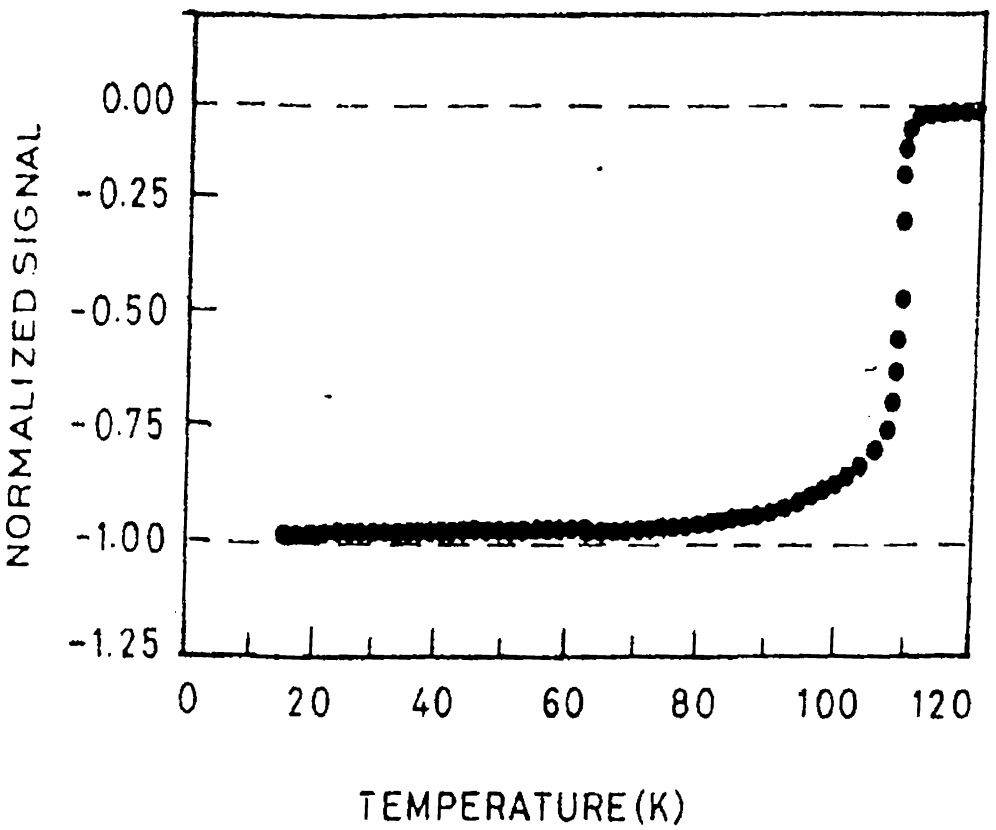

Fig. 7.7. AC susceptibility vs. temperature plot of a multifilamentary tape.

The magnetic field dependence on J_C at 77 K for a 45-filament tape is shown in Fig. 7.8. The field-applied parallel to the c-axis shows a strong J_C dependence dropping from 15.5 to 4 kAcm^{-2} by applying a field of 100 mT. While the field parallel to the a-b plane has a much weaker effect,

dropping J_C to only 10.8 $kAcm^{-2}$ by applying the same field. J_C as a function of increasing and decreasing field shows no irreversible loop, which is usually observed for Ag sheathed Bi-2223 tapes in cases where

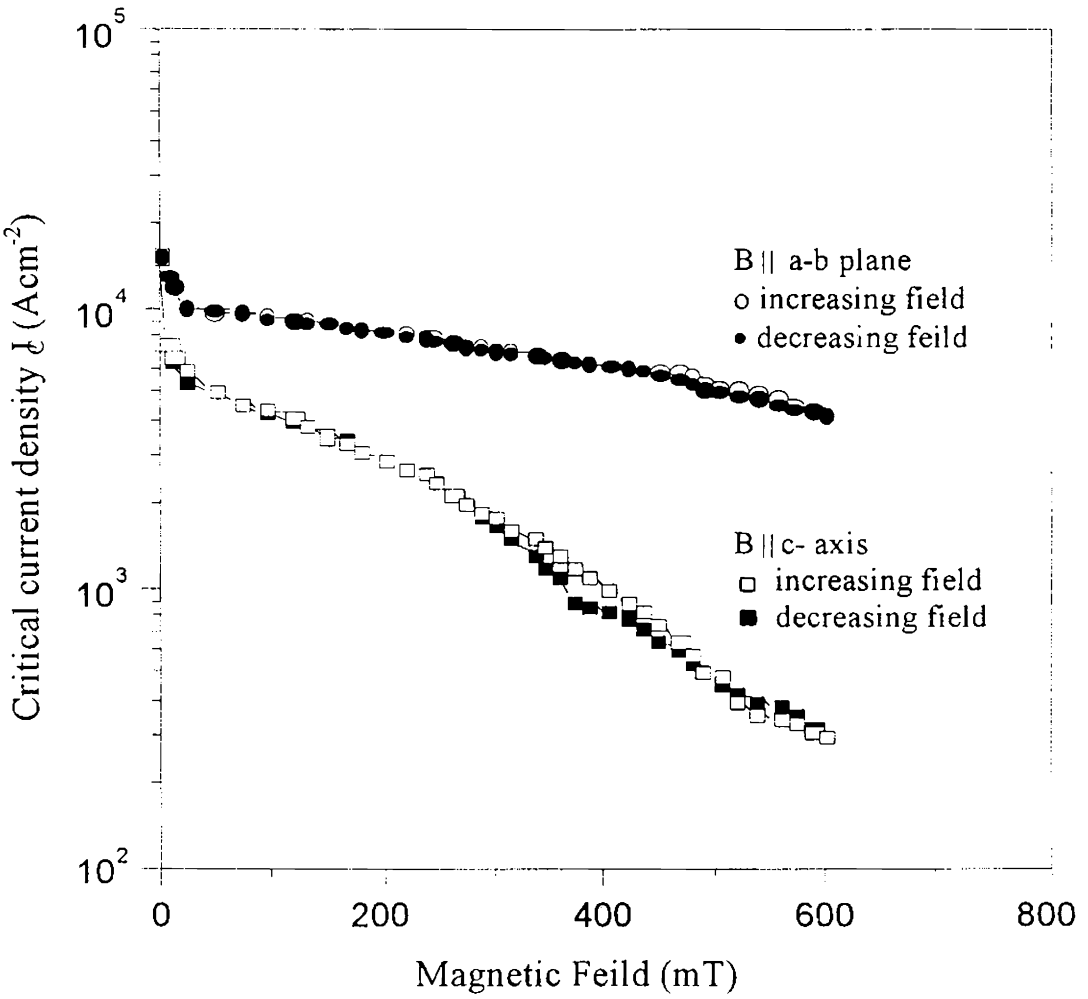

Fig. 7.8. The magnetic feild dependence of J_C at 77K

weak links are significant.[11-12] The absence of irreversible loops in the present case indicates that the effect of weak links is reduced to a great extend in the newly developed tapes.

Photograph of long multifilamentary superconducting tapes of length upto 12 m in solenoid form is shown in Fig. 7.9.

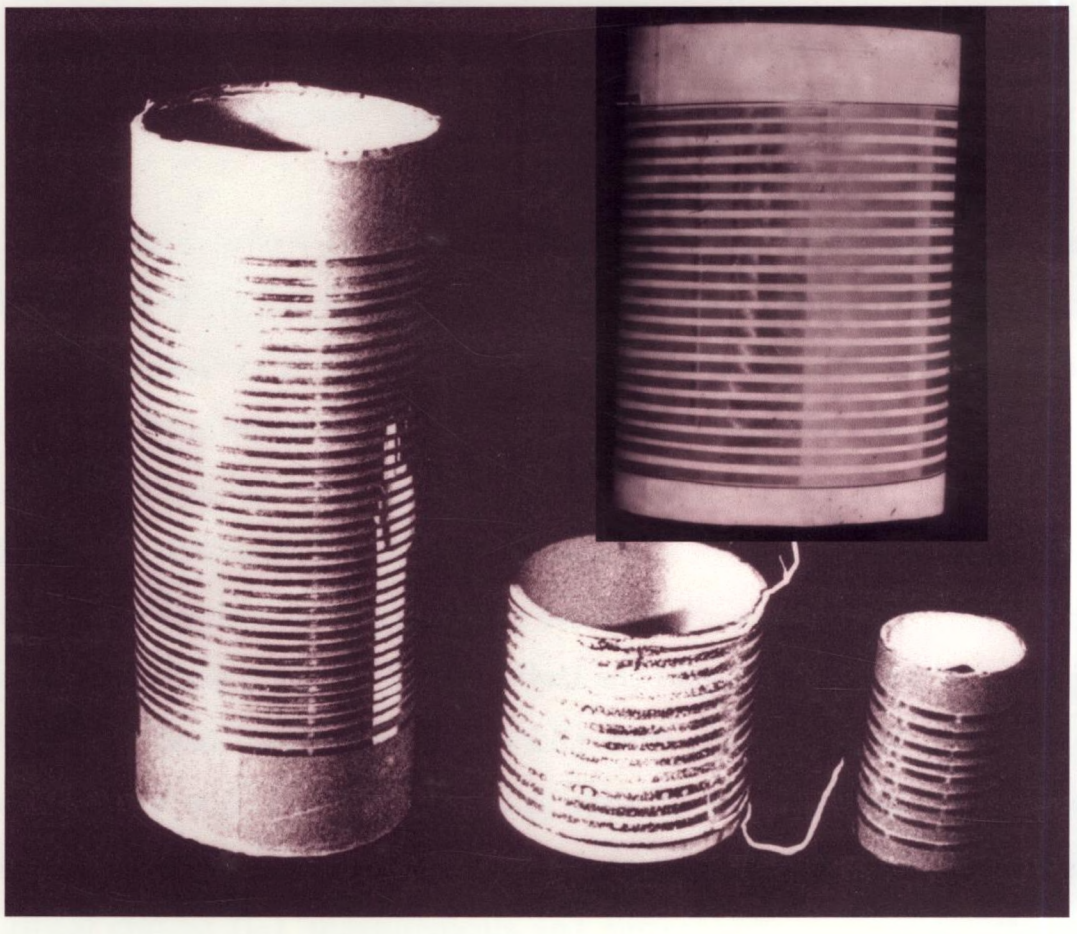

Fig.7.9. Photographs of long multifilamentary superconducting tapes

7.4. Pancake Coils

In order to assess the performance of the tape for practical applications in which the flexibility/ bend strain of the conductor is important, long superconducting tapes of different length were used to wind in the form of pancake coils.

7.4.1. Preparation and Characterization of Pancake Coils

Pancake coils with an inner winding diameter of 5-8 cm and outer diameter 8-10 cm and turn number 20-50 have been fabricated by means of both 'wind and react' (W&R) and 'react and wind' (R&W) methods using long multifilamentary tapes of varying lengths. Specially designed spools with provisions for varying the spacing and easy separation of the spool discs with different diameters were used for making the pancakes. The winding of the coils were electrically insulated from each other using a thin layer of alumina paint for W&R method and teflon tape for R&W method. After the heat treatment (for W&R) both the types of coils were impregnated with a cryostable epoxy resin of low viscosity in order to obtain a strongly fixed winding and for necessary strength and protection. Critical current (I_C) measurements and current-voltage characteristics of the coils have been conducted by using the procedures as described in chapter 2.

7.4.2. Results and Discussion

In order to fabricate pancake coils both R&W and W&R methods were investigated. Fig. 7.10. shows the relationship between normalised I_C and radius of the coils made by R&W and W&R methods. It shows that the W&R technique is better than R&W for obtaining higher critical current, but W&R was limited by many factors such as high temperature insulation, limitations in the shape of the coils etc. The choice of the method,

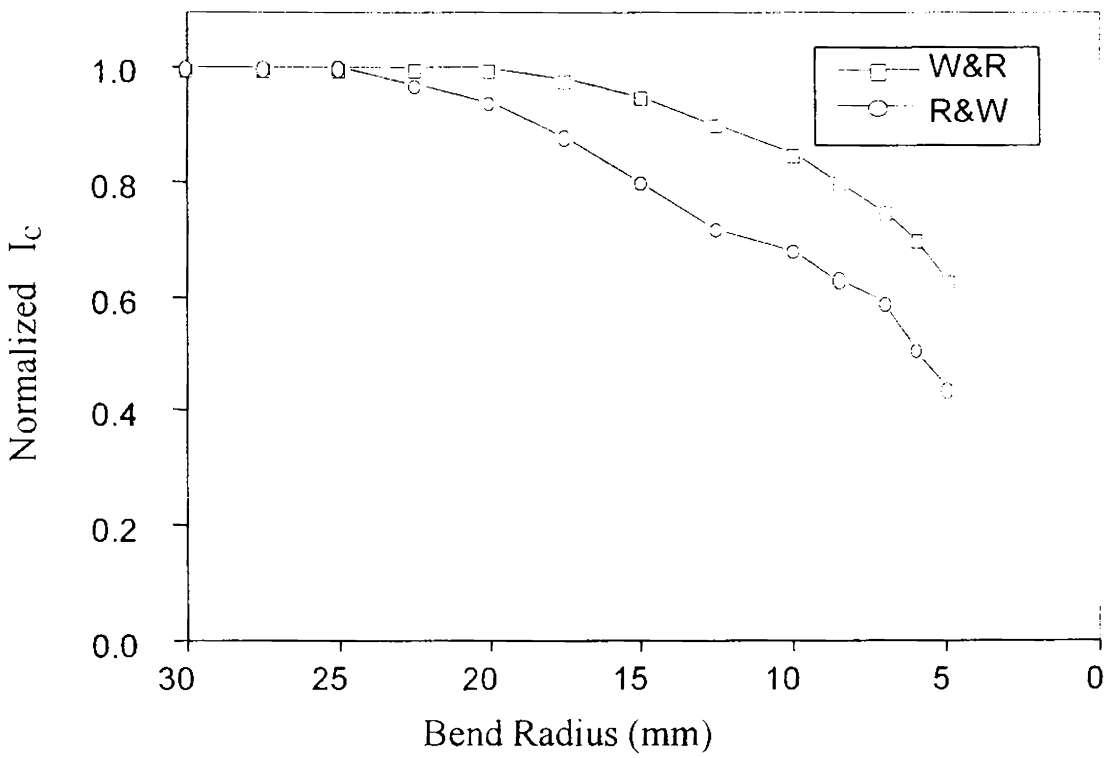

Fig 7.10. Relationship between normalized I_C and radius of the coils made by R&W and W&R method

therefore, depends on the nature of application. Thus larger size coils for practical application can be fabricated by the react and wind approach although smaller ones can easily be produced by the wind and react technique.

Ten pancake coils were made and the critical current of the coils in whole length as well as in different sections were measured at 77 K and 64K. Some of the typical I_C measurement results at 77K are given in table 7.3.

Table 7.3. Typical Ic values measured in pancake coils

Sample Code	Tape Length (m)	Type	ID/ OD (cm)	No. of Turns	Ic at 77K, 0 T (A)
PC 1	12.0	W&R	7/10	48	27
PC 2	10.5	W&R	5/8.2	50	29
PC 3	7.57	W&R	6/8	32	31
PC 4	9.08	R&W	6/8.5	39	24
PC5	10.5	R&W	5/8.2	50	23
PC6	12.0	R&W	7/10	48	22
PC7	6.5	W&R	8/9.5	22	35

Different sections of a typical coil were investigated in more detail by measuring the voltage-current (V-I) characteristics. A number of voltage tabs were placed at different positions of the pancake coil in order to characterize the inner, middle and outer section of the coil. Fig. 7.11 shows

the V-I characteristics of the coil (PC1 in the table 7.3) measured at 77K with 1μV criterion.

As shown in Fig. the V-I characteristics of the coils follow an exponential law and the different sections of the coil have about the same slope. The critical current decreases from the outer section to the inner section due to the magnetic field generated in the coil.

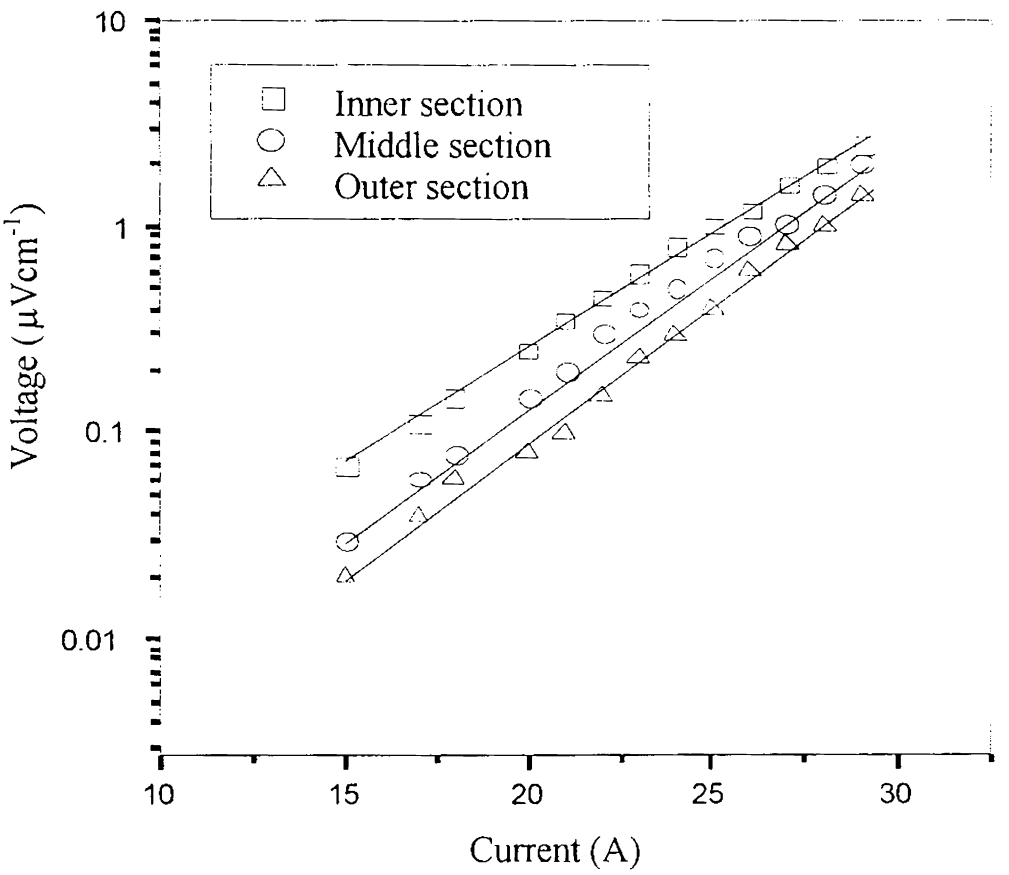

Fig. 7.11. V-I characteristics of the different sections of a pancake coil at 77 K

Photograph of some of the pancake coils fabricated by both W&R and R&W method are shown in Fig. 7.12.

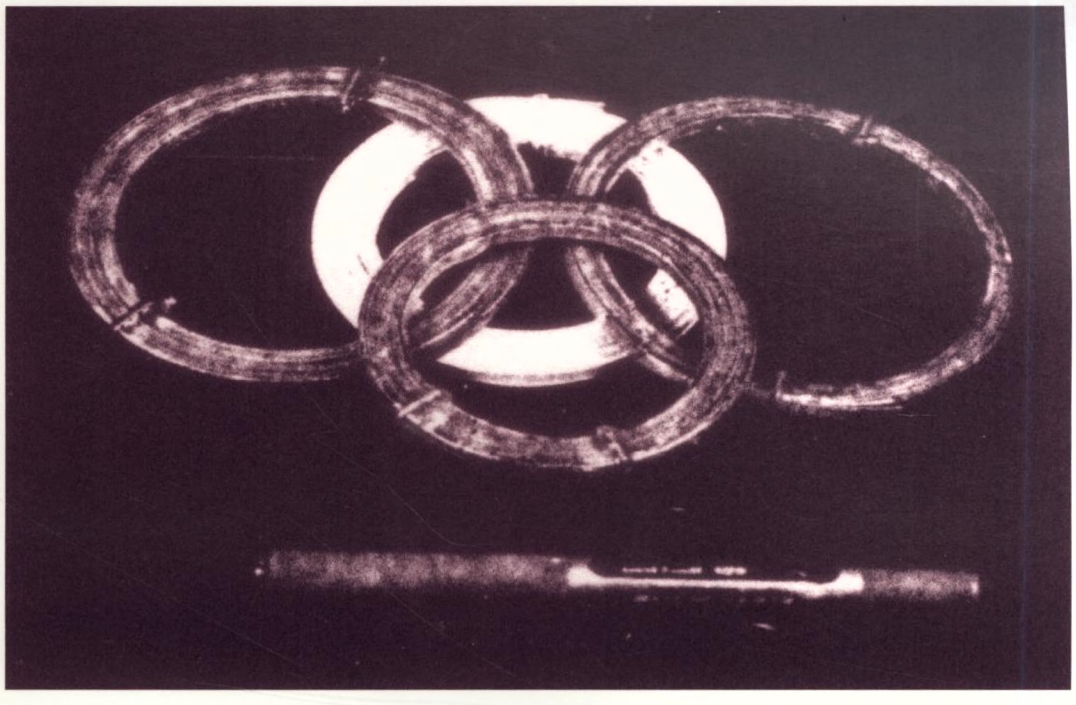

Fig. 7.12. Photograph of some of the pancake coils fabricated by both W&R and R&W method

7.5. Conclusions

Long multifilamentary Bi-2223/Ag composite tapes upto a length of 12 m have been developed by powder-in-tube (PIT) method followed by wire-in-tube (WIT) process. Critical current densities in the range 14-16 $kAcm^{-2}$ have been achieved in these tapes by an optimised processing. Pancake shaped coils of inner diameters 50-80 mm and outer diameter 80-100 mm and turn number upto 50 have been made using long multifilamentary tapes of length upto 12m by 'react & wind' and 'wind &

react' approaches. W&R technique is found to be better than R&W for obtaining higher critical currents in the coils.

References

[1]. L.Masur, E. Podtburg, D. Buczek, W. Carter, D. Daly, U. Kosasih, S. J Loong, K. Manwiller, D. Parker, P. Miles, M. Tanner, and J. Scudiere, *Adv. Crygenic Eng.* **46**, 871 (2000)

[2]. S. Norman et al. *Jicable, Paper* **A3.5**, 97 (1999)

[3]. J. K. Sykulski, et al. *IEE Proc.- Electr. Power Appl.*, **146 (1)**, 41 (1999)

[4]. T. Masuda, et al, *EUCAS, **E4**.*1-05 (2001)

[5]. U. Balachandran, A. N. Iyer, R. Jammy, M. Chudzik, M.Lelovic, P. Krishnaraj, N. G. Eror, and P. Haldar, IEEE Trans on Appl. Supercond, 1997, 7, 2207-2210

[6]. A. Sobha, R. P Aloysius, P. Guruswamy, and U. Syamaprasad, Supercond. Sci. Technol. **13**, 1 (2000)

[7]. S. Salib and C. Vipulanandan, Mater. Res. Bull **32(10)**, 1333 (1997)

[8]. P. Kovac, I. Husek and L. Cesnak, Supercond. Sci. Technol. **7**, 583 (1994)

[9]. R. P Aloysius, A. Sobha, P. Guruswamy, and U. Syamaprasad, Supercond. Sci. Technol. **14**, 1 (2001)

[10] K. Sato, T. Hikata, H. Mukai, M. Ueyama, N. Shibuta, T. Sato, T. Masuda, M. Nagata, K. Iwata and T. Mitsui, IEEE Trans. On Magnetics, 1991, **27** , 1231

[11]. D.P.Hampshire, Physica C, **296**, 153 (1998)

[12]. H. Kitaguchi, H. Kumakura and K. Togano, Applied Superconductivity, **3**(11-12), 535 (1995)

CHAPTER 8

SUMMARY AND CONCLUSIONS

High temperature superconductors have many superior superconducting properties over metallic low temperature superconductors. However, these new superconductors have various shortcomings, which restrict their applications. For Bi-based superconducting tapes/ wires suitable for power applications, these problems can be classified mainly as mechanical, electrical, magnetic and more general reliability problems. Usually for practical application, tapes are prepared in multifilamentary for enhanced mechanical strength, reduced AC loss and better reliability. Multifilamentary tapes are prepared by powder-in- tube (PIT) method followed by wire-in tube technique (WIT). In this technique, a ductile metal tube is filled with a suitable ceramic precursor and subjected to mechanical rolling operation and the rolled wires are cut into pieces and packed into another metal tube and are subjected to a second stage rolling. Finally the elongated and flexible conductor is heat treated so that the ceramic grains of the core get sintered and strong intergranular electrical current path get established. However the apparent simplicity of this approach is often deceptive and the target of getting better and reproducible critical current density is difficult. The reason for this is that (Bi, Pb)-2223 is a complex system which contains five cations and the processing parameters for obtaining good superconducting properties show wide

variations over sintering temperature, duration and atmosphere. Also many connectivity limitations occur in Bi-2223 tapes, amongst which are grain-to grain misalignments, cracks, porosity and impurity phase. In the work presented in this thesis, a systematic investigation has been carried out on ways to improve mechanical and superconducting properties of silver sheathed Bi-2223 tapes by adding silver in the matrix and the results thus obtained have been utilised successfully for the development of long multifilamentary superconducting tapes and pancake coils.

The thesis presents a brief review on the properties and processing aspects of Bi-based superconductors. Properties of the superconducting materials like mixed state, type II superconductor, irreversibility line, flux creep etc are mentioned. Also the structure of Bi- based superconductor, the reaction mechanism and stability of 2223 phase are discussed. The necessity of texture, need of PIT technique for the fabrication of tapes, general considerations for fabrication of PIT tape etc are explained. The importance of the mechanical strength of the tape for practical applications, role of silver in Bi-2223 superconductor, and the factors affecting the critical current density such as flux pinning, grain boundaries etc are also highlighted. Important applications of Bi- based superconductor in the form of long length tapes are also mentioned.

Against this background, the scope of the work included the effect of silver on mechanical and superconducting properties of long Ag/BPSCCO-Ag superconducting tapes. The investigations were focused mainly on (i). Optimise the suitable form, type and percentage of silver for improved superconducting and mechanical properties. (ii). Optimise the geometrical parameters of the multifilamentary tape with respect to critical

current and strain tolerance. (iii) Utilise the above information for development of long superconducting tape with improved mechanical and superconducting properties.

Processing of ceramic products with controlled properties is an area where a variety of techniques and instrumental methods are to be made use of. In the present study the main analytical methods used have been, particle size analysis using Micromeritics particle size analyser, phase analysis using XRD, microstructural examination using scanning electron microscope and optical microscopes and thermal analysis using DTA. Characterization techniques of the superconductor involved critical current density measurements with and without the application of external magnetic field and its dependence on bending strain and tensile stress, V-I characteristics, ac susceptibility measurements etc. Also the preparation techniques for preparing precursor powder, bulk pellets and Ag- sheathed mono and multifilamentary tapes have been described.

The preliminary studies were conducted by varying the particle size distribution of the precursor powder. A basic precursor with a stoichiometry of $Bi_{1.8}Pb_{0.4}Sr_2Ca_{2.2}Cu_{3.1}O_y$ was prepared by sol-gel method and was divided into different batches and milled in a planetary ball mill for different duration using agate balls in acetone. DTA results revealed that the reaction temperature of the precursor powder depends on the particle size and is minimum for the finest powder. (Bi,Pb)-2223/Ag sheathed tapes were prepared using precursor powders with different particle size distributions. The optimum heat treatment temperature was determined by heat-treating all the tapes at temperatures from 823 to 837^0C with an interval of 2^0C on the basis of DTA. After heat treating all the tapes

at their optimum temperature the tapes were characterized in order to evaluate the relative performance of the tape and to find out the optimum particle size of the precursor. Phase evolution studies, transport current measurement at 77K with and without the application of an external field, microstructural examination etc showed that the particle size has significant effects on the reaction kinetics, ultimate phase fraction, microstructure and transport critical current density. For the tapes fabricated using coarser powder, the reaction kinetics was found to be slower and the microstructure contained smaller grains with many misalignments and voids. On the other hand, use of extremely fine precursors yielded tapes with a larger fraction of secondary phases due to the degradation of crystallinity of the precursor and consequent change in the reaction sequence. The tapes prepared using a precursor with an average particle size of 3-4 μm showed the best results with respect to J_C, high-T_C phase fraction, microstructure and J_C-B characteristics.

With an effort to understand the effect of silver on superconducting and mechanical properties of the (Bi,Pb)-2223 /Ag sheathed tapes , studies were conducted initially in order to find out the relative effect of Ag powder, Ag_2O and $AgNO_3$ on the sequence of phase evolution , kinetics of (Bi,Pb)-2223 formation, density variation and finally the transport current in bulk BPSCCO system. Experiments were conducted by varying the silver content from 0 to 25 wt% in the composition. The reactants used were oxides or carbonates of metals and conventional ceramic route was followed for the preparation of sintered bar specimens. Phase evolution of the samples at different stages of heat treatment, microstructural examination and superconductivity measurements suggested that Ag

addition in BPSCCO accelerates the Bi-2223 phase formation and J_C to different extents depending on the form of Ag additive. Among the Ag additives Ag_2O and $AgNO_3$ were found to be much effective in promoting the Bi-2223 phase formation and J_C while the addition of higher percentage of Ag powder with larger particle size lead to segregation of Ag in bulk BPSCCO pellets. Sintered BPSCCO pellets with density as high as 90% of the theoretical density and critical current density about 400 Acm^{-2} could be prepared by addition of around 10 wt% Ag to the superconductor either in the form of Ag_2O or $AgNO_3$.

In Ag sheathed BPSCCO tapes addition of Ag to the precursor can lead to results different from bulk samples especially on phase evolution and J_C in view of the presence of Ag sheath. Studies on the effect of Ag powder, Ag_2O and $AgNO_3$ (10 wt% each) on (Bi,Pb)-2223/Ag tapes showed that the Ag addition reduces the rate of high T_C phase formation ultimate high T_C phase fraction and J_C to different extents depending on the form of additive which is in contrast to the result obtained in bulk sample. In the case of Ag powder and Ag_2O added tapes the reduction is significant while in $AgNO_3$ added samples the reduction is only to a lesser extent Microstructural examination showed larger grain growth in all the Ag added tapes with Ag particle size depending on the size and form of Ag additive.

Mechanical strain/ stress in superconducting composite leads to degradation of J_C. The effect was studied in mono and multifilamentary tapes containing different percentages of $AgNO_3$ (Ag: 0-7 wt%). The I_C of each sample was measured under increasing bending strains to determine the strain limit (ε_{irr}). Similarly, the stress tolerance of the samples under the

tensile mode was found by holding the sample in a vertical axis in liquid nitrogen and by applying the desired tensile load. The results showed that the bend strain tolerance and tensile stress tolerance of (Bi,Pb)-2223/Ag tapes improve remarkably as the Ag content in the matrix increases. The mechanical properties of multifilamentary tapes were found to be better than that of monofilamentary tape and multifilamentary tape with 7 wt% silver addition have a strain tolerance more than three times and a tensile stress tolerance of 142% higher than that of pure monofilamentary tape.

Improved grain connectivity accompanied by both grain alignment and densification is a necessity for improving the transport current. A study was conducted to improve the transport property and microstructure of Ag added tapes by introducing well dispersed ultrafine silver particles in molecular level to the precursor. Bi-2223/Ag nanocomposite tapes were prepared using these precursors with an intention to utilize the super plasticity of fine silver grain. The results showed that the silver addition in molecular level enhances the phase formation as well as J_C of (Bi,Pb)-2223/Ag tapes compared to other forms of silver addition. Transport property of 1 wt% and 3 wt% Ag added samples were found to be higher than the pure sample of which 3 wt% Ag added sample showed the highest J_C. Higher Ag addition (6 wt%) causes agglomeration of Ag particles leading to grain misorientation and reduced J_C.

Before going for the development of long multifilamentary tapes, geometrical parameters of the multifilamentary tapes such as filament number, initial and final wire diameter, final tape thickness etc were optimised with respect to J_C and strain tolerance in short length tapes. The experiments were conducted in short tapes of length 5-10 cm with filament

number ranging from 10-100, initial wire diameter from 0.8mm to 2.2 mm , final wire diameter from 2.2 to 4.5 mm and final tape thickness from 0.2 mm to 0.45 mm. The critical current density was found to be more influenced by the final tape thickness and to a lesser extent by the final wire diameter. The number of filaments have still lesser role in deciding the maximum J_C. The highest J_C and better strain tolerance was obtained in tapes having a thickness of around 0.3 mm, filament number around 45 and final wire diameter 3.0 mm.

Long multifilamentary Bi-2223/Ag composite tapes upto a length of 12 m have been successfully developed by powder-in-tube (PIT) method followed by wire-in-tube (WIT) process by incorporating the results obtained from the above experiments. Whole length critical current densities in the range 14-16 $kAcm^{-2}$ at 77K and self-field have been achieved in these tapes. The performance evaluation of the tape over the entire length showed a dispersion of J_C within ± 6% and dispersion of width and thickness as low as ± 2%. XRD studies as well as ac susceptibility measurements showed good phase purity with single step transition. Pancake coils of inner diameter 50-80 mm and outer diameter 80-100 mm and turn number upto 50 have been made using long multifilamentary tapes of length upto 12 m by 'wind and react' (W&R) and 'react and wind' (R&W) approaches. W&R technique was found to be better than R&W for obtaining higher critical current in the coils.